

Supramolecular aggregation patterns featuring Se^{···}N secondary-bonding interactions in mono-nuclear selenium compounds: A comparison with their congeners

Edward R. T. Tiekink

Research Centre for Crystalline Materials, School of Medical and Life Sciences, 5 Jalan Universiti, Sunway University, Bandar Sunway, Selangor Darul Ehsan 47500, Malaysia

E-mail: edwardt@sunway.edu.my

ORCID ID: 0000-0003-1401-1520

ABSTRACT

An evaluation of the Cambridge Structural Database for crystals containing Se^{···}N secondary-bonding interactions was conducted. The presence of Se^{···}N secondary-bonding interactions has been established in nearly 9% of crystals of mono-nuclear selenium compounds where such interactions can potentially form, **that is, having at least one nitrogen atom**. The Se^{···}N interactions feature in 71 zero-dimensional, usually di-nuclear aggregates, 63 one-dimensional chains and tapes, and smaller numbers of two- and three-dimensional arrays, that is seven and one, respectively. Selenium(II) compounds form the majority of the dataset with only eight selenium(IV) compounds included in the survey. In most cases (112 out of 142), the selenium centre forms a single Se^{···}N contact with 26 aggregates having a selenium atom forming two contacts and four examples where three Se^{···}N contacts are evident. The great propensity of selenadiazole rings (75%) and selenocyanates (50%) to form Se^{···}N secondary-bonding interactions in their crystals is particularly noteworthy.

Keywords: Se \cdots N interactions; supramolecular chemistry; secondary-bonding; crystal engineering; selenium; nitrogen

Table of Contents

1. Introduction
2. Methods
3. Assemblies featuring Se \cdots N secondary-bonding in mono-nuclear selenium compounds
 - 3.1 Two-molecule aggregates featuring one Se \cdots N interaction
 - 3.2 Two-molecule aggregates featuring two Se \cdots N interactions: selenadiazole rings
 - 3.3 Two-molecule aggregates featuring two Se \cdots N interactions: non-selenadiazole rings
 - 3.4 Higher nuclearity, zero-dimensional aggregates featuring two or more Se \cdots N interactions
 - 3.5 Linear chains featuring Se \cdots N interactions
 - 3.6 Zig-zag chains featuring Se \cdots N interactions
 - 3.7 Helical chains featuring Se \cdots N interactions
 - 3.8 Tapes featuring Se \cdots N interactions
 - 3.9 Two-and three-dimensional architectures featuring Se \cdots N interactions
 - 3.10 Multi-component crystals featuring Se \cdots N interactions
 - 3.11 Aggregates sustained by Se \cdots N interactions in selenium(IV)-containing crystals
- 4 Evaluating the crystals of congeners of 1-142 for the presence of related secondary-bonding interactions
5. Overview
6. Conclusions

Declaration of Competing Interest

Acknowledgements

Appendix A. Supplementary data

References

1. Introduction

The seemingly incongruous intermolecular interactions occurring between main group elements in low oxidation states, for example and relevant to the present survey, occurring between selenium(II)/(IV) and nitrogen atoms, that is, both electron-rich species, are well-established in molecular crystallography [1, 2] and have long been categorised as secondary-bonding interactions [3]. This is a generic term as it also encompasses more conventional Lewis acid/Lewis base interactions that might occur between, for example, a selenium(VI) centre and an electron-rich species [4]. Secondary-bonding interactions are readily recognised from crystallographic analyses in a contact that is longer than the sum of the relevant covalent radii but shorter than the sum of the assumed van der Waals radii. Naturally, any such interaction does not necessarily operate in isolation of other intermolecular forces and may very well cooperate with other obvious supramolecular synthons such as those formed by conventional hydrogen-bonding [5]. With the continuing surge of interest in identifying any number of intermolecular contacts in crystals [6-10], secondary-bonding interactions, including halogen-bonding [11], occupy a prominent position, so much so that a new lexicology has emerged [12-14]. Thus, the terms triel- [15], tetrel- [16], pnictogen- [17] and chalcogen-bonding [18] refer to the group the electrophilic element is derived. Terminology to one side, the question remains as to the nature of the interaction between two apparently electron-rich species.

Largely through the pioneering work of Politzer et al. [19-23], the interactions leading to attractive intermolecular contacts are rationalised in terms of the appearance of an electron-deficient region at the extension of, for example, a C–halogen bond leading to a polar cap or a σ -hole capable of functioning as an electron acceptor. Rather linear contacts between donor and acceptor atoms may be envisaged through interactions involving σ -holes. The polarization about a C–halogen bond this implies results in a relatively electron-rich region perpendicular

to the C–halogen bond that can also participate in intermolecular interactions. A complimentary concept to the σ -hole relates to a π -hole where an electron-deficient region occurs in a position perpendicular to an atom within a molecular residue. A comprehensive discussion and potential utility in supramolecular chemistry of σ - and π -holes has appeared [24]. Both σ - and π -hole interactions are noted in the present review of the supramolecular architectures featuring Se \cdots N interactions in molecular crystals. While these attractive interactions are stabilising, the next question relates to the energy of stabilisation these interactions provide.

Many of the structures described herein, see below, were determined in order to establish molecular connectivity as a part of a synthetic chemistry project, often motivated by the pharmacological potential of selenium-containing molecules [25-27]. Hence, relatively few studies include the results of supporting density function theory (DFT) calculations and comments on energies of stabilisation provided by Se \cdots N contacts, if they are mentioned at all. However, very recently, a detailed computational chemistry analysis of a common and important synthon described herein, that is, {Se–N \cdots }₂, formed in the theoretical dimers of a series of model compounds based on 1,3-benzoselenadiazole molecules [28] as well as their sulphur- and tellurium-congeners. This study showed the energy of stabilisation sustained by the four-membered {Se–N \cdots }₂ synthon and supporting, transannular N \cdots N pnictogen-bond, varied between a low -5.4 kcal/mol for sulphur to a high -16.8 kcal/mol for tellurium, matching other theoretical studies/experimental (NMR) studies [29] and consistent with the notion that such interactions can provide comparable energies of stabilisation as do conventional hydrogen-bonding [30]. Theory shows that for the studied compounds, the electrostatic contribution remains approximately constant for the sulphur-, selenium- and tellurium-containing compounds, at 58%, the orbital contribution increases from sulphur (25%) to tellurium (36%) and the dispersion term decreases from sulphur (18%) to tellurium (6%) [28].

While the focus of the present review is upon Se···N interactions occurring in crystals, it is salient to note that these and other chalcogen-bonding interactions play significant roles in biochemical processes, catalysis, anion recognition, etc., as noted in several recent reviews [31-36].

In continuation of a long-held interest of the supramolecular association in crystals mediated by secondary-bonding and related interactions involving the main group elements [37-51], the present survey focuses upon the delineation of the supramolecular architectures featuring Se···N interactions in the crystals of mononuclear selenium molecules which operate in the absence of other obvious supramolecular synthons, such as hydrogen-bonding. This survey reveals a full range of zero-, one-, two- and three-dimensional architectures featuring Se···N interactions. Subsequent to this bibliographic survey, attention is then directed to an analysis of the prevalence of analogous chalcogen-bonding in the oxygen, sulphur and tellurium analogues of the identified selenium compounds to ascertain any trends in the formation of chalcogen-bonding interactions among the chalcogens.

2. Methods

The Cambridge Structural Database (CSD; version 5.41 + three updates) [10] was searched employing ConQuest (version 2.0.4) [52] for Se···N contacts present in crystals of mononuclear selenium compounds. The primary criterion was distance-based so the separation between the selenium and nitrogen atoms had to be equal to or less than the sum of the van der Waals radii of selenium (1.90 Å) and nitrogen (1.55 Å), that is 3.45 Å [52]. Additional criteria were applied to enhance the reliability of the data/nature of the interaction in that structures with errors, that were charged and were polymeric were omitted. In all 181 structures were retrieved. These were then evaluated manually to ensure that the Se···N interaction was

operating in isolation of other obvious supramolecular synthons employing PLATON [53] and DIAMOND [54].

Three classes of compounds were rejected for further analysis to enable a focus upon Se \cdots N secondary-bonding interactions operating in isolation. Firstly, and most common, were structures that registered as a hit when in fact the putative Se \cdots N interaction was embedded within a N–H \cdots Se hydrogen bond. This is illustrated for the selenocarbamate ester [55] in Fig. 1a. An eight-membered { \cdots HNCSe \cdots }₂ synthon is formed in the crystal and the Se \cdots N interaction (3.45 Å) is the separation between the heteroatoms participating in the hydrogen-bond. Over half the excluded structures, that is 22, fell into this category; the significance of hydrogen-bonding interactions involving selenium has been reviewed recently [56]. The second class of Se \cdots N interactions that were omitted are those where the Se \cdots N contact cooperated with another secondary-bonding interaction. Thus, in the helical chain (2₁-screw axis) formed in the crystal of the benzoselenazole derivative [57] shown in Fig. 1b, Se \cdots N interactions (3.09 Å) cooperate with significantly shorter Se \cdots O (2.42 Å) interactions; six aggregates conforming to this pattern were omitted in the present survey. While more often than not, molecules with hydrogen-bonding potential were excluded as the Se \cdots N separation reflected the presence of a hydrogen-bond between these atoms, there were three instances where cooperation between hydrogen- and other secondary-bonding subsumed Se \cdots N interactions. This is illustrated for the co-crystal formed between co-formers 2,2-dimethylpropanoic acid and the heavily substituted selenadiazole derivative [58], as shown in Fig. 1c. The co-formers are connected via O–H \cdots N and N–H \cdots O hydrogen-bonds through an eight-membered { \cdots HOCO \cdots HNCN \cdots } hetero-synthon with two such dimers being connected via cooperating Se \cdots N (2.83 Å) and Se \cdots O (3.27 Å) secondary bonds. There are several co-crystals included in the present survey (see section 3.10) where Se \cdots N interactions form without supporting secondary and/or hydrogen bonds.

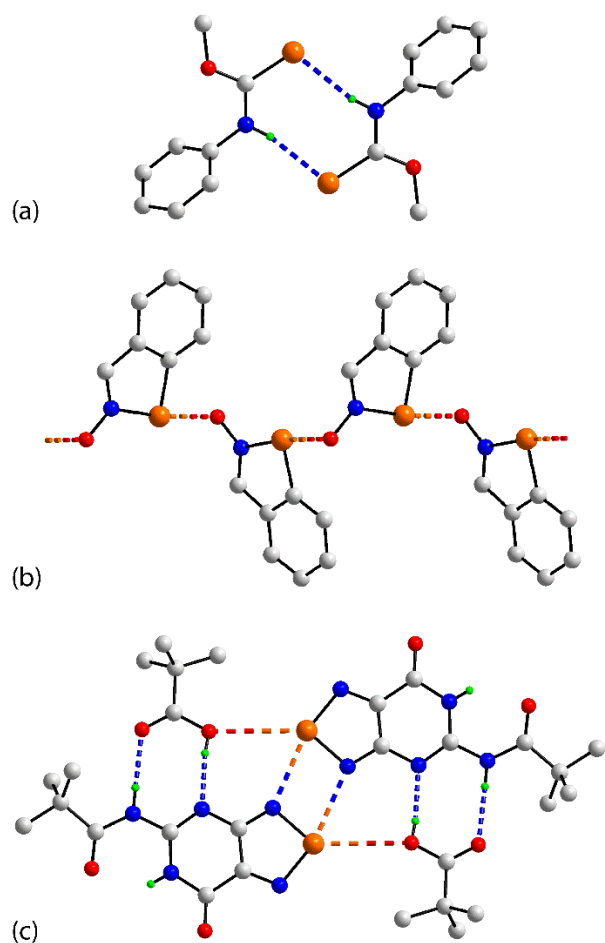


Fig. 1. Three examples of aggregates excluded from the survey as (a) the Se \cdots N atoms forming the contact are embedded within a amine-N–H \cdots Se hydrogen-bond, (b) the Se \cdots N contact (not shown) occurs within a helical chain which also features short Se \cdots O secondary-bonding interactions and (c) the Se \cdots N contacts occur within a tetra-molecule aggregate already sustained by a combination of Se \cdots O secondary-bonding interactions as well as O–H \cdots N and N–H \cdots O hydrogen-bonding. In this and subsequent diagrams, hydrogen bonds are shown as blue dashed lines, Se \cdots O and Se \cdots N contacts are shown as orange-red and orange-blue dashed lines, respectively, and non-acidic hydrogen atoms are omitted. Colour code: selenium (orange), oxygen (red), nitrogen (blue), carbon (grey) and hydrogen (bright-green).

After manual screening of the original 181 hits, 142 examples of supramolecular aggregation featuring Se \cdots N secondary-bonding interactions remained, **that is, after removing**

duplicates and aggregates sustained by additional supramolecular synthons (see above).

Information on all 142 structures are compiled in Appendix A, as Tables S1-S12. Thus, full details of the composition of the crystal, that is, including non-interacting species such as counter-ions, solvent and co-formers in the case of co-crystals, full citation details, selected distances and angles defining the Se \cdots N secondary-bonding interactions, comments on supramolecular aggregation along with image(s) and details of other significant intra- and inter-molecular contacts, that is hydrogen-bonding and additional secondary-bonding interactions, usually intramolecular. All crystallographic diagrams herein are original, being generated with DIAMOND [54].

3. Assemblies featuring Se \cdots N secondary-bonding in mono-nuclear selenium compounds

In the first instance, the aggregates are sorted into three broad categories: aggregates occurring between like-selenium(II) compounds (sections 3.1-3.9), multi-component crystals of selenium(II) compounds (section 3.10) and selenium(IV) compounds (section 3.11). Within each category, molecules are arranged in terms of the dimension of the supramolecular aggregation patterns sustained by the Se \cdots N secondary-bonding interactions, that is zero-, one-, two- and three-dimensional. To assist the flow of discussion and to enhance comparison of key geometric parameters, molecules with comparable interacting residues are grouped together within each sub-category, generally listed so crystals with shorter Se \cdots N interactions are covered before those with longer contacts.

In the ensuing discussion, Se \cdots N interactions are identified based on distance criteria, that is, contacts less than the sum of the van der Waals radii occurring in the absence of any other apparent supramolecular synthon. The van der Waals radii employed in this analysis are those assumed in the CSD [52] and PLATON [53] and are used as the benchmark in the

identification of Se \cdots N interactions in **1-142** and in the discussion of congeners of these. This is not to imply a stabilising contact can not occur beyond the assumed van der Waals separations. Indeed, the contrary is true, there being several discussions on this point [48, 51, 59-62]. Reflecting this, in the following descriptions, interactions beyond the van der Waals radii are also discussed but the basic database of 142 aggregates is established on the basis of the benchmark van der Waals radii. The application of the above criteria ensures a focus upon stronger, structure-directing Se \cdots N interactions.

3.1 Two-molecule aggregates featuring one Se \cdots N interaction

In seven crystals of mononuclear selenium(II) compounds zero-dimensional assemblies are formed mediated by a single Se \cdots N secondary-bonding interaction. The chemical diagrams for the interacting species in **1-7** [63-68] are given in Fig. 2. In this diagram and throughout, only the interacting species are shown with full details of the composition for the respective crystals given in the Tables comprising Appendix A, in this case Table S1. Key geometric details and citation details for **1-7** are presented in Table 1.

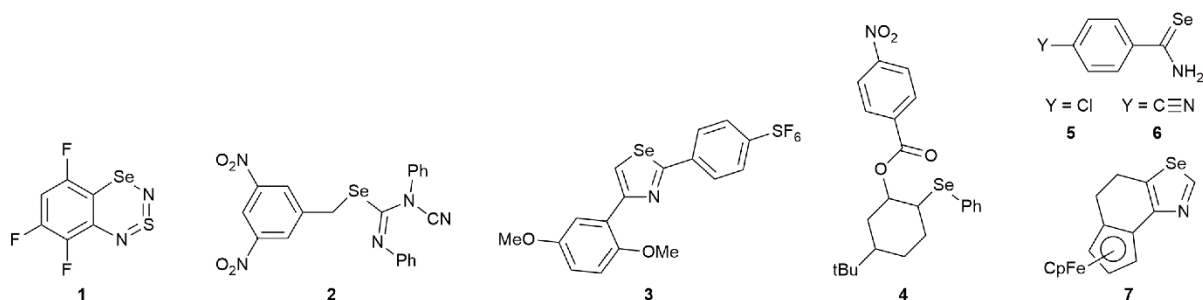


Fig. 2. Chemical diagrams for the interacting species in crystals **1-7** containing selenium(II) compounds featuring a single Se \cdots N contact leading to a zero-dimensional aggregate.

Despite there being only seven examples in this section, there is a wide variety of structural features which make this section a microcosm for subsequent sections. Crystals of

1, where the selenium(II) atom is encompassed within a six-membered hetero-ring, feature four independent formula units in the unit-cell and two pairs are connected via a single Se \cdots N chalcogen bond. Fig. 3a shows one pair of interacting molecules being representative of the second pair. The orientation of the molecular pair in the crystal of **1** is such to place nitrogen and sulphur atoms derived from adjacent six-membered rings in close proximity but the separations between them, that is, 3.456(6) and 3.533(6) Å, are outside the sum of their van der Waals radii [63]. It must be both acknowledged and appreciated interactions do not become negligible beyond van der Waals sums and hence, mention will be made of longer contacts when relevant to the discussion (see discussion above). A recurring theme is noted here in that the Se \cdots N interaction often occurs within a close to linear arrangement, Table 1. In this case, the C–Se \cdots N angles for the independent aggregates are 173.0(2)° for that shown in Fig. 3a and 171.3(2)° for the second pair.

Table 1Geometric (Å, °) details for aggregates in **1-7** which form zero-dimensional aggregates in their crystals mediated by a single Se···N interaction

Aggregate	Se···N (Å)	%(d/vdW) ^a (Å)	C–Se···N (°)	X / X–Se···N (°)	Y–N···Se (°)	Z / Z–N···Se (°)	REFCODE	Ref.
1	3.030(6)	87.8	173.0(2)	N / 76.4(2)	Se / 114.2(2)	S / 120.8(3)	EWACOV	[63]
	3.077(6)	89.2	171.3(2)	N / 76.5(2)	Se / 114.2(2)	S / 121.5(3)		
2	3.299(2)	95.6	171.03(7)	(C)C / 76.19(8)	C / 137.03(13)		YIPXUS	[64]
3	3.366(3)	97.6	142.69(13)	C / 111.39(13)	C / 102.6(2)	C / 102.5(2)	DIZTAJ	[65]
4	3.385(2)	98.1	140.78(9)	C / 116.51(9)	O / 90.84(14)	C / 85.13(13)	IGACUO	[66]
					O / 93.26(14)			
5	3.392(10)	98.3	146.1(4)		C / 123.5(7)	H / 69 & 113	BOPGOD	[67]
6	3.430(12)	99.4	82.8(4)		C / 118.8(8)	H / 50 & 113	BOPGAP	[67]
7	3.449(10)	100.0	165.4(3)	N / 84.6(4)	Se / 99.1(3)	N / 147.9(7)	SICMUP	[68]

^a %(d/vdW) = [d(Se···N)/3.45] × 100

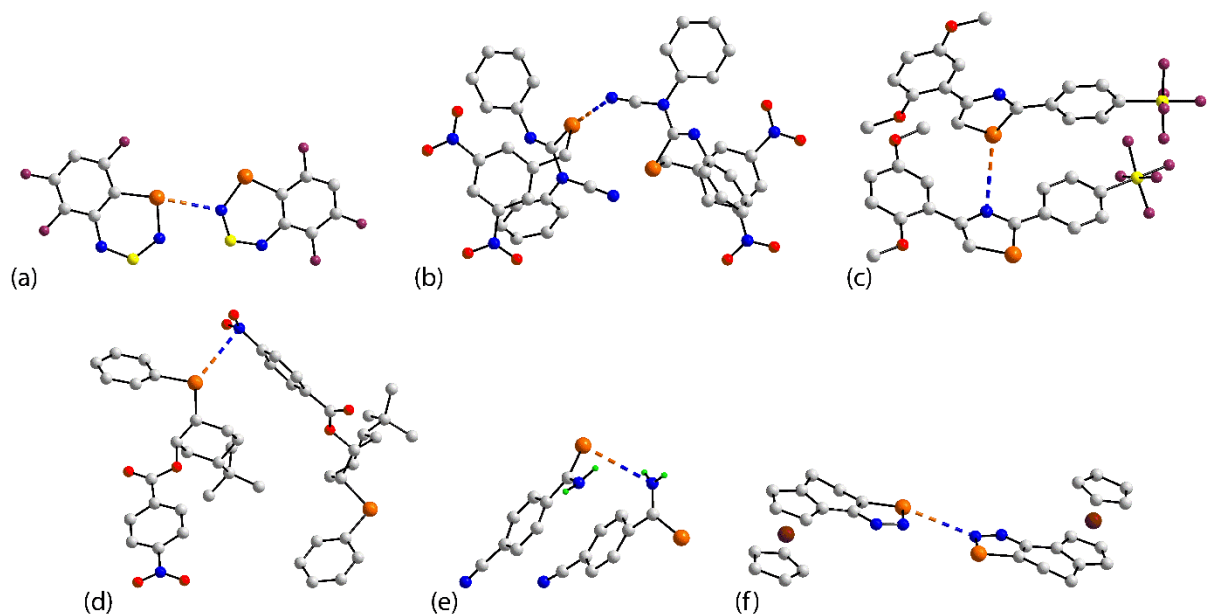


Fig. 3. Diagrams highlighting the formation of zero-dimensional aggregates featuring a single $\text{Se}\cdots\text{N}$ secondary-bonding interaction in crystals containing: (a) **1**, (b) **2**, (c) **3**, (d) **4**, (e) **6** and (f) **7**. Additional colour codes: iron (brown), sulphur (yellow) and fluoride (plum).

The common feature of the contacts formed in the crystals of **2-6** is that the $\text{Se}\cdots\text{N}$ interaction occurs between the two molecules comprising the crystallographic asymmetric-unit. Crystal **2** [64] manifests a contact involving diorganoselenium(II) and nitrile-nitrogen atoms, Fig. 3b, and in **3** [65], Fig. 3c, atoms within five-membered rings. In the latter case, the $\text{C}-\text{Se}\cdots\text{N}$ angle is contracted to $142.69(13)^\circ$, reflecting the constraints of the ring.

While the preceding examples can be classified as instances of $\text{Se}\cdots\text{N}$ contacts involving σ -hole interactions, in the crystal of **4** [66], Fig. 3d, this interaction can be classified a π -hole interaction as the selenium atom occupies a position almost plumb to the CO_2 -donor set about the nitrogen atom, Table 1. The selenide derivatives in each of **5** and **6** [67] contain hydrogen-bonding functionality with each amine-H atom forming a $\text{N}-\text{H}\cdots\text{Se}$ hydrogen-bond with a symmetry related selenium atom resulting in approximately trigonal-planar geometries for the nitrogen atoms. Based on angle considerations, the $\text{Se}\cdots\text{N}$ interactions for each of **5** and **6**

appears to be a π -hole interaction, as illustrated for the latter in Fig. 3e. The selenium atoms in **5** and **6**, being sp^2 hybridised adopt a more side-on approach to the nitrogen atoms. The final structure in this section, that is **7** [68], provides a convenient segue to the next section. There are four independent molecules in the asymmetric-unit and as for **1**, each participates in a $Se\cdots N$ interaction. As shown in Fig. 3f, one pair of molecules are connected by a single $Se\cdots N$ interaction. Despite the molecules being orientated to allow a complimentary $Se\cdots N$ interaction, the separation of 3.571(11) Å is outside the search criteria. Of the two remaining molecules, one does not form an equivalent $Se\cdots N$ interaction while the fourth independent molecule self-associates about a centre of inversion to form a dimer as discussed below for aggregate **45**.

3.2 Two-molecule aggregates featuring two $Se\cdots N$ interactions: selenadiazole rings

There is a total of 29 zero-dimensional aggregates featuring two $Se\cdots N$ interactions between two selenadiazole molecules to be described in this section: the chemical diagrams for these are shown in Fig. 4 and geometric data listed in Table 2. The majority of examples have the selenadiazole molecules disposed about a centre of inversion. In four examples, that is **16** [73], **19** [73], **23** [69] and **35** [77], two independent molecules comprise the crystallographic asymmetric-unit and these are connected into a supramolecular dimer. There is a single example, that is **12** [69], where there are two independent molecules and each of these self-associates about a centre of inversion. Finally, there is one example, namely **18** [69], where three independent molecules comprise the asymmetric-unit. Two of these are connected into a supramolecular dimer with the third self-associating about a centre of inversion.

A representative example a dimer formed by a selenadiazole molecule is shown in Fig. 5a, for **8** [69]. As indicated in Fig. 4, this supramolecular dimer features in seven crystals but, this is not to imply seven polymorphs. Rather this synthon is maintained in seven different co-

crystals where the co-former is usually a potential hydrogen bond donor. In the illustrated dimer of Fig. 5a, the co-crystallised iodine molecule forms I \cdots N halogen bonds with the nitrogen atoms not participating in the formation of the {SnN \cdots }₂ synthon, to form a four-molecule aggregate. In Fig. 5b, showing the dimer formed in the crystal of **9** [70], the {SnN \cdots }₂ synthon persists despite the steric demands of the remote substituents on the selenadiazole. There are several other closely related structures included in this section, Fig. 4, and these molecules feature prominently in the discussion of congeners of **1-142**, see section 4.

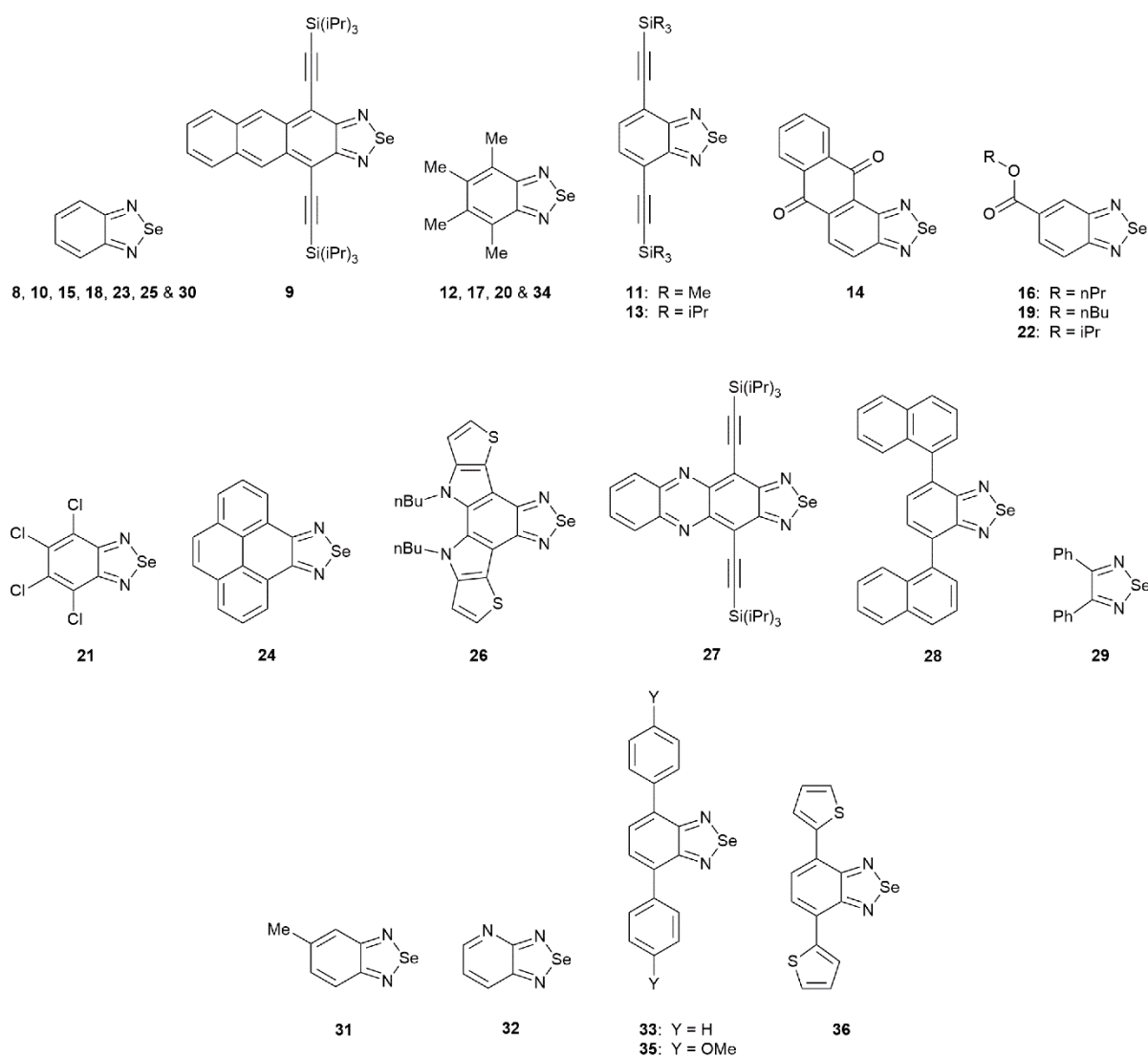


Fig. 4. Chemical diagrams for the interacting species in crystals **8-36** containing selenadiazole molecules featuring two Se \cdots N contacts leading to a zero-dimensional aggregate.

Table 2

Geometric (\AA , $^\circ$) details for aggregates in **8-36** which form zero-dimensional aggregates in their crystals mediated by two $\text{Se}\cdots\text{N}$ interactions:
selenadiazole derivatives

Aggregate	$\text{Se}\cdots\text{N}$ (\AA)	$\%(d/vdW)^a$ (\AA)	$\text{N}-\text{Se}\cdots\text{N}$ ($^\circ$)	$\text{N}-\text{Se}\cdots\text{N}$ ($^\circ$)	$\text{Se}-\text{N}\cdots\text{Se}$ ($^\circ$)	$\text{C}-\text{N}\cdots\text{Se}$ ($^\circ$)	REFCODE	Ref.
8	2.804(17)	81.3	164.5(7)	71.4(6)	108.6(7)	144(1)	GAJQUG	[69]
9	2.820(3)	81.7	168.11(10)	73.30(10)	106.70(11)	146.60(19)	BEVPOJ	[70]
10	2.8506(16)	82.6	162.45(6)	72.23(6)	107.77(7)	143.13(13)	GAJLAN	[69]
11	2.859(3)	82.9	165.72(9)	71.61(9)	108.39(10)	144.86(18)	BEVQEA	[70]
12^b	2.876(3)	83.4	167.28(10)	74.20(10)	105.80(11)	146.1(2)	GAJSOC	[69]
	2.905(3)	84.2	169.09(10)	77.55(10)	102.45(11)	149.3(2)		
13	2.877(5)	83.4	168.1(2)	74.01(18)	105.99(19)	147.2(4)	HARCOU	[71]
14^c	2.88	83.5	168.4	75.6	104.4	146.8	ANQSDZ	[72]
15	2.8911(14)	83.8	165.61(5)	73.47(5)	106.53(5)	145.89(11)	GAJRUH	[69]
16^d	2.901(5)	84.1	169.80(18)	77.44(17)	107.7(2)	141.6(4)	GASDUC	[73]
	2.970(4)	86.1	164.20(19)	72.61(17)	104.60(19)	150.7(4)		
17	2.904(4)	84.2	167.95(16)	74.05(14)	105.95(16)	147.3(3)	GAJSAO	[69]
18^e	2.905(4)	84.2	168.17(15)	74.08(16)	108.88(18)	142.6(4)	GAJQIU	[69]
	3.025(4)	87.7	164.47(16)	70.74(16)	104.20(17)	148.0(4)		

	2.922(4)	84.7	167.37(16)	73.44(15)	106.57(17)	146.3(4)		
19^d	2.910(5)	84.4	170.0(2)	74.80(18)	107.3(2)	141.9(4)	GASFEO	[73]
	2.973(5)	86.2	164.7(2)	73.24(18)	104.25(19)	151.9(4)		
20	2.9116(17)	84.4	165.74(8)	72.03(6)	107.97(7)	145.12(16)	GAJSAO01	[69]
21	2.924(3)	84.8	165.25(10)	71.05(10)	108.95(11)	144.7(2)	ACIYOD	[74]
22	2.924(2)	84.8	164.84(8)	71.25(8)	108.75(9)	143.71(17)	GASFAK	[73]
23^d	2.9255(17)	84.8	172.49(8)	78.89(8)	112.22(9)	139.99(16)	GAJROB	[69]
	3.2620(17)	94.6	163.15(8)	69.52(7)	98.92(8)	154.16(15)		
24	2.9276(17)	84.9	166.78(6)	73.90(6)	106.10(6)	146.62(12)	VIBTAD	[75]
25	2.941(3)	85.2	164.31(13)	71.12(13)	108.88(15)	143.5(3)	GAJRIV	[69]
26	2.944(2)	85.3	167.32(9)	74.32(9)	105.68(11)	147.55(19)	VEHVUC	[76]
27	2.9487(18)	85.5	157.42(8)	71.82(8)	108.18(8)	140.68(15)	BEVPID	[70]
28	2.950(6)	85.5	160.0(3)	70.3(3)	109.7(3)	143.2(6)	WUSJUR	[77]
29	2.953(8)	85.6	164.3(2)	73.12(19)	106.9(2)	145.9(4)	DPSEAZ	[78]
30	2.972(3)	86.1	164.39(11)	73.33(11)	109.97(12)	142.4(2)	GAJRER	[69]
31	2.9824(18)	86.4	170.30(7)	76.03(6)	103.97(7)	149.58(13)	ZARZEA	[79]
32	2.9918(19)	86.7	164.42(7)	71.97(7)	108.03(8)	145.62(15)	YANQOV	[80]
33	2.993(4)	86.8	170.43(19)	76.02(16)	103.78(18)	149.5(3)	SOLPIU	[81]
34	3.021(3)	87.6	163.41(9)	72.49(8)	107.51(9)	143.64(17)	GAJSIW	[69]
35^d	3.0698(18)	89.0	170.92(8)	76.42(7)	102.79(8)	150.01(15)	WUSKAY	[77]

	3.0713(19)	89.0	162.79(8)	76.42(7)	102.63(8)	149.82(15)		
36	3.424(10)	99.2	175.1(4)	82.5(4)	97.6(4)	155.3(8)	SOLPOA	[81]

a $\%(\text{d/vdW}) = [\text{d}(\text{Se}\cdots\text{N})/3.45] \times 100$

b Two independent molecules, each self-associates about a centre of inversion

c Standard uncertainty values are not available

d Two independent molecules are connected into a supramolecular dimer

e Three independent molecules, two are connected into a supramolecular dimer (first two entries) with the third self-associating about a centre of inversion

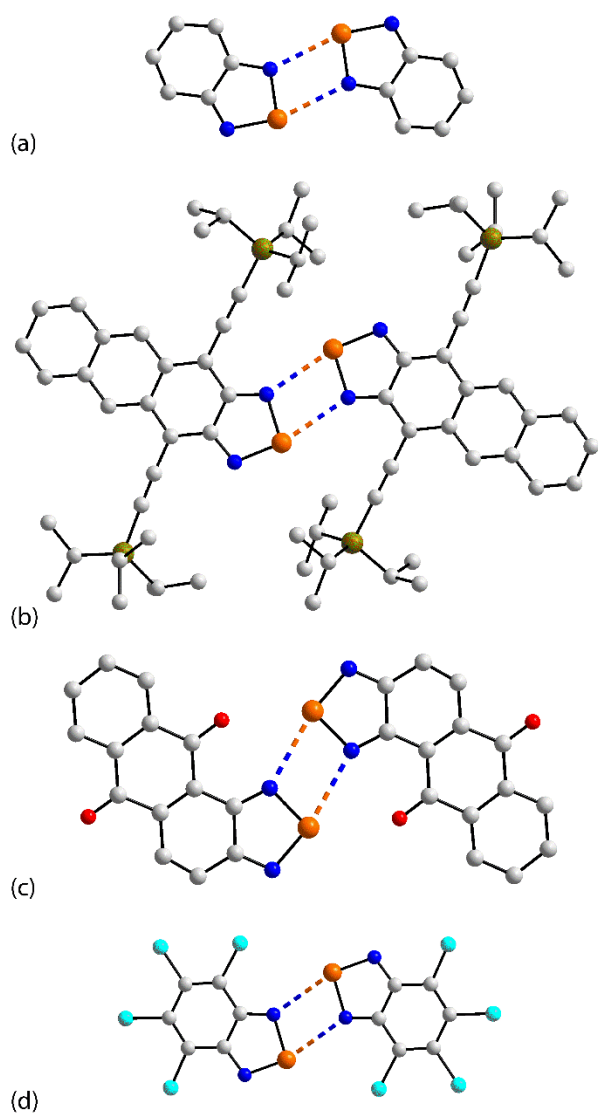


Fig. 5. Diagrams highlighting the formation of zero-dimensional aggregates featuring two $\text{Se}\cdots\text{N}$ secondary-bonding interactions in crystals containing selenadiazole molecules: (a) **8**, (b) **9**, (c) **14** and (d) **21**. Additional colour codes: silicon (dark-yellow) and chloride (cyan).

The dimer shown in Fig. 5c forms in the crystal of **14** [72] and features additional stabilisation owing to the presence of longer $\text{Se}\cdots\text{O}$ interactions (3.10 Å) in a role reversal of the aggregate shown in Fig. 1b. The robustness of the $\{\text{SnN}\cdots\}_2$ synthon is illustrated in Fig. 5d for **21** [74], that is, a perchlorinated derivative. In this instance, the dimer forms in preference to putative $\text{Se}\cdots\text{Cl}$ interactions.

In the first example of polymorphs to be described herein, **17** and **20** are polymorphic [69]. In the former, the molecule lacks crystallographically-imposed symmetry which contrasts the latter, wherein the molecule lies on a mirror plane containing the hetero-atoms comprising the fused-ring system. The same basic dimeric motif is noted in each crystal.

From the data collated in Table, it is evident the Se \cdots N interactions described in this section are of the type σ -hole as the N–Se \cdots N angles approach linearity, ranging from a low value of 157.42(8) $^\circ$, in **27**, to a wide 175.1(4) $^\circ$, in **36**. The Se \cdots N separations span a wide range, that is, from a short 2.804(17) Å in **8** to a long 3.424(10) Å in **36**. There are no obvious correlations between N–Se \cdots N angles and Se \cdots N distances, even among this relatively homogeneous series. This observation is borne out by the parameters associated with the dimer formed between the independent molecules in the crystal of **35**. Here, both Se \cdots N separations are 3.07 Å and yet the N–Se \cdots N angles vary by over 8 $^\circ$. This lack of correlation is to be expected owing to the various substitution patterns around participating atoms, differences in experimental conditions of the X-ray experiments, etc.

3.3 Two-molecule aggregates featuring two Se \cdots N interactions: non-selenadiazole rings

In this section, aggregates featuring Sn \cdots N interactions leading to two-molecule aggregates formed by non-selenadiazole derivatives are summarised. Clearly, a greater diversity of chemical species and synthons are described compared to the homogeneity of the previous section (3.2). The chemical diagrams for **37-53** are shown in Fig. 5 and pertinent data are included in Table 3.

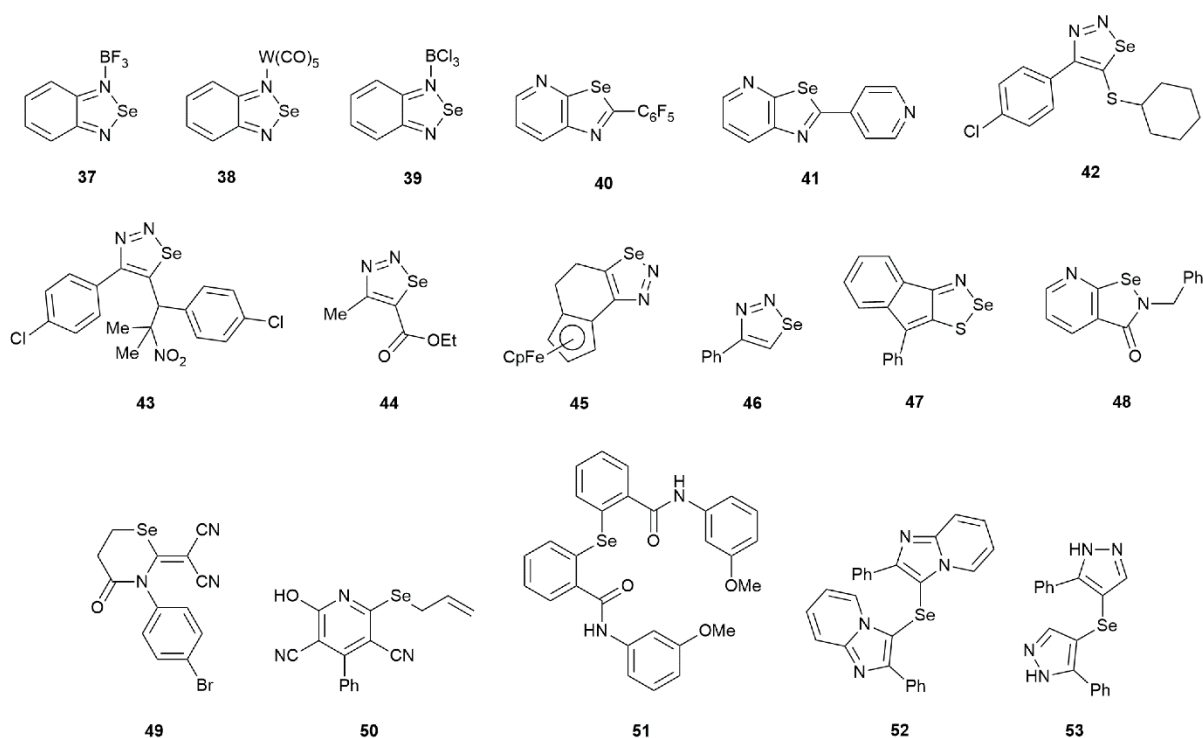


Fig. 6. Chemical diagrams for the interacting species in crystals **37-53**, containing non-selenadiazole derivatives featuring two $\text{Se}\cdots\text{N}$ contacts leading to a zero-dimensional aggregate.

With six exceptions, all two-molecule aggregates are situated about a centre of inversion in a crystal where one selenium-containing molecule comprises the asymmetric-unit. In **39** [82], where the fused-ring system is located on a mirror plane, and **48** [91], the aggregate has 2-fold symmetry. In the crystal of **41** [85], two independent molecules comprise the asymmetric-unit and one of these self-associates about a centre of inversion to form the aggregate. As mentioned above for aggregate **7**, the crystal comprises four independent molecules. Two of these associate via a single interaction as shown in Fig. 3f, whereas the two-molecule aggregate in **45** [68] is disposed about a centre of inversion like most aggregates in this section; the fourth independent molecule does not form equivalent $\text{Se}\cdots\text{N}$ interactions. In **51** [94], the two crystallographically-independent molecules associate to form the dimer with two distinct $\text{Se}\cdots\text{N}$ contacts. Finally, for **53** [96], there are four selenium-containing

molecules as shown for the tautomer in Fig. 6, four molecules of a second tautomer, whereby the nitrogen-bound hydrogen atom has migrated to the second nitrogen in one of the rings, and two ethanol molecules of solvation. Only one of the four original tautomers (shown in Fig. 6) forms Se \cdots N contacts to form a centrosymmetric dimer.

In each of **37** [82], **38** [83], shown in Fig. 7a, and **39** [82], the familiar four-membered {SeN \cdots }₂ synthon noted in the previous section (3.2) sustains the two-molecule aggregate, despite the presence of substituents on the non-participating nitrogen atoms; the molecule in **39** has mirror symmetry encompassing the fused-ring system. The molecules in **40** [84] and **41** [85] feature pyridyl-nitrogen atoms in the six-membered ring fused to the selenadiazole ring. In this case, the Se \cdots N interactions involve the pyridyl-nitrogen atoms and lead to the formation of six-membered {SeCN \cdots }₂ synthons, as shown in Fig. 7b for **41**. It is notable that in **41** an appended pyridyl substituent is also available for interaction but it does not do so. The next five crystals, that is, **42** [86], **43** [87], **44** [88], Fig. 7c, **45** [68] and **46** [89] feature 1,2,3-selenadiazole rings and form centrosymmetric dimers via {SeN \cdots }₂ synthons. In **47** [90], two 1,2,3-thiaselenaazole rings associate about a centre of inversion to form the {SeN \cdots }₂ synthon, as illustrated in Fig. 7d.

Table 3

Geometric (\AA , $^\circ$) details for aggregates in **37-53** which form zero-dimensional aggregates in their crystals mediated by two $\text{Se}\cdots\text{N}$ interactions:

non-selenadiazole derivatives

Aggregate	$\text{Se}\cdots\text{N}$ (\AA)	$\%(\text{d}/\text{vdW})^a$ (\AA)	W / W– $\text{Se}\cdots\text{N}$ ($^\circ$)	X / X– $\text{Se}\cdots\text{N}$ ($^\circ$)	Y / Y–N $\cdots\text{Se}$ ($^\circ$)	Z / Z–N $\cdots\text{Se}$ ($^\circ$)	REFCODE	Ref.
37	2.7851(18)	80.7	N / 162.63(7)	N / 72.46(7)	Se / 107.54(7)	C / 142.44(14)	QIBROL	[82]
38	2.823(6)	81.8	N / 162.2(2)	N / 70.5(2)	Se / 109.5(3)	C / 142.1(5)	DEXTEI	[83]
39	2.8644(8)	83.0	N / 165.31(4)	N / 74.66(4)	Se / 105.34(5)	C / 142.21(7)	QIBREB	[82]
40	2.964(5)	85.9	C / 175.17(17)	C / 91.72(17)	Se(C) / 143.8(4)	C / 101.2(4)	BEYJEX	[84]
41	3.294(5)	95.5	C / 156.93(16)	C / 88.68(17)	Se(C) / 143.1(3)	C / 96.3(3)	WUMCIT	[85]
42	3.034(4)	87.9	C / 152.24(12)	N / 66.74(12)	Se / 113.26(14)	N / 135.1(2)	PIWCEE	[86]
43	3.0946(8)	89.7	C / 154.33(3)	N / 73.76(3)	Se / 106.24(4)	N / 138.95(6)	SITJAH	[87]
44	3.137(4)	90.9	C / 154.68(14)	N / 68.45(14)	Se / 111.55(16)	N / 137.3(3)	TITDEG	[88]
45	3.292(11)	95.4	C / 160.9(4)	N / 75.4(4)	Se / 104.6(5)	N / 144.5(8)	SICMUP	[68]
46	3.379(5)	97.9	C / 166.88(18)	N / 92.07(16)	Se / 87.93(15)	N / 157.7(4)	DANJIM	[89]
47	2.7303(17)	79.1	S / 166.65(4)	N / 73.81(7)	Se / 106.19(8)	C / 138.68(14)	DESFAL	[90]
48	2.5845(17)	74.9	N / 169.24(7)	C / 88.85(8)	C / 109.02(14)	C / 128.22(14)	BAHBOD	[91]
49	3.119(4)	90.4	C / 158.08(12)	C / 77.21(14)	C / 119.8(3)		LEYZUL	[92]
50	3.371(12)	97.7	C / 172.8(3)	C / 75.7(3)	C / 118.6(8)		HAWZUA	[93]

51 ^b	3.373(7)	97.8	C / 116.1(2)	C / 124.9(3)	(O)C / 98.4(4)	C / 108.0(4)	ZEGHEA	[94]
					H / 61			
	3.422(7)	99.2	C / 114.3(3)	C / 125.6(2)	(O)C / 99.1(4)	C / 107.4(4)		
					H / 59			
52	3.403(3)	98.6	C / 158.66(9)	C / 96.41(9)	(Se)C / 89.87(15)(N)C / 94.39(19)		NUXRIK	[95]
					C / 87.20(19)			
53 ^b	3.307(4)	95.9	C / 154.27(14)	C / 78.82(13)	N / 82.5(2)	C / 107.0(3)	VADVIH	[96]
	3.407(4)	98.8	C / 173.66(14)	C / 78.87(13)	N / 74.3(3)	C / 107.5(3)		

$$a \%(\text{d}/\text{vdW}) = [\text{d}(\text{Se}\cdots\text{N})/3.45] \times 100$$

b Two independent molecules are connected into a supramolecular dimer

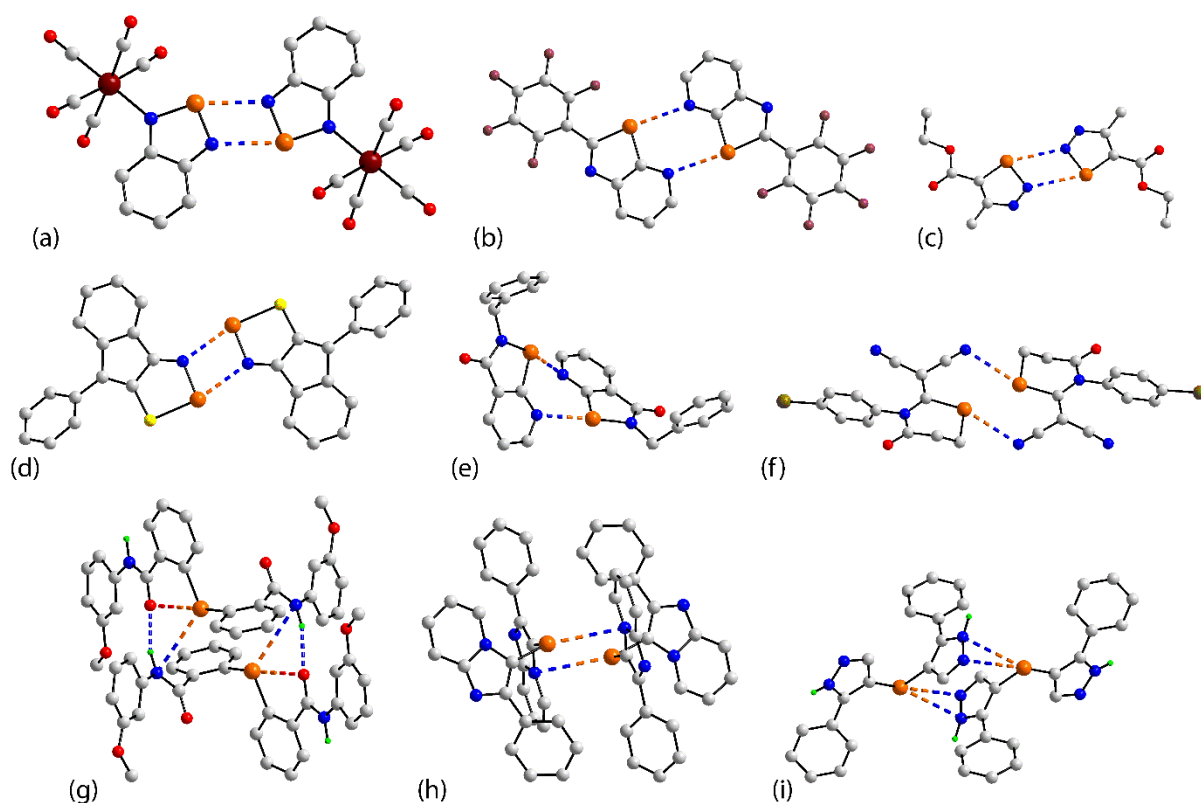


Fig. 7. Diagrams highlighting the formation of zero-dimensional aggregates featuring two $\text{Se}\cdots\text{N}$ secondary-bonding interactions in crystals containing other than selenadiazole molecules: (a) **38**, (b) **41**, (c) **44**, (d) **47**, (e) **48**, (f) **49**, (g) **52**, (h) **52** and (i) **53**. Additional colour codes: tungsten (brown) and bromide (dark-yellow). The intramolecular $\text{Se}\cdots\text{O}$ interaction in (g) is represented by a red-orange dashed line.

Molecules having a 1,2-selenazole ring bearing a carbonyl group, as in **48** [91], have been noted previously to have a high propensity to form intermolecular $\text{Se}\cdots\text{O}$ chalcogen-bonding interactions [50]. Indeed, where such $\text{Se}\cdots\text{O}$ chalcogen-bonding can potentially occur, they do in 48% cases which nearly matches with the 50% adoption of $\text{Se}\cdots\text{O}$ interactions in all selenium-containing molecules also featuring a carbonyl group [50]. In **48**, the $\text{Se}\cdots\text{N}$ interaction involves the participation of a pyridyl-nitrogen atom and gives rise to a six-membered $\{\text{SeCN}\cdots\}_2$ synthon disposed about a 2-fold axis of symmetry as seen in Fig. 7e. A larger supramolecular synthon, that is, a 10-membered $\{\text{SeC}_3\text{N}\cdots\}_2$ synthon is seen in the

crystals of **49** [92] and **50** [93] with the former highlighted in Fig. 7f. In each centrosymmetric aggregate, the nitrogen donor to the diorganoselenium(II) centre is a nitrile-nitrogen atom with the transannular Se \cdots Se separation within each dimer being 3.7828(7) and 3.730(14) Å, each value under the sum of the van der Waals radii for selenium (3.80 Å) [52]. In the crystals of **51** [94] and **52** [95] Se \cdots N π -hole interactions are apparent with the ensuing two-molecule aggregates shown in Fig. 7g and 7i, respectively. The aggregate in **51**, an acyclic diorganoselenium(II) species, also features intramolecular Se \cdots O [2.704(6) and 2.721(6) Å] interactions in each of the independent molecules forming the aggregate. Encompassing the core are conventional amine-N–H \cdots O(carbonyl) hydrogen bonds which lead to a pair of four-membered { \cdots Se \cdots NH \cdots O} synthons which serve to emphasise the cooperative nature of different intermolecular interactions in sustaining supramolecular aggregates [5]. In **51**, the participating nitrogen atom is an amine-nitrogen while that in **52**, also an acyclic species, is an imine-nitrogen atom. In the last aggregate to be described in this section, namely **53** [96], for which the asymmetric-unit is rather complex, as described above, one of the tautomers self-associates about a centre of inversion with the distinctive feature setting this aggregate apart from the aforementioned being the formation of two Se \cdots N π -hole interactions per acyclic diorganoselenium atom. As the two independent Se \cdots N separations differ by about 0.1 Å, the interaction might be better described as a semi-localised interaction [97], occurring between the selenium and the nitrogen atoms connected by a bond having some π -electron density, that is, Se $\cdots\pi$ (NN).

3.4 Higher nuclearity, zero-dimensional aggregates featuring two or more Se \cdots N interactions

Whereas in sections 3.2 and 3.3, two-molecule aggregates were summarised, in this section, higher-nuclearity, zero-dimensional aggregates are described. The chemical diagrams

for the three molecules in this section are shown in Fig. 8 with selected geometric data summarised in Table 4.

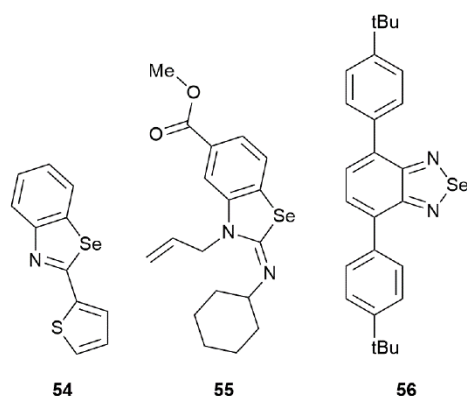


Fig. 8. Chemical diagrams for the interacting species in crystals **54-56**, featuring two or more $\text{Se}\cdots\text{N}$ contacts leading to zero-dimensional aggregates.

Despite there being only three examples in this section, there are three distinct aggregation patterns. A three-molecule aggregate is noted in the crystal of **54** [98]. Here, there are three independent molecules in the asymmetric-unit. The selenium atom of one of these, incorporated within a five-membered, 1,3-selenazole ring, forms contacts with the nitrogen atom of each of the other two molecules to form the aggregate shown in Fig. 9a. Four molecule aggregates are formed in the crystals of **55** [99] and **56** [100]. In the former, four, 3-selenazole derivatives assemble about a site of crystallographic symmetry $\bar{4}$ with the $\text{Se}\cdots\text{N}$ interactions being of the type π -hole. While the shape of the aggregate in **55**, Fig. 9b, is approximately that of a sphere, the four-molecule aggregate in **56** is an isolated zig-zag chain, Fig. 9c. The core of the chain in **56** is a centrosymmetric $\{\text{SeN}\cdots\}_2$ synthon, as noted for the 1,2,5-selenadiazole examples described in section 3.2, and appended to the core at either side are two additional molecules, via analogous $\{\text{SeN}\cdots\}_2$ synthons.

Table 4

Geometric (\AA , $^\circ$) details for aggregates in **54-56** which form zero-dimensional aggregates in their crystals mediated by two or more $\text{Se}\cdots\text{N}$ interactions

Aggregate	$\text{Se}\cdots\text{N}$ (\AA)	$\%(\text{d}/\text{vdW})^a$ (\AA)	X / W– $\text{Se}\cdots\text{N}$ ($^\circ$)	Y / X– $\text{Se}\cdots\text{N}$ ($^\circ$)	Z / Y–N $\cdots\text{Se}$ ($^\circ$)	C–N $\cdots\text{Se}$ ($^\circ$)	REFCODE	Ref.
54 ^b	3.217(15)	93.3	C / 166.4(3)	C / 84.5(4)	C / 109.0(9)	109(1)	OLUQOD	[98]
	3.423(15)	99.2	C / 159.2(4)	C / 117.2(3)	C / 108(1)	131(1)		
55	3.4102(19)	98.9	C / 162.24(7)	C / 110.01(8)	C / 87.05(11)	89.88(12)	JEWTEEN	[99]
				C / 97.13(12)				
56 ^c	2.959(3)	85.8	N / 77.10(10)	N / 177.07(9)	Se / 102.92(11)	C / 150.2(2)	SAYKIN	[100]
	2.977(3)	86.3	N / 74.48(10)	N / 168.74(10)	Se / 116.50(11)	C / 128.3(2)		
	3.430(3)	99.4	N / 62.05(9)	N / 129.77(10)	Se / 98.42(10)	C / 150.60(19)		

$$a \ \%(\text{d}/\text{vdW}) = [\text{d}(\text{Se}\cdots\text{N})/3.45] \times 100$$

b Three independent molecules are connected into a three-molecule aggregate with one selenium atom forming contacts to nitrogen atoms of the other two molecules

c Two independent molecules. The first entry is for the contacts defining the centrosymmetric core.

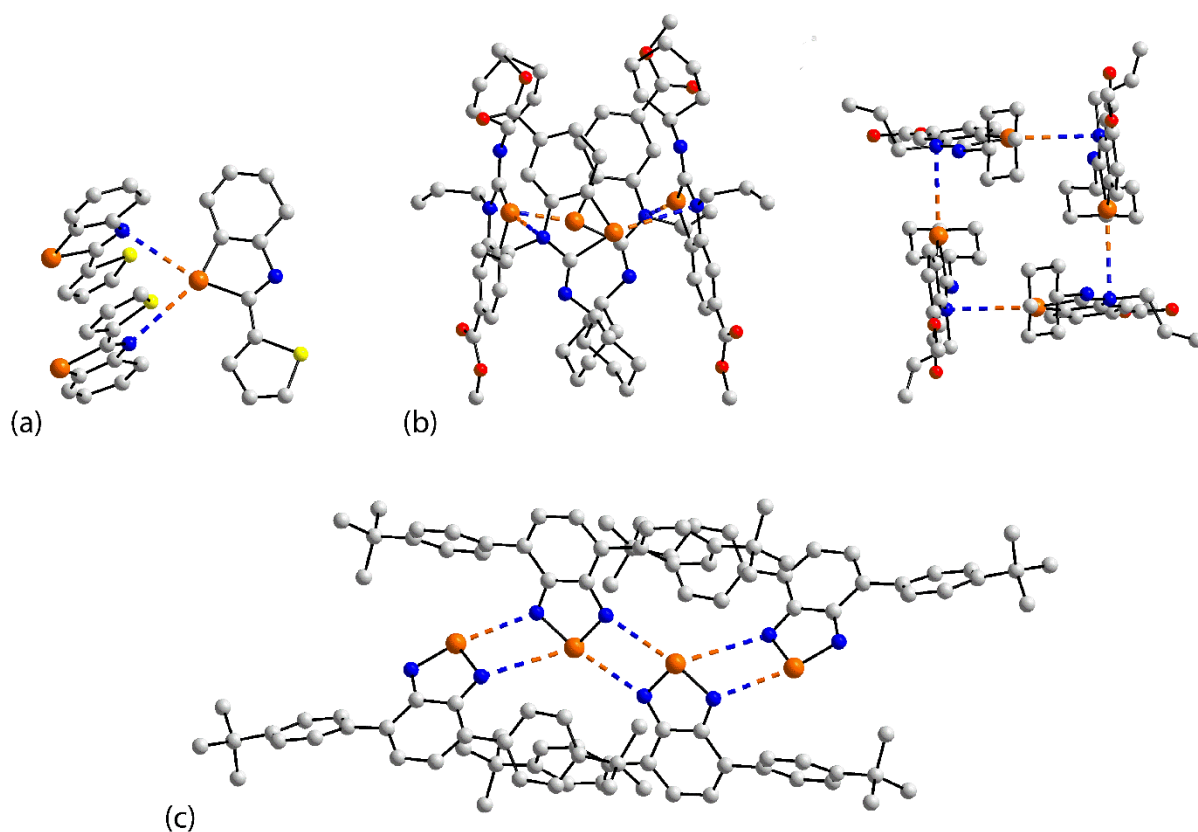


Fig. 9. Diagrams highlighting the formation of zero-dimensional aggregates featuring Se...N secondary-bonding interactions in crystals: (a) **54**, (b) **55** (side- and end-on views) and (c) **56**.

3.5 Linear chains featuring Se...N interactions

Fourteen aggregates included in this survey are one-dimensional chains with a linear topology: chemical diagrams for the interacting species and geometric data are given in Fig. 10 and Table 5, respectively.

Four organoselenium cyanate species, namely **57** [101], **58** [102] **59** [103] and **60** [102] adopt simple linear assemblies in their crystals mediated by Se...N secondary-bonding interactions, as exemplified in Fig. 11a for **59**. Of interest is the observation the asymmetric-unit of **57** comprises two independent molecules and that each assembles into a linear chain. Further Se...N connections are evident for the second independent chain which leads to supramolecular tapes as discussed below for aggregate **112**. Crystals **59** and **60** are polymorphic.

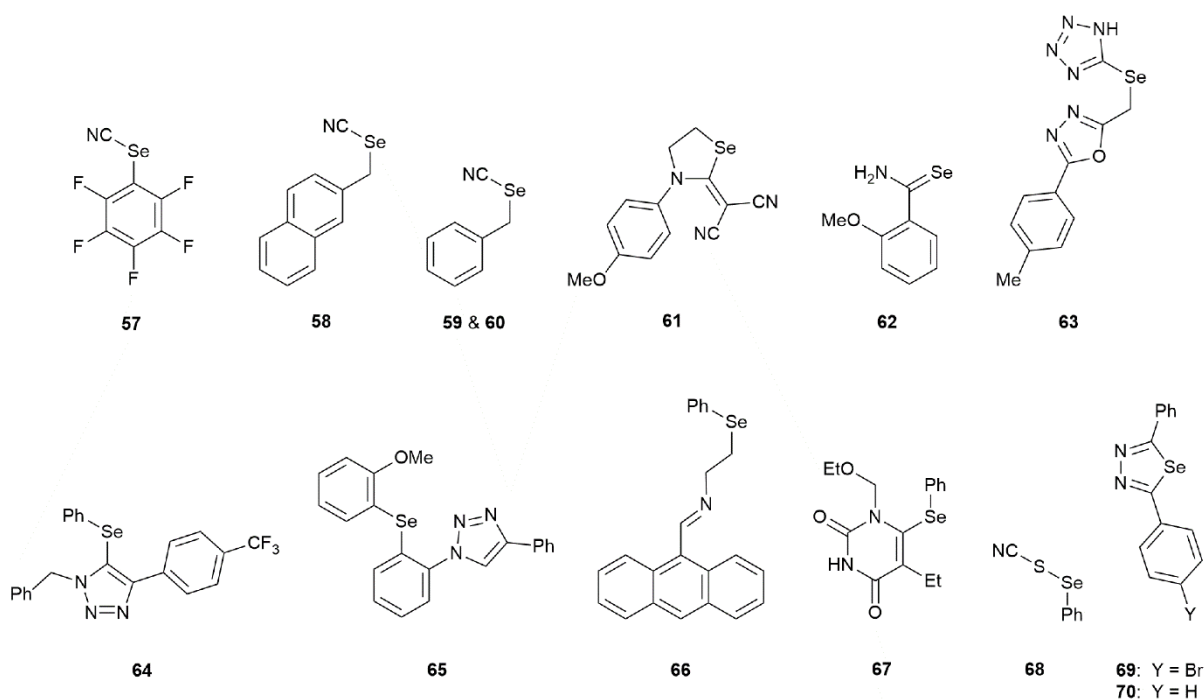


Fig. 10. Chemical diagrams for the interacting species in crystals **57-70**, featuring $\text{Se}\cdots\text{N}$ contacts leading to one-dimensional chains with a linear topology.

While the aforementioned assemblies feature acyclic centres, selenium incorporated within a five-membered ring features in the linear chain formed in the crystal of **61** [103], see Fig. 11b. The supramolecular chain of crystal of **62** [104] is cause for special comment, see Fig. 11c. First and foremost, the selenium atom is well separated from the acidic hydrogen atoms with the closest $\text{Se}\cdots\text{H}$ separation of 2.72 Å associated with the hydrogen atom forming the short intramolecular $\text{N}-\text{H}\cdots\text{O}$ hydrogen bond of 2.04 Å. The second hydrogen atom is even further away, at 3.32 Å, but forms a $\text{N}-\text{H}\cdots\text{Se}$ hydrogen bond with a centrosymmetrically-related selenium atom. Under these, circumstances, with a well-defined geometry for the nitrogen atom, a $\text{Se}\cdots\text{N}$ π -hole type interaction might be anticipated but, based on the angle data in Table 5, this is likely not the case, indicating a detailed theoretical analysis is required to delineate the nature of the bonding in this species.

Table 5Geometric (\AA , $^\circ$) details for aggregates in **57-70** which form linear chains in their crystals mediated by $\text{Se}\cdots\text{N}$ interactions

Aggregate	$\text{Se}\cdots\text{N}$ (\AA)	$\%(\text{d}/\text{vdW})^a$ (\AA)	W / W– $\text{Se}\cdots\text{N}$ ($^\circ$)	X / X– $\text{Se}\cdots\text{N}$ ($^\circ$)	Y / Y– $\text{N}\cdots\text{Se}$ ($^\circ$)	Z / Z– $\text{N}\cdots\text{Se}$ ($^\circ$)	REFCODE	Ref.
57	2.965(9)	85.9	(N)C / 172.1(4)	C / 78.1(3)	C / 175.6(8)		BATDIJ	[101]
58	2.995(4)	86.8	(N)C / 176.57(17)	C / 81.2(3)	C / 175.3(4)		HOFXOS	[102]
59	3.107(4)	90.1	(N)C / 167.12(15)	C / 79.92(16)	C / 167.3(3)		CIGGOO	[103]
60	3.1086(18)	90.1	(N)C / 169.11(7)	C / 80.43(7)	C / 169.22(15)		HOFXIM	[102]
61	3.0946(18)	89.7	(N)C / 162.98(6)	C / 75.86(8)	C / 176.31(15)		TEFBIQ	[103]
62	3.403(3)	98.6	C / 150.0(2)		C / 133.63(12)		BOPFUI	[104]
63	3.289(3)	95.3	(N)C / 167.96(11)	C / 74.64(10)	N / 87.95(15)	C / 141.0(2)	BAXGIT	[105]
64	3.302(2)	95.7	C / 165.52(9)	(N)C / 95.28(8)	N / 95.87(14)	C / 93.96(14)	HEMWUU	[106]
65	3.3362(19)	96.7	C / 178.96(6)	C / 84.74(6)	N / 107.19(11)	C / 118.50(11)	HUDJEX	[107]
66	3.340(5)	96.8	(Ph)C / 159.2(2)	C / 82.2(2)	(C=N) / 134.3(5)	C / 91.4(4)	VEFFOE01	[108]
67	3.411(8)	98.9	C / 169.9(4)	(N)C / 80.9(3)	C / 82.6(6)	C / 91.8(6)	CUDQOH	[109]
68	3.348(4)	97.0	C / 172.10(13)	S / 88.50(7)	C / 102.7(3)		CIBGAW	[110]
69^b	3.210(8)	93.0	C / 146.60(7)	C / 129.81(8)	C / 159.48(13)	N / 82.29(10)	FOYGUW	[111]
	3.327(6)	96.4	C / 154.53(8)	C / 121.93(7)	C / 165.30(12)	N / 72.95(10)		
70	3.250(5)	94.2	C / 151.9(2)	C / 127.3(2)	C / 168.3(4)	N / 77.7(3)	SADVUQ01	[112]

$$a \text{ \%}(d/vdW) = [d(\text{Se}\cdots\text{N})/3.45] \times 100$$

b The selenium atom forms two contacts

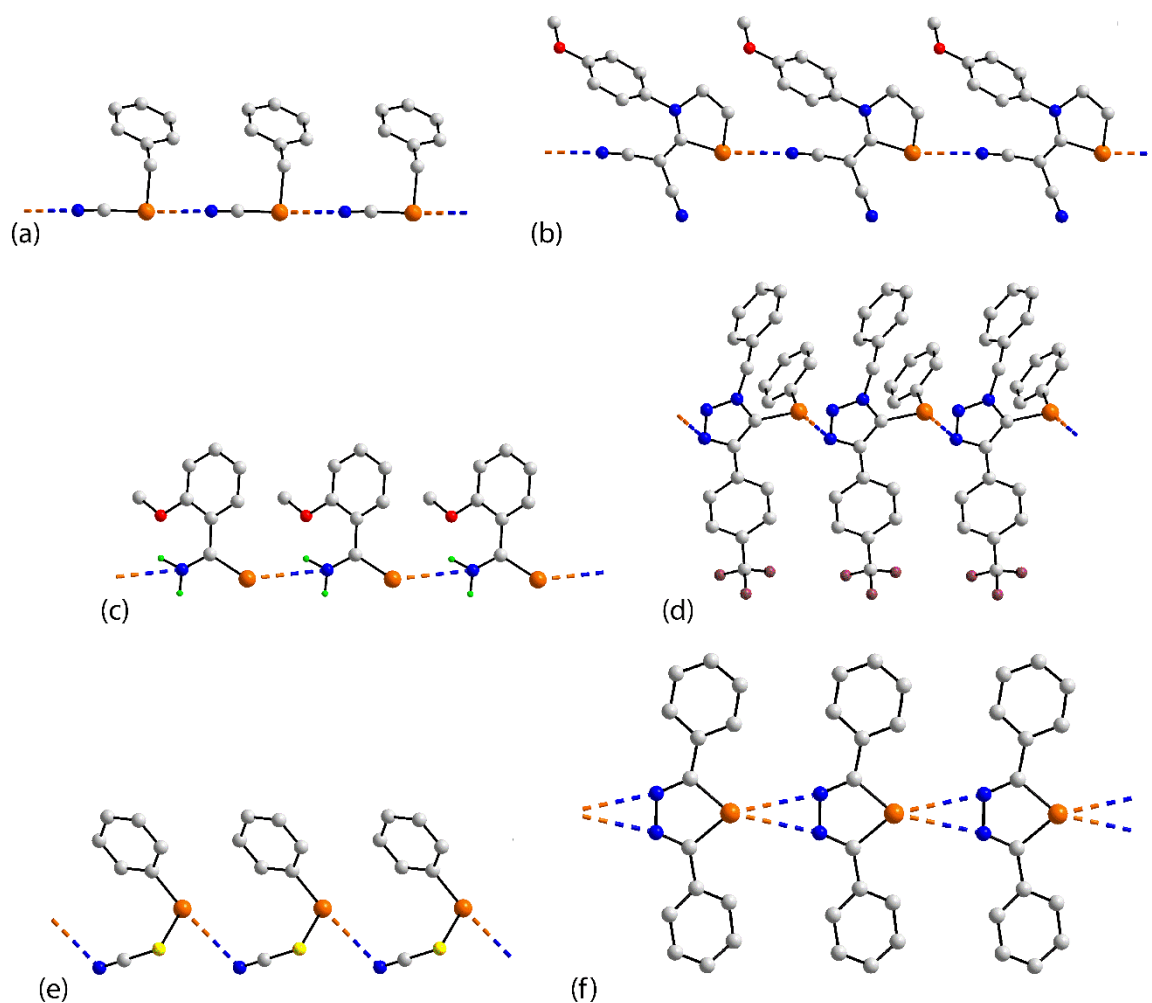


Fig. 11. Diagrams highlighting the formation of linear, supramolecular chains featuring Se \cdots N secondary-bonding interactions in crystals: (a) **59**, (b) **61**, (c) **62**, (d) **64**, (e) **68** and (f) **70**.

Selenium interacting with nitrogen atoms within five-membered rings are evident in **63** [105], **64** [106], Fig. 11d, and **65** [107], with Se \cdots N π -hole type interactions suggested for the latter two chains. In **66** [108], the contact involves an imine-nitrogen atom and in **67** [109], the Se \cdots N π -hole type interaction involves an uracil-nitrogen atom. While all preceding examples involve diorganoselenium species, in **68** [110], a bent CS donor set is apparent for selenium, with the resulting chain shown in Fig. 11e. The final two examples in this section, **69** [111] and **70** [112], Fig. 11f, see selenium forming two Se \cdots N contacts with adjacent nitrogen atoms incorporated within a 1,3,4-selenadiazole ring, resembling the situation found in the crystal of

53 [96], Fig. 7i, where a $\text{Se}\cdots\pi(\text{NN})$ was suggested based on angle considerations; **70** is situated about a 2-fold axis. The close to linear angles noted in each of **69** [111] and **70** [112], again indicate a computational chemistry study is required to understand more fully the nature of the $\text{Se}\cdots\text{N}$ interactions in these crystals.

3.6 Zig-zag chains featuring $\text{Se}\cdots\text{N}$ interactions

Complementing the linear, supramolecular chains described above in 3.5 are 18 chains with a zig-zag topology. The chemical diagrams for the interacting species in **71-88** are given in Fig. 12 and associated geometric data presented in Table 6.

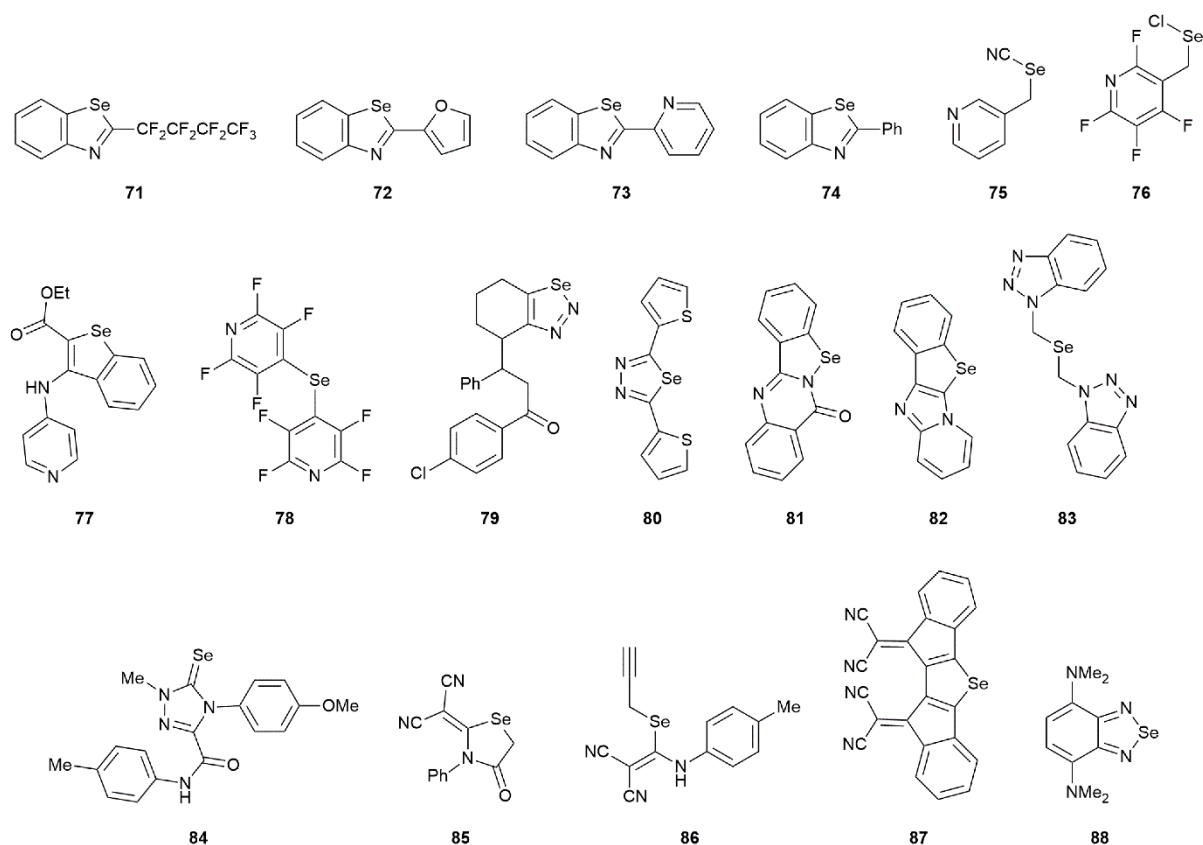


Fig. 12. Chemical diagrams for the interacting species in crystals **71-88**, featuring $\text{Se}\cdots\text{N}$ contacts leading to one-dimensional chains with a zig-zag topology.

Table 6Geometric (\AA , $^\circ$) details for aggregates in **71-88** which form zig-zag chains in their crystals mediated by Se \cdots N interactions

Aggregate	Se \cdots N (\AA)	%(d/vdW) ^a (\AA)	W / W-Se \cdots N ($^\circ$)	X / X-Se \cdots N ($^\circ$)	Y / Y-N \cdots Se ($^\circ$)	Z / Z-N \cdots Se ($^\circ$)	REFCODE	Ref.
71	3.192(6)	92.5	(N)C / 172.3(2)	C / 88.7(2)	C / 112.7(4)	C / 128.8(4)	SOCWEP	[113]
72	3.253(8)	94.3	(N)C / 171.9(3)	C / 89.4(3)	C / 116.5(6)	(Se)C / 126.0(6)	OLUGEJ	[98]
73	3.327(13)	96.4	(N)C / 166.5(6)	C / 86.1(5)	C / 109(1)	(Se)C / 119(1)	OLUFUY	[98]
74	3.355(2)	97.3	(N)C / 171.04(8)	C / 88.15(11)	(Se)C / 134.72(18)	C / 110.04(15)	OLUGAF	[98]
75	2.843(7)	82.4	(N)C / 174.0(2)	C / 91.2(2)	C / 98.0(4)	C / 144.4(5)	WERYAT	[114]
76^b	2.881(3)	83.5	Cl / 175.89(7)	C / 82.28(13)	C / 112.3(2)	C / 128.4(3)	XELBAT	[115]
	2.980(4)	86.4	Cl / 172.12(8)	C / 80.81(14)	C / 116.3(3)	C / 125.5(3)		
77	3.073(2)	89.1	C / 177.60(8)	C / 94.48(9)	C / 105.25(17)	C / 128.76(18)	NARXUB	[116]
78^b	3.146(3)	91.2	C / 171.94(10)	C / 81.61(9)	C / 108.48(18)	C / 134.52(19)	BECFUM	[117]
	3.217(3)	93.3	C / 170.79(10)	C / 74.67(11)	C / 103.96(18)	C / 138.0(2)		
79	3.141(3)	91.0	C / 166.47(10)	N / 85.92(9)	N / 104.94(18)	C / 120.67(17)	HAMKOX	[118]
80	3.433(6)	99.5	C / 150.5(2)	C / 101.1(2)	N / 104.5(4)	C / 138.2(4)	ATABAZ01	[112]
81	2.808(2)	81.4	N / 178.59(8)	C / 96.57(9)	(N)C / 108.29(16)	C / 109.68(15)	GOBYUU	[119]
82	3.1857(19)	92.3	C / 175.75(8)	(N)C / 97.15(8)	C / 112.06(14)	C / 121.33(15)	ODASEU	[120]
83	3.2941(18)	95.5	C / 166.27(7)	C / 75.46(6)	N / 147.70(13)	C / 104.25(12)	GIWRAG02	[121]

84	3.381(4)	98.0	C / 157.45(19)		N / 124.4(3)	C / 131.1(3)	MOGZOY	[122]
85	3.1452(19)	91.2	N(C) / 161.35(8)	C / 73.81(7)	C / 166.22(18)		TEFBOW	[104]
86	3.2269(16)	93.5	(H)C / 157.12(6)	C / 78.16(5)	C / 107.46(11)		BIYVUB	[123]
87	3.422(5)	99.2	C / 166.34(18)	C / 105.69(18)	C / 94.0(4)		ZEJDUQ	[124]
88^c	2.975(4)	86.2	N / 177.98(16)	N / 82.29(18)	C / 95.4(3)	C / 102.3(3)	XOQBUA	[125]
				C / 112.3(3)				
	3.249(6)	94.2	N / 153.1(2)	N / 93.9(2)	C / 91.8(4)	C / 99.0(4)		
				C / 120.3(3)				

$$a \%(\text{d/vdW}) = [d(\text{Se}\cdots\text{N})/3.45] \times 100$$

b Each of two independent molecules forms a zig-zag chain in the crystal

c The first entry gives geometric details for the zig-zag chain and the second entry for the appended molecule

The common feature of all examples in this section is the propagation of the zig-zag chain by glide symmetry. With four exceptions, all crystals comprise one independent molecule. Three crystals feature two independent molecules in the asymmetric-unit, that is, **73** [98], **76** [115] and **78** [117]. In **73** only one of the independent molecules assembles into a zig-zag chain whereas in each of **76** and **78**, each molecule self-assembles into an independent chain. The molecule in **87** [125] is disposed about a 2-fold axis of asymmetry which encompasses the selenium atom.

The first four molecules, that is, **71** [113], **72**, **73** and **74** [98], contain the 1,3-benzoselenazole five-membered ring. A representative example, namely **73**, is illustrated in Fig. 13a, in which a pendent 2-pyridyl residue is present yet, it is the ring-nitrogen of the five-membered ring that forms the Se \cdots N contact. Contrary behaviour is noted by the molecules of **75** [114], **76** [115], **77** [116] and **78** [117] where pyridyl-nitrogen atoms are also present: in each case the Se \cdots N contact involves a pyridyl-nitrogen atom. The zig-zag chain in **76** is represented in Fig. 13b and is noteworthy for having both chloride and fluoride atoms available to form secondary-bonding interactions. Regardless of there being two pyridyl-nitrogen atoms in the molecule of **78**, as opposed to one each in **75-77**, only one independent Se \cdots N interaction is evident. The nitrogen atom in the five-membered ring of the 1,2,3-selenadiazole residue in **79** [118], 1,3,4-selenadiazole in **80** [112], shown in Fig. 13c, and 1,2-selenaazole in **81** [119] interacts with a selenium atom derived from the same ring to form the chain. In **82** [120], heteroatoms from each of the fused five-membered rings form the Se \cdots N interaction. In **83** [121], the acyclic selenium atom has a geometry defined by two carbon atom and forms only one chalcogen-bond despite there being four available ring-nitrogen atoms of the two pendant 1,2,3-triazole substituents; two additional nitrogen atoms are available for putative π -hole interactions. A selenide-selenium atom comes to the fore in **84** [122] to interact with a ring-nitrogen of the 1,2,4-triazole ring. In each of **85** [104] and **86** [123], nitrile-nitrogen atoms

form the Se...N contacts with end- and side-on approaches, respectively, based on the angle data included in Table 6. The two remaining supramolecular aggregation patterns are quite distinct.

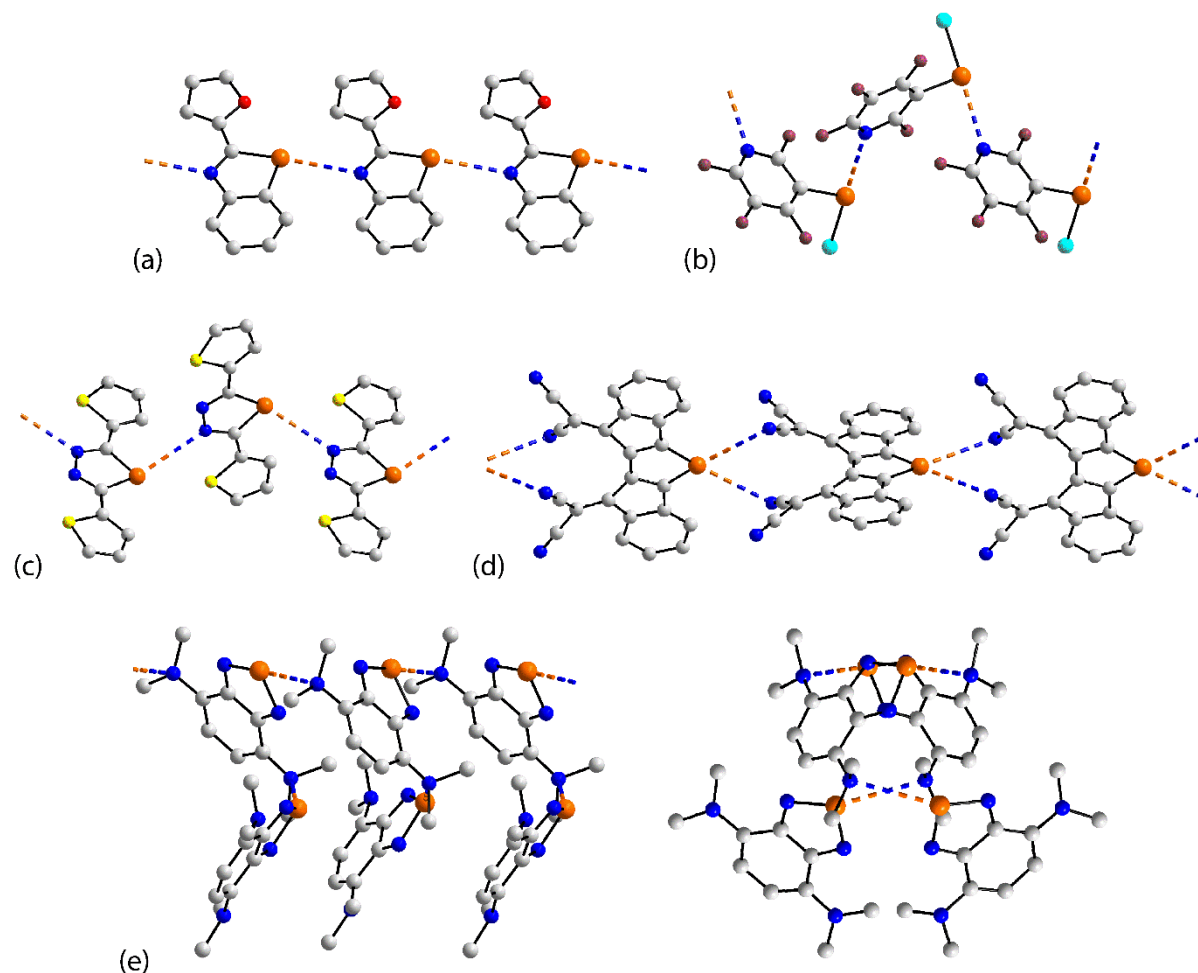


Fig. 13. Diagrams highlighting the formation of zig-zag, supramolecular chains featuring Se...N secondary-bonding interactions in crystals: (a) **73**, (b) **76**, (c) **80**, (d) **87** and (e) **88** (side- and end-on views).

In 2-fold symmetric **87** [124], the selenium atom forms two Se...N interactions, again with nitrile-nitrogen atoms to sustain the assembly shown in Fig. 13d. The most complicated architecture in this section is found in the crystal of **88** [125]. Here, one of the independent molecules, shown in the upper portions of the side- and end-on views of Fig. 13e, assembles into a zig-zag chain via Se...N interactions as seen above for the chains in **71-86** but dangling

from the chain via an additional $\text{Se}\cdots\text{N}$ contact per repeat unit is an additional molecule. As the $\text{Se}\cdots\text{N}$ interactions involve tertiary amine atoms, these are π -hole contacts as confirmed by the $\text{C}-\text{N}\cdots\text{Se}$ angle data listed in Table 6.

3.7 Helical chains featuring $\text{Se}\cdots\text{N}$ interactions

Helical, supramolecular chains are found in crystals **89-104**: the chemical diagrams for the interacting species are given in Fig. 14 and salient geometric data given in Table 7. From a crystallographic standpoint, the 16 crystals are homogeneous with a single molecule comprising the asymmetric-unit in each case and all crystals are solvent-free. The other common feature is that 2_1 -screw symmetry uniformly propagates the helical chain in each crystal.

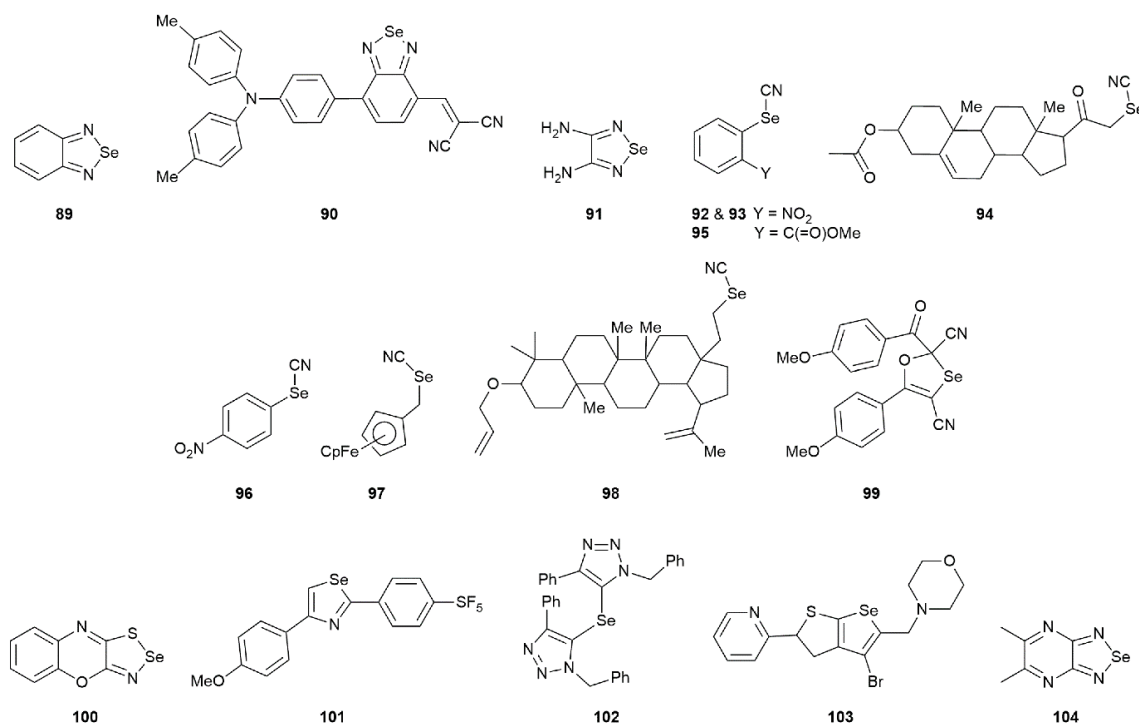


Fig. 14. Chemical diagrams for the interacting species in crystals **89-104**, featuring $\text{Se}\cdots\text{N}$ contacts leading to one-dimensional chains with a helical topology.

Table 7Geometric (\AA , $^\circ$) details for aggregates in **89-104** which form helical chains in their crystals mediated by $\text{Se}\cdots\text{N}$ interactions

Aggregate	$\text{Se}\cdots\text{N}$ (\AA)	$\%(\text{d}/\text{vdW})^a$ (\AA)	W / W– $\text{Se}\cdots\text{N}$ ($^\circ$)	X / X– $\text{Se}\cdots\text{N}$ ($^\circ$)	Y / Y– $\text{N}\cdots\text{Se}$ ($^\circ$)	Z / Z– $\text{N}\cdots\text{Se}$ ($^\circ$)	REFCODE	Ref.
89	3.155(6)	91.4	N / 169.16(11)	N / 83.9(2)	Se / 110.1(3)	C / 120.6(4)	BESEAZ01	[126]
90	3.289(3)	95.3	N / 153.76(11)	N / 103.34(12)	C / 145.0(3)		GORXAO	[127]
91	3.1289(14)	90.7	N / 163.69(5)	N / 75.25(4)	C / 150.00(10)		AHINUC	[128]
92	3.221(3)	93.4	C / 178.91(10)	(N)C / 83.10(11)	C / 130.3(3)		HEPPIE01	[129]
93	3.259(2)	94.5	C / 175.50(7)	(N)C / 81.96(8)	C / 150.77(19)		HEPPIE	[129]
94	3.260(5)	94.5	C / 165.03(12)	(N)C / 83.67(17)	C / 127.5(4)		JOHNEC	[130]
95	3.271(2)	94.8	C / 167.29(6)	C / 74.29(7)	C / 147.39(16)		AHEQIN	[131]
96	3.333(5)	96.6	C / 173.33(13)	(N)C / 76.71(15)	C / 135.2(4)		HEPPUQ	[129]
97	3.3504(19)	97.1	(N)C / 166.43(7)	C / 81.25(7)	C / 101.90(14)		SOHQOX	[132]
98	3.358(16)	97.3	(N)C / 157.9(7)	C / 96.2(5)	C / 87(1)		ZUTTAL02	[133]
99	3.4190(17)	99.1	(O)C / 159.37(6)	C / 90.72(7)	C / 98.20(13)		HOYHIP	[134]
100	2.962(3)	85.9	N / 159.87(12)	S / 71.90(6)	(S)C / 109.4(2)	C / 133.9(2)	DERQOJ	[90]
101	3.427(6)	99.3	C / 114.84(16)	C / 92.77(17)	C / 82.6(3)	C / 88.6(3)	DIZSEM	[65]
102	3.2688(16)	94.8	C / 146.87(6)	C / 113.61(5)	N / 88.36(9)	N / 158.72(11)	DOGYIK	[135]
103	3.155(5)	91.4	C / 163.6(2)	(S)C / 78.19(19)	C / 106.7(4)	C / 132.9(4)	DUBTIF	[136]

104 ^b	2.975(10)	86.2	N / 174.0(4)	N / 89.8(4)	(N)C / 102.9(7)	C / 140.8(8)	AHIKIN	[128]
	3.264(9)	94.6	N / 133.6(3)	N / 132.0(4)	C / 91.2(7)	Se / 162.3(5)		

$$a \%(\text{d/vdW}) = [\text{d}(\text{Se}\cdots\text{N})/3.45] \times 100$$

b The first entry refers to the Se \cdots N(pyridyl) interaction

Three helical chains are sustained by Se \cdots N interactions derived from selenium atoms within a 1,2,5-selenadiazole ring: **89** [126], shown in Fig. 15a, where the nitrogen atom is also contained within the ring, **90** [127], with a nitrile-nitrogen donor, and **91** [128] with an amine donor, akin to that discussed above for **62** (Fig. 11c). There are seven examples of organoselenocyanate molecules in this section, namely **92** [129], **93** [129], **94** [130], **95** [131], **96** [129], **97** [132], **98** [133] and **99** [134]. A representative helical chain is shown for **92** in Fig. 15b, which is of interest for a number of reasons. Firstly, it has a polymorph, that is, **93** which differs in the magnitude of the intramolecular Se \cdots O contact which relates to the length of the Se \cdots N contact. Thus, in **92**, Se \cdots N = 3.221(3) Å and Se \cdots O = 2.523(3) Å, values which are shorter and longer, respectively, than the equivalent separations in **93** of 3.259(2) and 2.515(2) Å. The crystal of **92** is also isostructural with the 4-nitro isomer, **96**, where no such Se \cdots O contact is apparent. Close, intramolecular Se \cdots O contacts are noted in each of **94**, **95** and **99**, see Table S8 in Appendix A for details. It is of interest to note that while the C–Se \cdots N angles in the seven organoselenocyanate structures are close to linear across the series, ranging from 157.9(7)° in **98** to 178.91(10)° in **92**, the C–N \cdots Se angles vary significantly from a low 87(1)° in **98** to 150.77(19)° in **93**, consistent with varying side- to end-on approaches, but these present no systematic trends, Table 7.

The selenium atom is incorporated within a 1,2,3-thiaselenazole ring in **100** [90] and in a 1,3-selenazole ring in **101** [66]. The interactions leading to the helical chain involve pyridyl-nitrogen atoms in **100**, Fig. 15c, and atoms comprising the five-membered ring in **101**. A symmetric, acyclic diorganoselenium atom features in **102** [135] with each organic ligand bearing a 1,2,3-triazole residue. Despite the relatively large number of nitrogen atoms, only a single Se \cdots N interaction features in the helical chain. Compound **103** [136] is a tetracyclic system with the selenium within a C₄Se five-membered ring interacting with a pyridyl-nitrogen atom within the helical chain. While the foregoing examples in this section feature a single

Se \cdots N contact per repeat unit, compound **104** [129] features two such interactions. As illustrated in Fig. 15d, the selenium atom forms a contact with a pyrazine-nitrogen atom, the shorter of the two contacts, Table 7, and also with a nitrogen atom of the 1,2,5-selenadiazole ring to form a four-membered $\{\cdots\text{Se}\cdots\text{NCN}\}$ synthon.

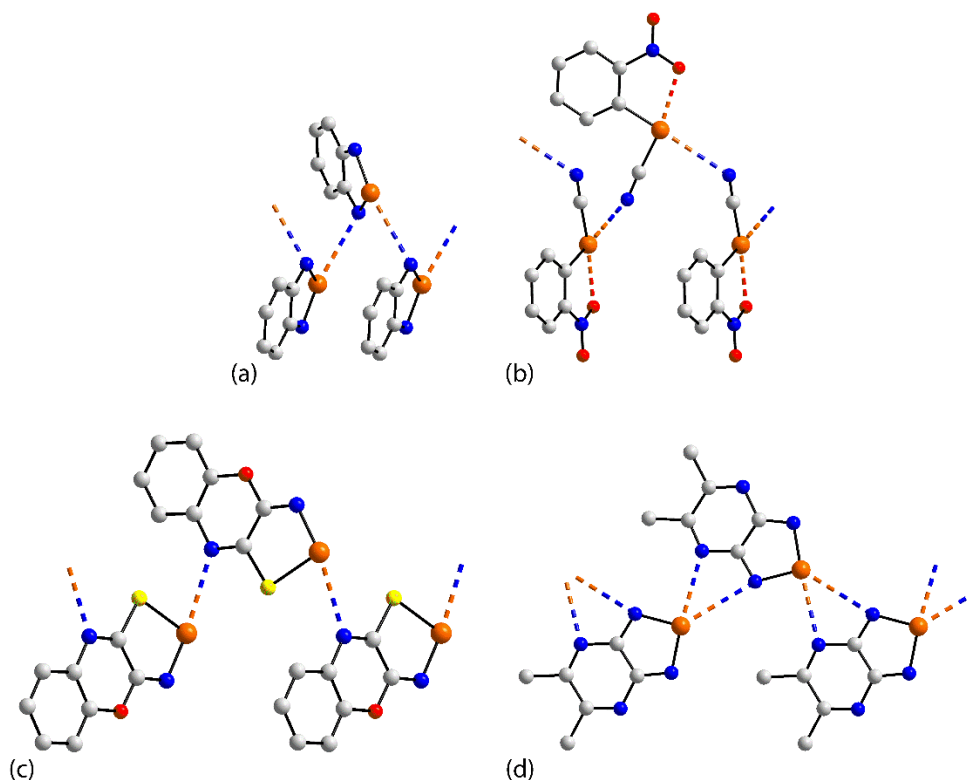


Fig. 15. Diagrams highlighting the formation of helical, supramolecular chains featuring Se \cdots N secondary-bonding interactions in crystals: (a) **89**, (b) **92**, (c) **100** and (d) **104**.

3.8 Tapes featuring Se \cdots N interactions

While the overwhelming majority of aggregation patterns described thus far, feature a single Se \cdots N interaction per selenium atom, with one or two notable exceptions, in this and the next two sections (3.9 and 3.10), the selenium atom, at a minimum, forms two Se \cdots N contacts. The chemical diagrams for **105-115** are shown in Fig. 16 with the geometric parameters summarised in Table 8.

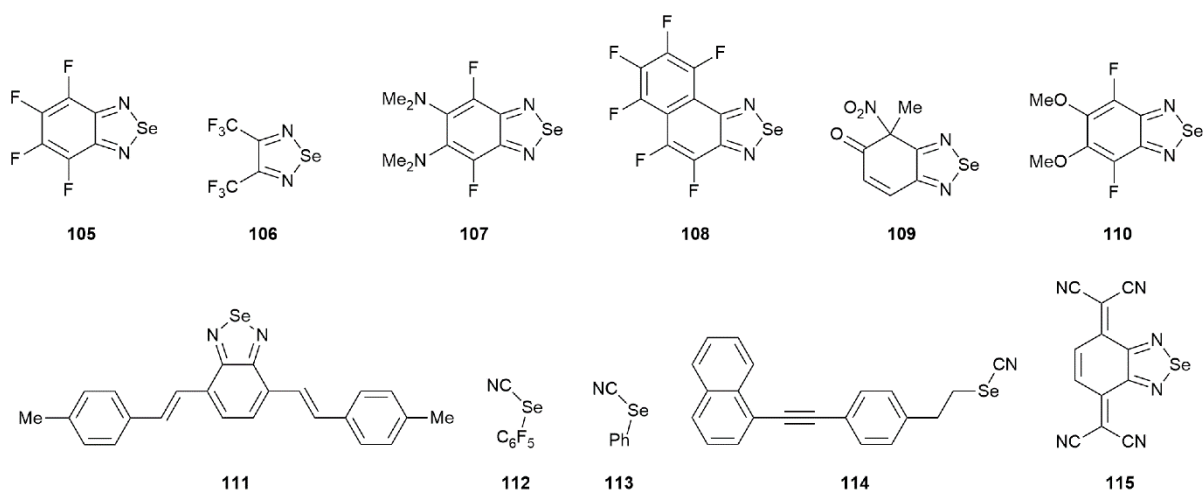


Fig. 16. Chemical diagrams for the interacting species in crystals **105-115**, featuring $\text{Se}\cdots\text{N}$ contacts leading to one-dimensional chains with a helical topology.

The first seven tapes in this section feature the now familiar 1,2,5-selenadiazole ring and a common, to a first approximation, supramolecular motif: **105** [137], **106** [138], **107** [137], **108** [139], **109** [140], **110** [137] and **111** [141]. The prototypical tape for this series is shown in Fig. 17a, for **106**. Here, molecules assemble into a tape with a zig-zag topology via a sequence of connected $\{\text{SeN}\cdots\}_2$ synthons as the selenium atom links to two nitrogen atoms of adjacent molecules and each nitrogen forms a single $\text{Se}\cdots\text{N}$ contact. The crystal of **105** is notable in having eight independent molecules in the asymmetric-unit leading to four independent tapes as each molecule participates in the $\text{Se}\cdots\text{N}$ contacts. In **106**, each of the two independent molecules assembles into a tape while in **110**, the two independent molecules are connected into a single tape. Generally, molecules **105-110** are flat, at least the $\{\text{SeN}\cdots\}_n$ core of the tape.

Table 8Geometric (\AA , $^\circ$) details for aggregates in **105-115** which form supramolecular tapes in their crystals mediated by $\text{Se}\cdots\text{N}$ interactions

Aggregate	$\text{Se}\cdots\text{N}$ (\AA)	$\%(d/vdW)^a$ (\AA)	W / W– $\text{Se}\cdots\text{N}$ ($^\circ$)	X / X– $\text{Se}\cdots\text{N}$ ($^\circ$)	Y / Y– $\text{N}\cdots\text{Se}$ ($^\circ$)	Z / Z– $\text{N}\cdots\text{Se}$ ($^\circ$)	REFCODE	Ref.
105 ^b	2.884(15)	83.6	N / 164.4(6)	N / 73.6(5)	Se / 115.9(7)	C / 132(1)	NABSAN	[137]
	3.172(13)	91.9	N / 156.8(5)	N / 65.9(6)	Se / 104.2(6)	C / 152(1)		
	2.915(12)	84.5	N / 163.4(6)	N / 73.1(5)	Se / 116.3(5)	C / 138(1)		
	3.159(15)	91.6	N / 160.0(5)	N / 67.6(5)	Se / 102.9(5)	C / 151(1)		
	2.919(15)	84.6	N / 169.2(5)	N / 74.4(6)	Se / 113.8(7)	C / 140(1)		
	3.170(16)	91.9	N / 160.6(5)	N / 67.3(6)	Se / 104.2(7)	C / 145(1)		
	2.946(18)	85.4	N / 168.7(5)	N / 74.8(6)	Se / 110.8(7)	C / 137(1)		
	3.174(15)	92.0	N / 158.6(5)	N / 67.3(6)	Se / 106.4(6)	C / 146(1)		
106	2.886(7)	83.7	N / 164.6(3)	N / 73.7(2)	Se / 110.1(3)	C / 139.0(5)	LOSMAK	[138]
	3.023(6)	87.6	N / 160.8(2)	N / 70.0(3)	Se / 104.6(3)	C / 145.2(5)		
107 ^c	2.8811(16)	83.5	N / 167.94(7)	N / 75.44(6)	Se / 119.05(7)	C / 131.43(15)	NABSOB	[137]
	3.3503(17)	97.1	N / 155.55(7)	N / 62.73(6)	Se / 105.05(6)	C / 150.47(15)		
	2.9104(17)	84.4	N / 168.32(6)	N / 74.82(6)	Se / 117.79(7)	C / 134.01(12)		
	3.2932(16)	95.5	N / 157.57(6)	N / 64.44(6)	Se / 102.17(7)	C / 150.78(12)		
108	3.001(7)	87.0	N / 164.4(2)	N / 73.1(2)	Se / 106.3(3)	C / 141.4(5)	ZUCTUO	[139]

	3.065(6)	88.8	N / 162.4(2)	N / 71.2(2)	Se / 104.3(2)	C / 142.3(5)		
109	3.015(4)	87.4	N / 161.31(12)	N / 71.88(10)	Se / 104.49(11)	C / 148.7(3)	JURLAJ	[140]
	3.063(3)	88.8	N / 160.85(9)	N / 69.15(10)	Se / 110.85(12)	C / 141.64(18)		
110	3.071(3)	89.0	N / 163.62(14)	N / 70.55(13)	Se / 109.45(15)	C / 143.7(3)	NABSER	[137]
	3.121(3)	90.5	N / 162.12(13)	N / 69.50(13)	Se / 110.50(15)	C / 142.3(3)		
111	3.086(2)	89.5	N / 170.49(8)	N / 82.14(8)	Se / 97.86(8)	C / 153.83(16)	TORTOM	[141]
	3.427(2)	99.3	N / 146.92(8)	N / 71.92(7)	Se / 108.08(8)	C / 134.68(16)		
	3.0071(16)	87.2	N / 153.80(7)	N / 78.21(8)	Se / 101.73(8)	C / 149.53(15)		
	3.1175(17)	90.4	N / 167.68(7)	N / 75.13(7)	Se / 97.61(8)	C / 153.24(15)		
	3.375(2)	97.8	N / 157.90(8)	N / 75.04(8)	Se / 100.47(8)	C / 142.31(15)		
	3.518(3)	102.0	N / 131.19(7)	N / 71.00(7)	Se / 95.34(8)	C / 158.08(17)		
112	2.958(10)	85.7	(N)C / 173.4(4)	C / 78.0(3)	C / 175.6(8)		BATDIJ	[101]
	3.449(10)	100.0	C / 149.1(2)	(N)C 76.4(3)	C / 106.1(7)			
113	3.023(3)	87.6	(N)C / 172.94(13)	C / 91.42(12)	C / 170.9(3)		CIBFUP	[142]
	3.065(4)	88.8	(N)C / 166.07(13)	C / 95.53(13)	C / 164.9(3)			
	3.329(4)	96.5	C / 166.75(13)	(N)C / 75.64(13)	C / 108.1(3)			
	3.444(4)	99.8	C / 162.48(13)	(N)C / 73.52(13)	C / 106.0(3)			
114^d	2.935(4)	85.1	(N)C / 173.07(17)	C / 80.20(19)	C / 173.3(4)		ZUNWEN	[143]
	2.946(4)	85.4	(N)C / 172.27(17)	C / 81.1(2)	C / 173.3(4)			
	3.410(7)	98.8	C / 167.57(19)	(N)C / 75.1(2)	C / 110.6(4)			

	3.674(6)	106.5	(N)C / 71.2(2)	C / 119.24(18)	C / 103.7(4)		
115	3.019(5)	87.5	N / 169.24(12)	N / 75.55(15)	C / 152.4(3)	NONZIZ	[144]
	3.313(5)	96.0	N / 127.80(13)	N / 137.17(15)	Se / 104.4(4)		
	3.434(3)	99.5	N / 154.69(13)	N / 80.66(12)	Se / 99.19(13)	C / 142.8(2)	

a $\%(d/vdW) = [d(\text{Se}\cdots\text{N})/3.45] \times 100$

b There are four independent chains in the crystal, hence eight entries

c There are two independent chains in the crystal, hence four entries

d The first two values link molecules into a chain and the second two values define the rungs

The exceptional tape is found in the crystal of **111**, with end- and side-on views illustrated in Fig. 17b and c, respectively. One of the Se \cdots N contacts connecting the three independent molecules into the tape is at a separation greater than the sum of the van der Waals radii; these are indicated by an asterisk in Fig. 17c. This feature of the supramolecular aggregation may contribute the highly twisted topology highlighted in Fig. 17b brought forth by the proximity of the bulky substituents.

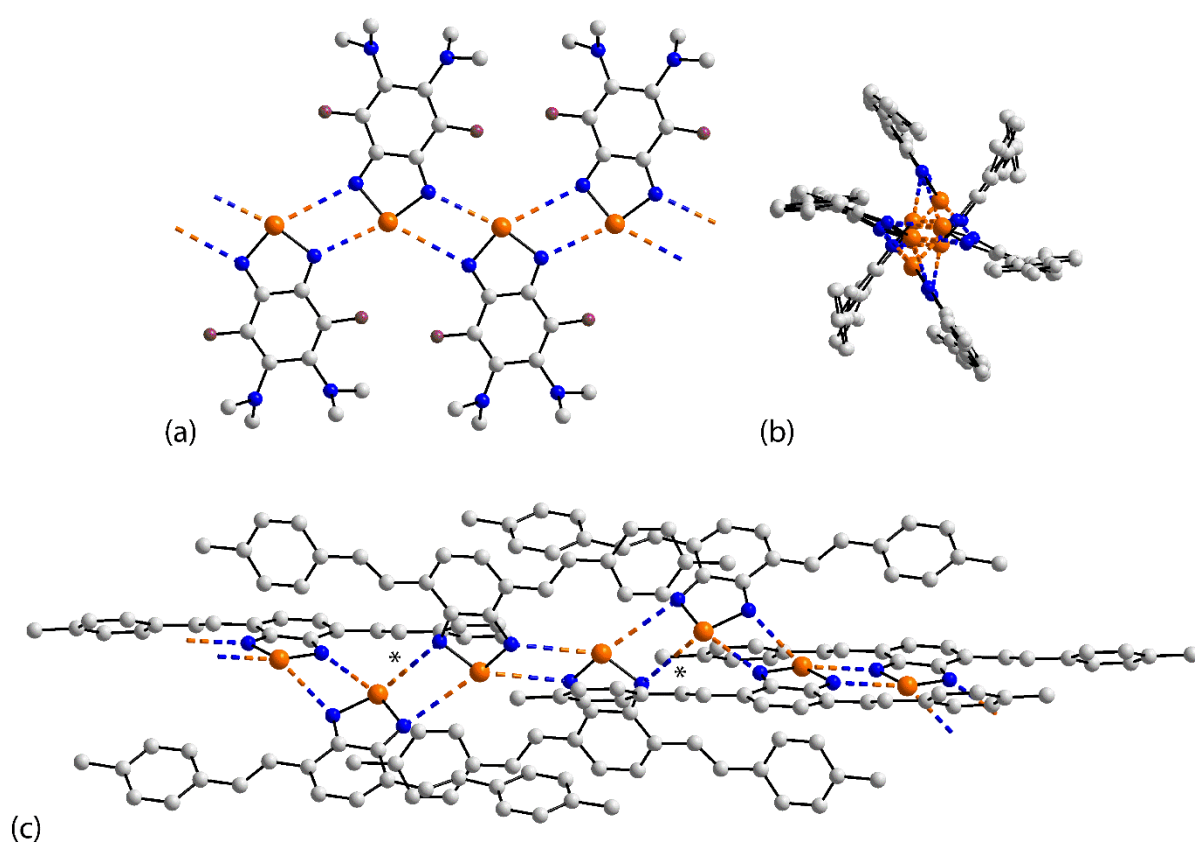


Fig. 17. Diagrams highlighting the formation of supramolecular tapes featuring Se \cdots N secondary-bonding interactions in crystals: (a) **106** and (b) **111** (end-on view) and (c) **111** (side-on view). In (c), the Se \cdots N interactions indicated by an * occur at 3.518(3) Å, that is, beyond the sum of van der Waals radii.

A different topology for the supramolecular tapes is observed in the crystals of **112** [101], **113** [142] and **114** [143], being based on edge-shared rectangles. The three molecules are organoselenium cyanates. The starting point for the construction of the tapes are the linear supramolecular chains described above for **59**, illustrated in Fig. 11a and homologues. Short Se \cdots N connections connect the molecules into a linear chain and symmetry-related chains are linked via longer Se \cdots N connections, as exemplified for **112** in Fig. 18a. This separation, at 3.449(10) Å, is just below the van der Waals limit (3.45 Å) and is the longest contact distance among the 142 aggregates described in this review. Indeed, for **112**, two molecules comprise the asymmetric-unit. One of the aggregates is a linear chain noted above for **57** and the second forms aggregate **112**. While chains line up to potentially form inter-chain Se \cdots N interactions in **57**, the separation, at 3.663(10) Å, is beyond the sum of the van der Waals radii. In a variation, the two independent molecules of **113** self-assemble into a single chain and connect the tape via longer Se \cdots N interactions. As noted from Table 8, the selenium atom forming the shorter of the contacts within the chain also forms the shorter of the inter-chain contacts. Akin to that described above for **111**, one of the links between chains is missing in the aggregate formed in **114** so that tape comprises edge-shared connections between significantly elongated rectangles; the missing rung in the ladder has a Se \cdots N separation of 3.674(6) Å. The reason for this difference between the pattern of aggregation in **112** and **113** compared to that in **114** may also be steric in origin. It is also noted that ladders in **112** and **113** are propagated by a centre of inversion as opposed to the 2-fold symmetry of **114** with the important consequence the organic substituents are orientated to the same side of the core in the latter.

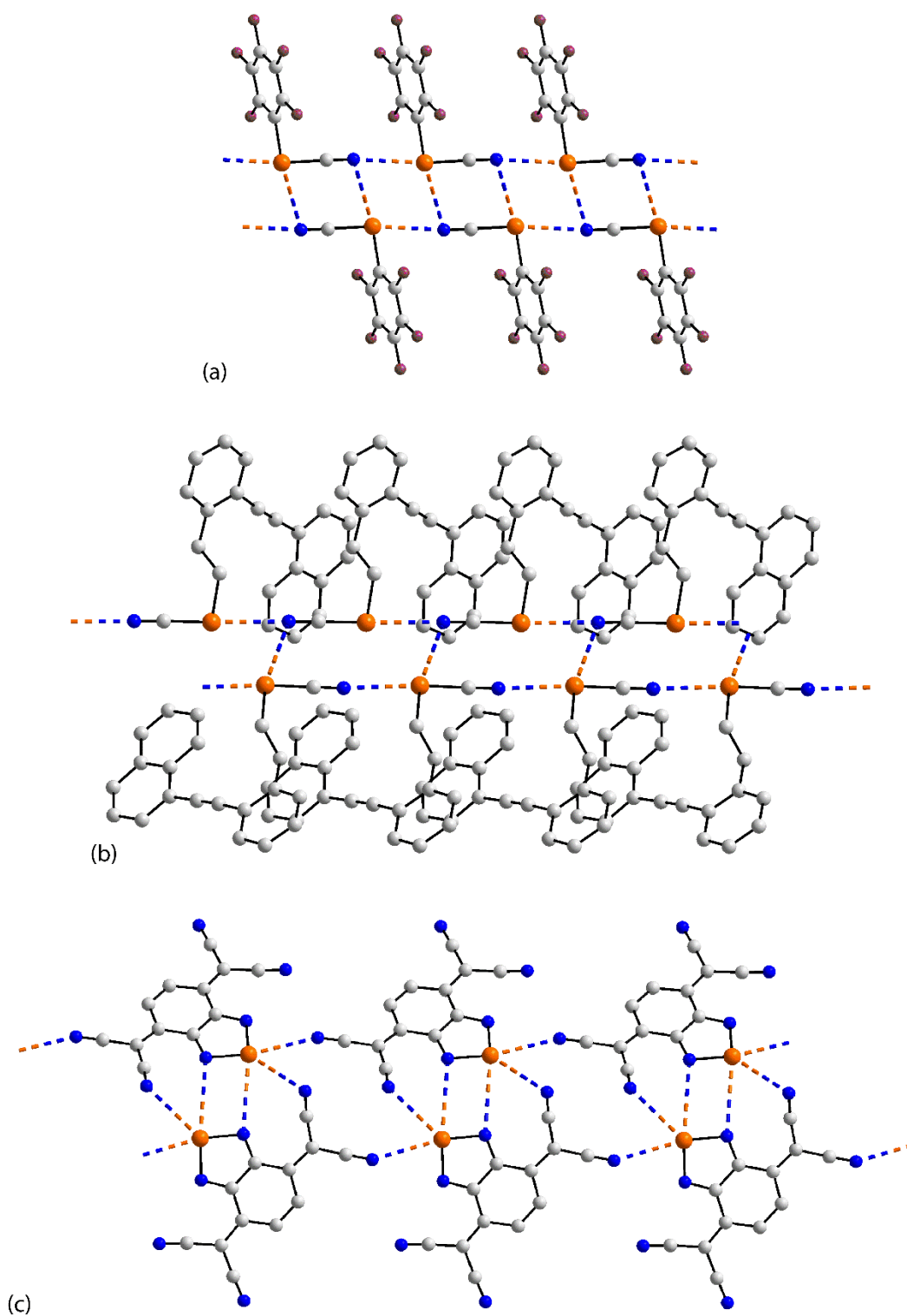


Fig. 18. Diagrams highlighting the formation of supramolecular tapes featuring Se \cdots N secondary-bonding interactions in crystals: (a) **112**, (b) **114** and (c) **115**.

The selenium atom in **115** [144] forms three Se \cdots N contacts to form the tape shown in Fig. 18c. Two 1,2,5-selenadiazole rings, related by a 2-fold axis of symmetry, connect via a {SeN \cdots }₂ synthon. The selenium atom is also connected to a nitrile-nitrogen atom derived from the same molecule as well as a translationally-related molecule to form a supramolecular tape. The mode of association leads to the formation of 7-membered {Se \cdots NC₄N \cdots } and 12-membered {Se \cdots NC₃N \cdots }₂ synthons.

3.9 Two-and three-dimensional architectures featuring Se \cdots N interactions

There are seven two-dimensional arrays featuring Se \cdots N interactions between the molecules: **116** [145], **117** [146], **118** [147], **119** [128], **120** [148], **121** [149] and **122** [150]. There is one further example of a molecule, in the crystal of **123** [151], where Se \cdots N interactions feature within a three-dimensional architecture. The chemical diagrams for the eight compounds are given in Fig. 19 and key geometric parameters associated with the Se \cdots N contacts are summarised in Table 9.

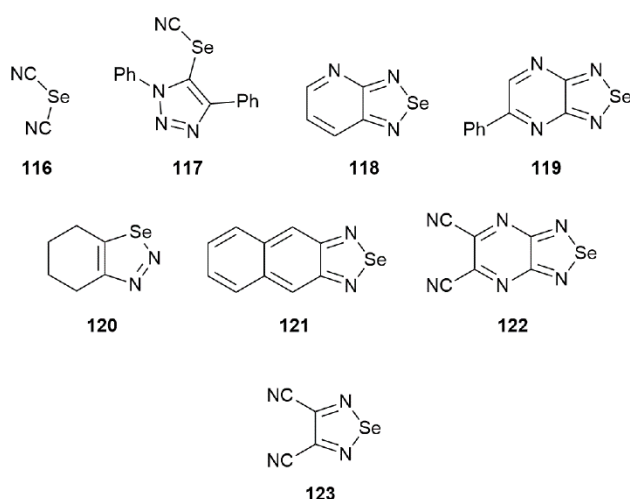


Fig. 19. Chemical diagrams for the interacting species forming Se \cdots N contacts leading to two-dimensional arrays in crystals **116-122**, and to a three-dimensional architecture in the crystal of **123**.

Table 9

Geometric (\AA , $^\circ$) details for aggregates in **116-123** which form two- or three-dimensional architectures their crystals mediated by $\text{Se}\cdots\text{N}$ interactions

Aggregate	$\text{Se}\cdots\text{N}$ (\AA)	$\%(\text{d/vdW})^a$ (\AA)	W / W– $\text{Se}\cdots\text{N}$ ($^\circ$)	X / X– $\text{Se}\cdots\text{N}$ ($^\circ$)	Y / Y– $\text{N}\cdots\text{Se}$ ($^\circ$)	Z / Z– $\text{N}\cdots\text{Se}$ ($^\circ$)	REFCODE	Ref.
116	2.813(6)	81.5	C / 166.3(3)	C / 75.0(2)	C / 153.8(5)		UQAXUH	[145]
	2.835(6)	82.2	C / 170.4(2)	C / 79.1(2)	C / 133.4(5)			
117^b	3.177(3)	92.1	(N)C / 165.98(11)	C / 71.94(9)	N / 131.4(2)	C / 108.41(19)	DUBPEY	[146]
	3.229(3)	93.6	C / 174.10(9)	(N)C / 80.71(10)	N / 154.9(2)			
118^{c-c}	2.889(5)	83.7	N / 166.76(19)	N / 72.80(15)	Se / 109.53(17)	C / 143.9(4)	WEJXEQ	[147]
	2.958(5)	85.7	N / 164.11(18)	N / 70.92(15)	Se / 106.73(16)	C / 147.2(4)		
	3.362(5)	97.4	N / 158.99(14)	N / 97.33(15)	C / 106.8(3)	C / 131.3(3)		
	3.389(4)	98.2	N / 151.23(14)	N / 114.06(17)	Se / 93.50(15)	C / 134.5(3)		
119^e	2.991(3)	86.7	N / 165.74(9)	N / 71.84(8)	C / 145.72(18)	Se / 108.16(9)	AHIKEJ	[128]
	3.022(3)	87.6	N / 166.02(8)	N / 75.18(9)	C / 115.90(17)	C / 127.94(15)		
120^e	3.195(11)	92.6	C / 154.6(4)	N / 71.3(4)	Se / 108.7(4)	N / 138.5(8)	FENFIO	[148]
	3.154(10)	91.4	N / 175.8(4)	C / 91.4(4)	N / 121.2(7)	C / 121.6(7)		
121^d	3.005(2)	87.1	N / 160.67(8)	N / 74.78(8)	Se / 105.22(9)	C / 143.67(17)	PUBBAS	[149]
	2.890(2)	83.8	N / 167.63(9)	N / 73.02(8)	Se / 106.98(9)	C / 146.10(17)		

	3.375(2)	97.8	N / 96.06(8)	N / 82.53(8)	Se / 97.47(8)	C / 91.73(15)		
122 ^g	3.071(2)	89.0	N / 161.44(7)	N / 97.70(7)	C / 174.29(18)		KOWGAH	[150]
	3.073(2)	89.1	N / 162.95(7)	N / 96.55(7)	C / 120.27(18)			
	3.396(2)	98.4	N / 78.52(7)	N / 80.43(7)	Se / 114.82(8)	C / 128.49(14)		
123 ^{e, h}	3.0437(16)	88.2	N / 161.36(6)	N / 81.74(6)	Se / 124.09(7)	C / 118.70(11)	HAMFUY	[151]
	3.2869(18)	95.3	N / 135.27(6)	N / 81.05(6)	C / 114.17(14)			
	3.0232(16)	87.6	N / 167.76(6)	N / 80.90(6)	C / 158.70(16)			
	3.0427(16)	88.2	N / 162.55(6)	N / 82.11(6)	Se / 132.10(7)	C / 119.30(11)		
	3.300(2)	95.7	N / 129.40(6)	N / 113.34(6)	C / 162.24(18)			

a $\%(\text{d/vdW}) = [\text{d}(\text{Se}\cdots\text{N})/3.45] \times 100$

b The first entry is for Se \cdots N(tetrazole) and the second for Se \cdots N(cyanate)

c There are two independent molecules

d The first two entries are for dimer formation, the others occur between dimers

e The third entry is for Se \cdots N(pyridyl), the fourth for Se \cdots N(diazole)

f The first entry is for Se \cdots N(diazole)

g The first two entries are for Se \cdots N(cyanate), the third for Se \cdots N(azole)

h The first two entries are for the first independent selenium and are for Se···N(diazole) and Se···N(bridging cyanate), the remaining entries are for Se···N(bridging cyanate), Se···N(diazole) and Se···N(terminal cyanate)

As might be anticipated from the adoption of higher-dimensional aggregation patterns by quite disparate molecules, there exists a wide variety of supramolecular architectures to be described in this section. The only possible exception to this is found in the crystals of **116** and **117**. In the simplest molecule described in this review, that is, $\text{Se}(\text{CN})_2$ in **116**, in its crystal each nitrile-nitrogen atom forms a $\text{Se}\cdots\text{N}$ contact resulting in the formation of distinctive 12-membered rings arising as a result of translational and glide symmetry containing one SeC_2N_2 formula unit, two SeCN entities and one selenium atom. As noted from Table 9, the $\text{Se}\cdots\text{N}$ separations are close to each other in magnitude, the $\text{C}-\text{Se}\cdots\text{N}$ angles approximate linearity but the cyanate-donors do not approach the selenium atoms end-on. The resulting two-dimensional array is shown in Fig. 20a.

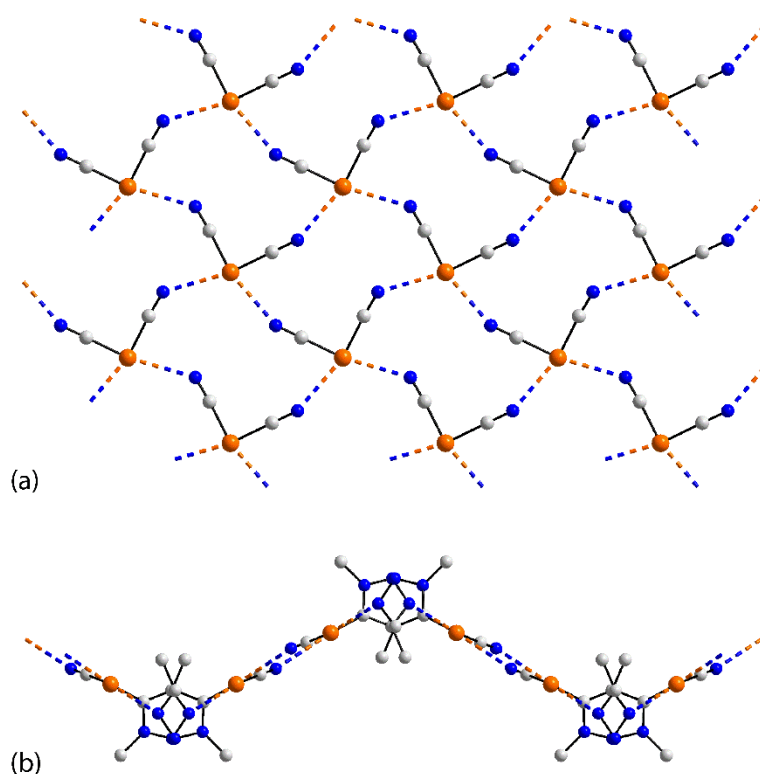


Fig. 20. Diagrams highlighting the formation of two-dimensional arrays featuring $\text{Se}\cdots\text{N}$ secondary-bonding interactions in crystals: (a) **116** and (b) **117**.

In the crystal of **117**, essentially the same arrangement is found with the obvious difference being in the nature of the bridges between selenium atoms as one of the cyanate ligands of **116** has been replaced by a 1,2,3-triazole ring to give **117**. This has the result that two of the bridges giving rise to the tetra-selenium supramolecular ring comprises an extra carbon atom leading to 14-membered rings; the layer is generated by a combination of 2_1 -screw and translational symmetry. The key difference between **116** and **117** is that the topology of the layer in the former is distinctly flat while that in the latter is zig-zag, as emphasised in Fig. 20b.

Two independent molecules comprise the asymmetric-unit of **118** and these form distinctive Se \cdots N interactions. The two molecules form a dimer via two close Se \cdots N(selenadiazole) contacts and the first independent molecule forms a second Se \cdots N(selenadiazole) contact with a second dimer. The selenium atom of the second molecule self-associates via Se \cdots N(pyridyl) contacts involving a third dimer. The result, illustrated in the two views of Fig. 21a, are columns of dimers with alternating orientations connected by the longer Se \cdots N contacts into a two-dimensional array.

As evident from the views of Fig. 21b, a more symmetric two-dimensional arrangement is formed in the crystal of **119** despite there being, potentially, more nitrogen atoms available for interaction. A single molecule comprises the asymmetric-unit and these self-assemble about an inversion centre to form a two-molecule aggregate via Se \cdots N(selenadiazole) interactions. Dimers are connected to either side via Se \cdots N(pyrazine) interactions. While the separations associated with the latter contacts are longer than the former, the difference in magnitude is not great. In the two-dimensional packing, translationally-related stacks of dimers are connected into a flat topology. In common with **118** but in contrast to **116** and **117**, the layer is two molecules thick.

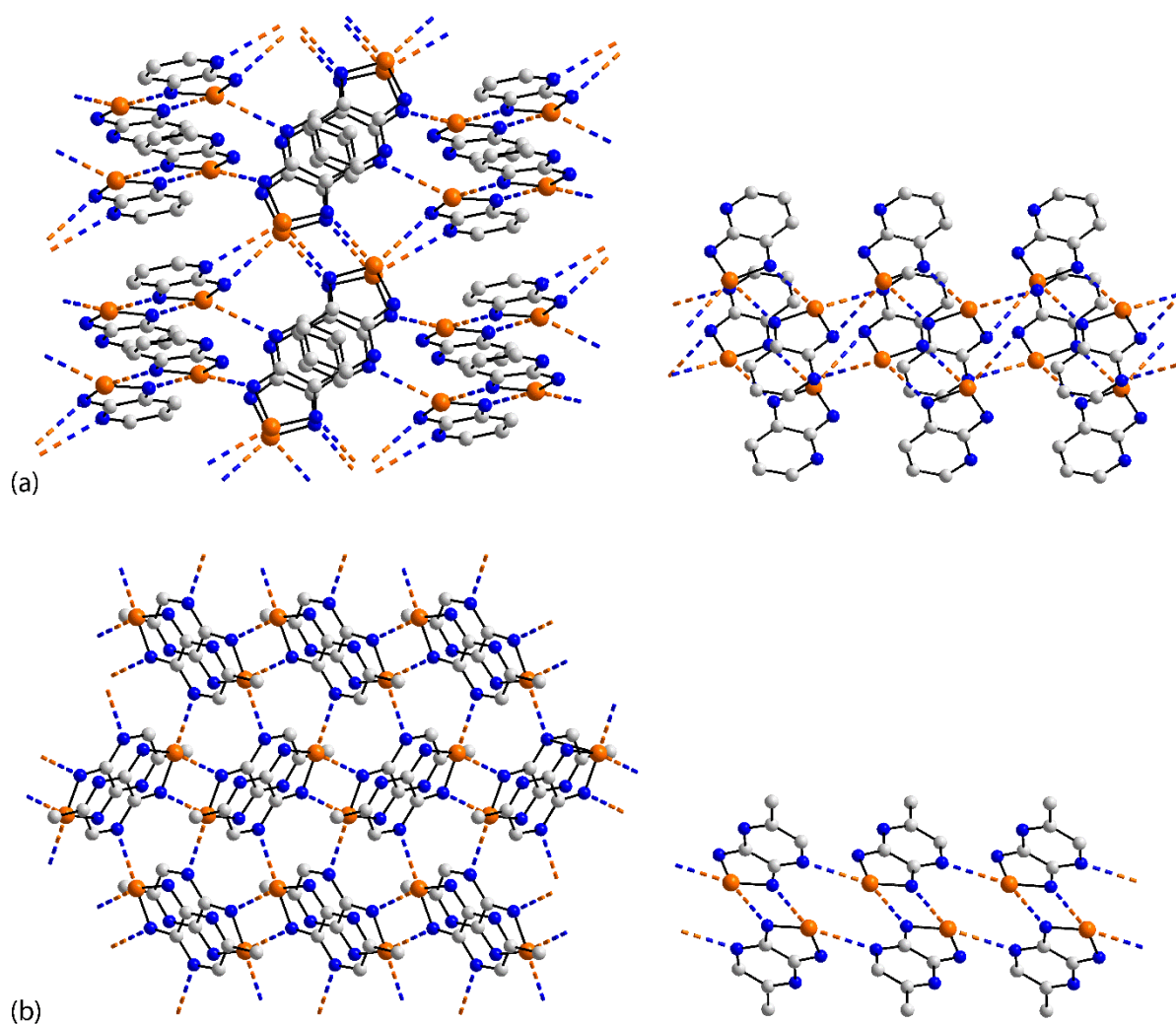


Fig. 21. Diagrams highlighting the formation of two-dimensional arrays featuring $\text{Se}\cdots\text{N}$ secondary-bonding interactions in crystals: (a) **118** and (b) **119**.

In the crystals of **120**, each atom comprising the 1,2,3-selenadiazole ring participates in a $\text{Se}\cdots\text{N}$ interaction, firstly to form a dimer, over a centre of inversion and via a four-membered $\{\text{SeN}\cdots\}_2$ synthon. The second $\text{Se}\cdots\text{N}$ interaction, marginally shorter than the first, serves to link the dimers into a layer, two molecules thick as can be noted from the images of Fig. 22a. Centrosymmetric $\{\text{SeN}\cdots\}_2$ synthons are also formed in **121**. In this case, the second nitrogen atom of the selenadiazole ring bridges two selenium atoms to form the two-dimensional array. Thus, the selenium atom forms three $\text{Se}\cdots\text{N}$ contacts with the separation associated with dimer formation being intermediate between the other two contacts.

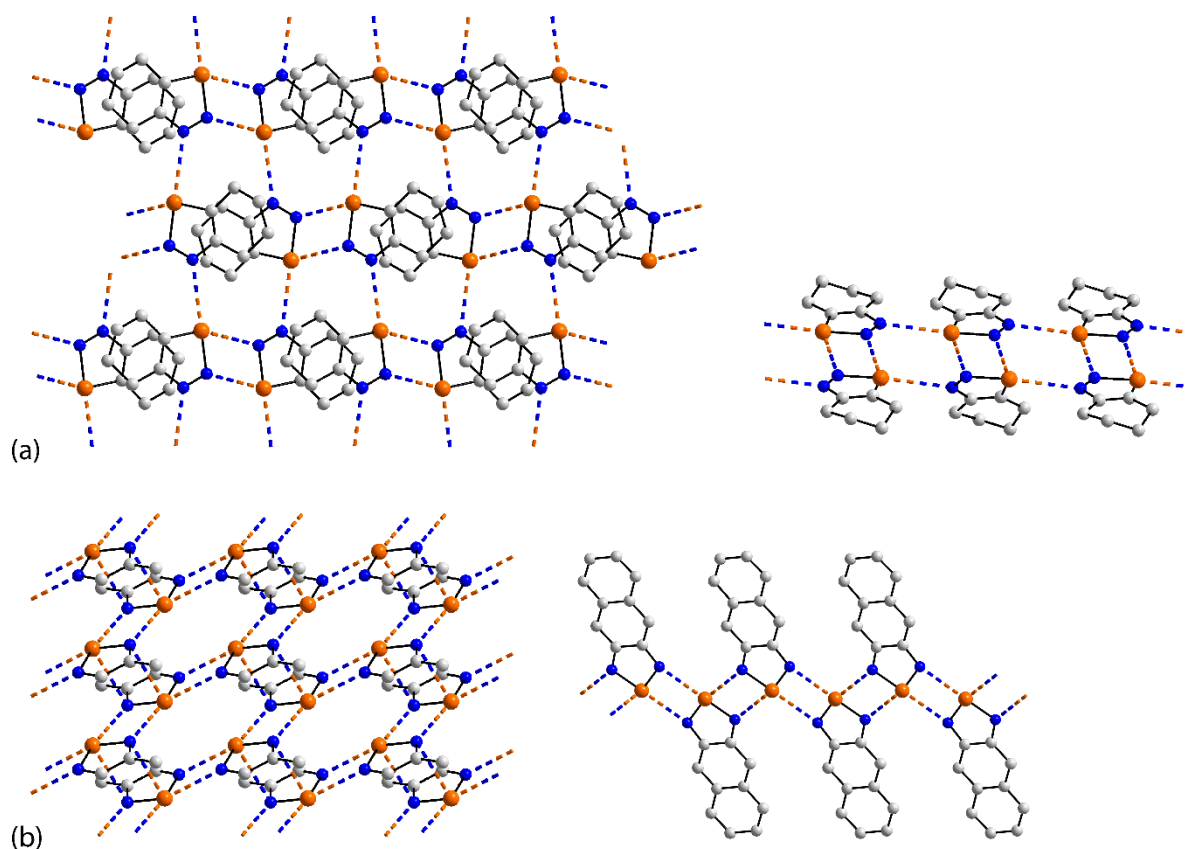


Fig. 22. Diagrams highlighting the formation of two-dimensional arrays featuring $\text{Se}\cdots\text{N}$ secondary-bonding interactions in crystals: (a) **120** and (b) **121**. For reasons of clarity, in the plan view of (b), only the carbon atoms bound to nitrogen are retained.

The last two-dimensional array to be described in this section is found in the crystal of **122**. The molecule is nitrogen-rich, having two each of selenadiazole-, pyrazine- and nitrile-nitrogen atoms. The selenium atom forms a $\text{Se}\cdots\text{N}$ interaction with a nitrile-nitrogen atom derived from two different molecules to stabilise the array; the $\text{N}-\text{Se}\cdots\text{N}(\text{nitrile})$ angles are close to linearity. The $\text{Se}\cdots\text{N}(\text{nitrile})$ separations are shorter than the $\text{Se}\cdots\text{N}(\text{selenadiazole})$ contact which contributes to the stability of the array, which, as seen from Fig. 23, is two molecules thick.

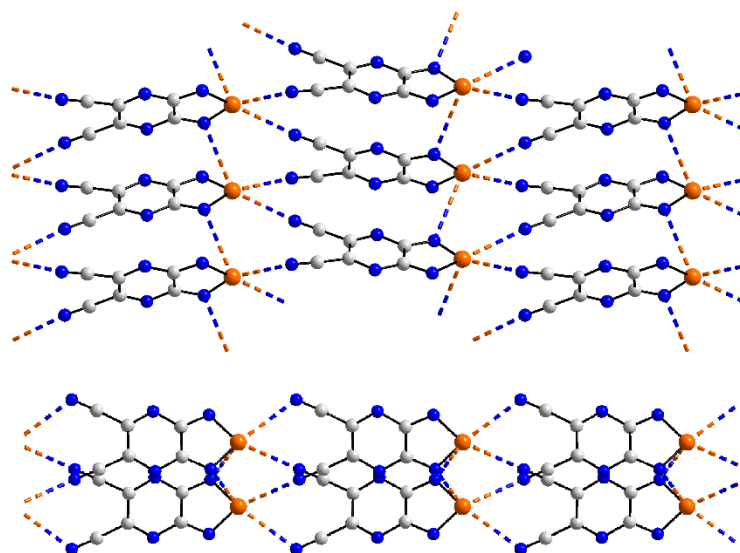


Fig. 23. Diagrams highlighting the formation of the two-dimensional arrays featuring Se...N secondary-bonding interactions in the crystal of **122**.

The sole example of a three-dimensional architecture featuring Se...N interactions in three directions is found in the crystal of **123**. Two nitrile-nitrogen atoms are present in the molecule along with two nitrogen atoms within the 1,2,5-selenadiazole ring. The crystallographic asymmetric-unit comprises two independent molecules and each has a distinct pattern of participation in Se...N interactions, as indicated in the upper views of Fig. 24. The common feature of the molecules is that each employs a ring- and nitrile-nitrogen in the supramolecular association with the difference being, the nitrile-nitrogen atom in the second molecule is bridging, linking selenium atoms derived from each independent molecule. The selenium atom in the first molecule is therefore, connected to a bridging nitrile-nitrogen atom and at the same to a 1,2,5-selenadiazole-nitrogen. The second selenium atom associates with an additional nitrile-nitrogen atom, forming three Se...N interactions in all. Of the Se...N(nitrile) contacts, a bridging contact is shorter than the other two interactions. The net result is the architecture shown in the lower view of Fig. 24.

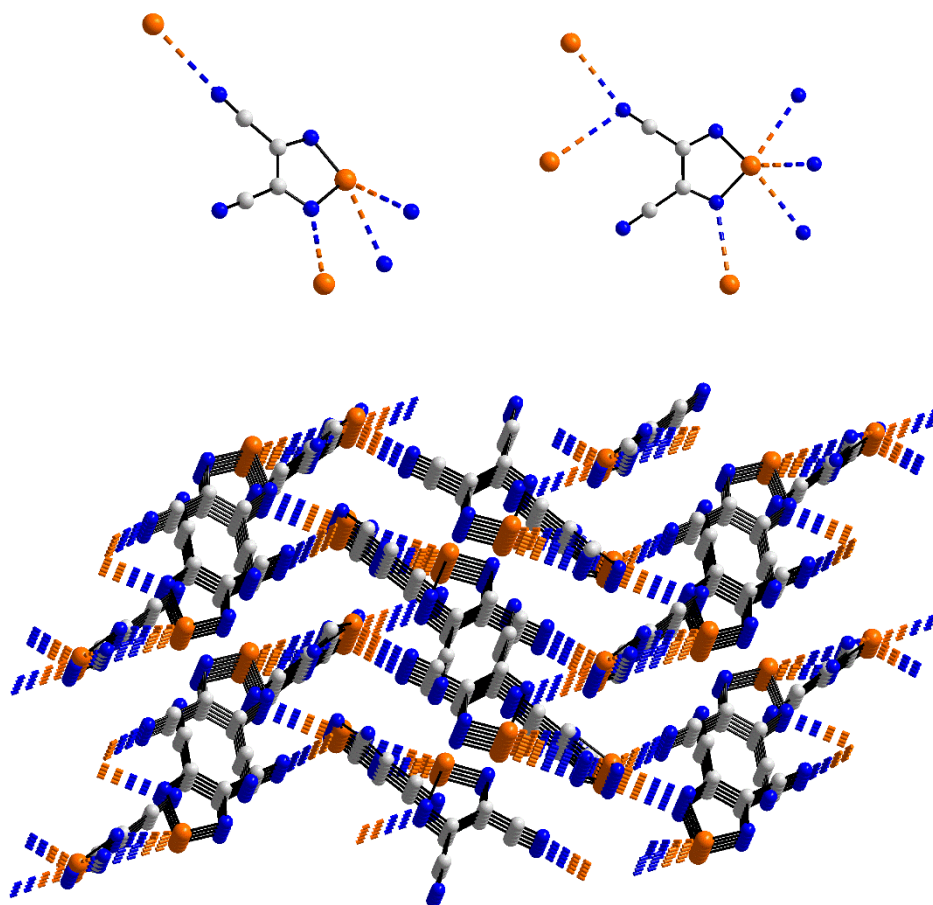


Fig. 24. Diagrams highlighting the formation of a three-dimensional array featuring Se...N secondary-bonding interactions in the crystal of **123**.

3.10 Multi-component crystals featuring Se...N interactions

This section covers multi-component crystals, **124-134**, featuring Se...N interactions between the constituents, chemical diagrams for these are given in Fig. 25 and geometric data in Table 10.

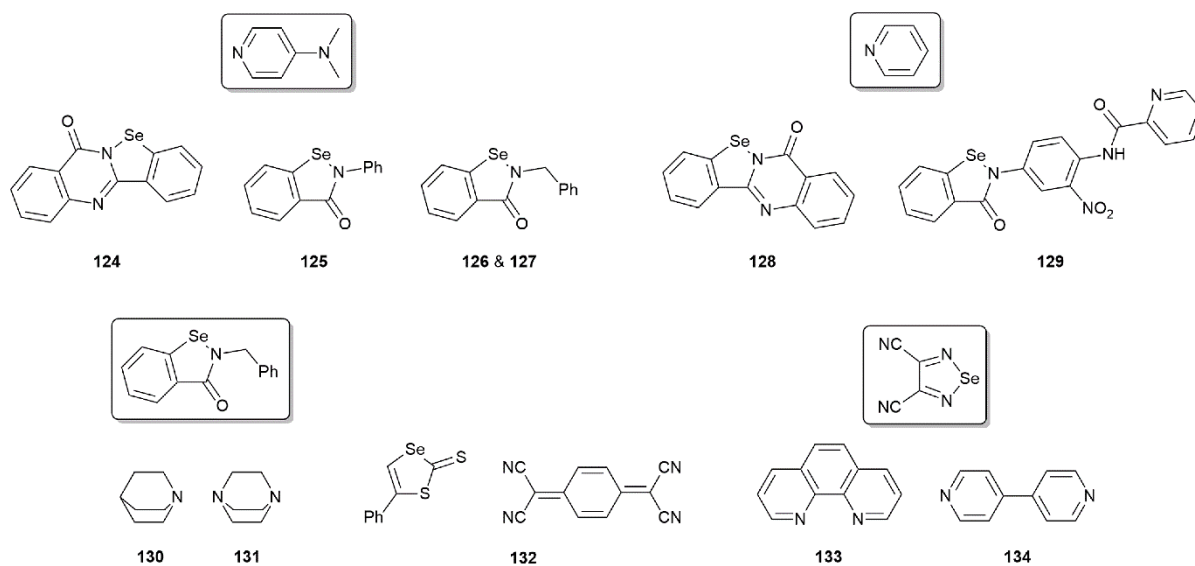


Fig. 25. Chemical diagrams for the interacting species in the crystals of **124-134**, forming $\text{Se}\cdots\text{N}$ contacts in multi-component crystals with selenium(II) co-formers. The highlighted molecules form multi-component crystals with the molecules underneath the boxes.

The first six aggregates in this section are derived from systematic structural studies of chalcogen-bonding [123, 152], feature similar molecules, having a 1,2-benzoselenazole core, the same type of two-molecule aggregate and are characterised by relatively short $\text{Se}\cdots\text{N}$ interactions, Table 10. Thus, **124-128** [119] and **129** [152], exemplified in Fig. 26a for **125**, feature a pyridyl-type molecule interacting with a selenium-containing molecule bearing at least one carbonyl group available for competitive $\text{Se}\cdots\text{O}$ interactions. The $\text{Se}\cdots\text{N}$ separation of 2.3038(11) Å in **124** has the distinction of being the shortest contact among the 142 structures described herein. The $\text{N}-\text{Se}\cdots\text{N}$ angle is greater than 173° in each case. The aggregates in **130** and **131** [119], Fig. 26b, are very similar to the aforementioned but involve an amine-nitrogen donor to selenium within a 1,2-benzoselenazole residue; the $\text{N}-\text{Se}\cdots\text{N}$ angles are greater than 175° . The interaction leading to the two-molecule aggregate in **132** [153] involves a selenium atom within a 1,3-thiaselenole ring interacting with a nitrile-nitrogen atom.

The approach of the nitrile-nitrogen atom is neither end- nor side-on with the C–N \cdots Se angle being 143.33(11)°.

Table 10Geometric (\AA , $^\circ$) details for aggregates in multi-component crystals **124-134** mediated by $\text{Se}\cdots\text{N}$ interactions

Aggregate	$\text{Se}\cdots\text{N}$ (\AA)	$\%(d/vdW)^a$ (\AA)	W / W– $\text{Se}\cdots\text{N}$ ($^\circ$)	X / X– $\text{Se}\cdots\text{N}$ ($^\circ$)	Y / Y– $\text{N}\cdots\text{Se}$ ($^\circ$)	Z / Z– $\text{N}\cdots\text{Se}$ ($^\circ$)	REFCODE	Ref.
124	2.3038(11)	66.8	N / 173.81(4)	C / 91.64(5)	C / 119.71(9)	C / 122.90(9)	GOBZOP	[119]
125	2.3715(11)	68.7	N / 174.18(4)	C / 90.26(5)	C / 120.68(8)	C / 122.26(8)	GOBYEE	[119]
126	2.4047(15)	69.7	N / 173.55(6)	C / 90.52(6)	C / 118.57(12)	C / 123.58(13)	GOBZUV	[119]
127^b	2.4279(13)	70.4	N / 173.92(6)	C / 90.09(6)	C / 120.44(11)	C / 123.34(11)	GOBZAB	[119]
	2.4328(14)	70.5	N / 175.31(5)	C / 91.97(5)	C / 118.97(11)	C / 119.72(10)		
128	2.461(3)	71.3	N / 174.11(10)	C / 92.23(10)	C / 116.5(2)	C / 124.3(2)	GOBZIJ	[119]
129	2.466(6)	71.5	N / 173.20(19)	C / 90.1(2)	C / 119.2(4)	C / 120.6(4)	BUJSAD	[152]
130	2.5873(16)	75.0	N / 176.76(6)	C / 97.98(7)	C / 92.15(12)	C / 114.11(13)	GOBYOO	[119]
				C / 121.91(13)				
131	2.6163(13)	75.8	N / 175.77(6)	C / 98.34(6)	C / 91.52(10)	C / 114.38(11)	GOBYII	[119]
				C / 123.63(11)				
132	3.106(3)	90.0	(S)C / 167.98(8)	C / 76.46(6)	C / 143.33(11)		PTSTCQ	[153]
133	2.780(2)	80.6	N / 175.08(8)	N / 83.32(8)	C / 113.97(18)	C / 128.52(15)	XUHGEP	[154]
	3.0880(19)	89.5	N / 139.12(8)	N / 128.80(8)	C / 117.63(14)	C / 124.58(17)		
134^c	2.585(5)	74.9	N / 175.34(18)	N / 83.83(17)	C / 114.8(4)	C / 128.7(4)	XUHTEC	[154]

2.648(5)	76.8	N / 172.84(18)	N / 80.61(17)	C / 115.1(3)	C / 128.2(4)
3.099(4)	89.8	N / 166.83(14)	N / 76.55(15)	Se / 100.75(17)	C / 151.2(3)
3.017(4)	87.5	N / 170.86(15)	N / 78.79(15)	Se / 103.88(18)	C / 147.4(3)

a $\%(\text{d/vdW}) = [\text{d}(\text{Se}\cdots\text{N})/3.45] \times 100$

b There are two independent pairs of co-formers

c The first two entries are for Se \cdots N(pyridyl) and the remaining for Se \cdots N(diazole)

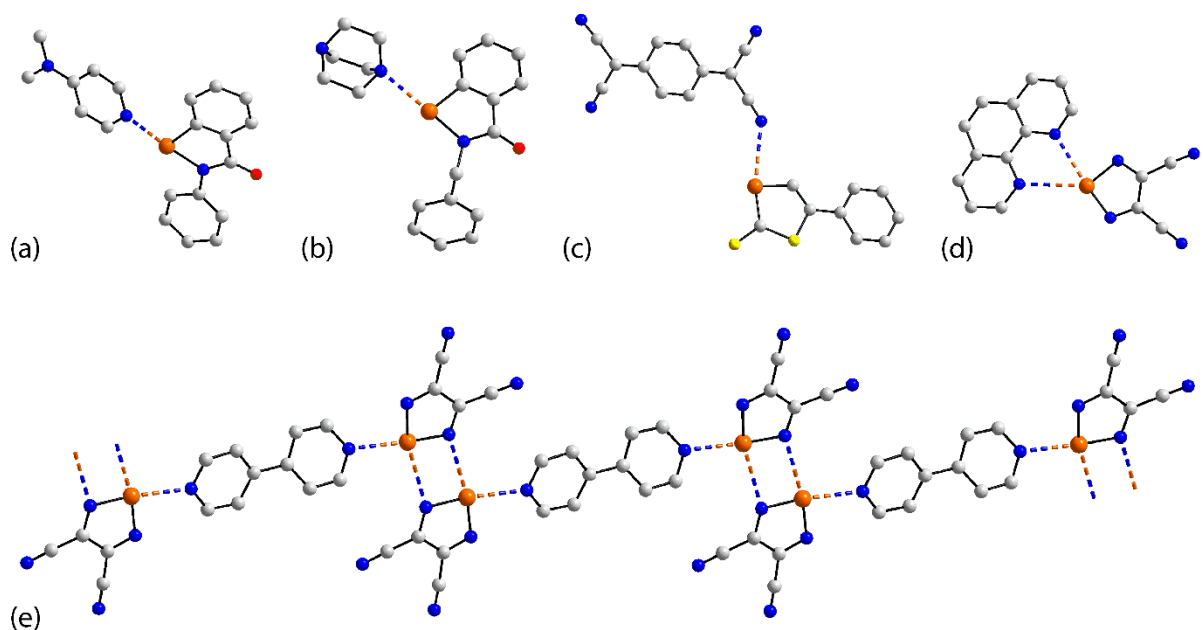


Fig. 26. Diagrams of multi-component species featuring Se \cdots N secondary-bonding interactions in their crystals: (a) **125**, (b) **131**, (c) **132**, (d) **133** and (e) **134**.

A variation occurs in **133** [154] in that two Se \cdots N contacts are formed between a 1,2,5-selenadiazole-bound selenium atom and both 1,10-phenanthroline-nitrogen atoms, Fig. 26d. One Se \cdots N separation is significantly shorter, by 0.30 Å, than the second interaction and the associated N–Se \cdots N angle is 175.08(8)°, perhaps suggesting the second interaction is an artefact. The last structure to be discussed in this section is a supramolecular polymer. In the crystal of **134** [154], a 1:2 co-crystal between 4,4'-bipyridyl and a 1,2,5-selenadiazole derivative, features non-symmetric {SeN \cdots }₂ synthons. The associated Se \cdots N separations are longer than those involving pyridyl-nitrogen atoms, Table 10, which serve to connect the dimers into the chain illustrated in Fig. 26e.

3.11 Aggregates sustained by Se \cdots N interactions in selenium(IV)-containing crystals

In this last section surveying aggregation patterns, attention turns to selenium(IV)-containing species. Compared to their selenium(II) counterparts, there is only a limited number

of examples and the ensuing discussion is in the order of the size of the aggregate. Each of the described aggregates have precedents among the selenium(II)-containing crystals. The chemical diagrams for the interacting species, **135-142**, are given in Fig. 27 and selected geometric data in Table 11.

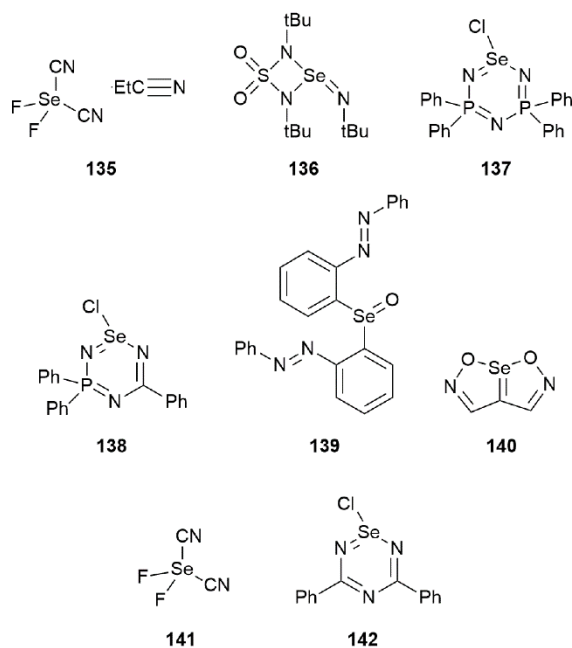


Fig. 27. Chemical diagrams for the interacting species in crystals **135-142**, highlighting the selenium(IV) species forming $\text{Se}\cdots\text{N}$ contacts.

The only multi-component crystal in this section involving a solvate is a simple two-molecule aggregate formed between $(\text{NC})_2\text{SeF}_2$ and propionitrile in the crystal of **135** [155]. As can be seen from Fig. 28a, a linear $\text{C}-\text{N}\cdots\text{SeCN}$ arrangement ensues. The aggregates in **136** [156], **137** [157], **138** [158] and **139** [159] are dimeric; all but **136** are centrosymmetric. In the first three examples, the $\text{Se}\cdots\text{N}$ interaction occurs at the extension of the $\text{N}-\text{Se}$ bond, as shown for **138** in Fig. 28b. By contrast, in **139**, an oxoselenium compound, Fig. 28c, the linear arrangement is $\text{C}-\text{Se}\cdots\text{N}$, Table 11. The remaining three crystals feature supramolecular polymers.

Table 11Geometric (\AA , $^\circ$) details for aggregates in selenium(IV)-containing crystals **135-142** which feature Se \cdots N interactions

Aggregate	Se \cdots N (\AA)	%(d/vdW) ^a (\AA)	W / W–Se \cdots N ($^\circ$)	X / X–Se \cdots N ($^\circ$)	Y / Y–N \cdots Se ($^\circ$)	Z / Z–N \cdots Se ($^\circ$)	REFCODE	Ref.
135	2.7504(13)	79.7	F / 91.16(4) N(C) / 167.90(4)	F / 95.83(4) N(C) / 75.29(4)	C / 177.33(10)		QUHYUP	[155]
136^b	3.187(2)	92.4	N / 151.68(7) N / 78.84(9)	N / 127.09(8)	Se / 101.62(9)	C / 120.79(15)	HUBXOR	[156]
	3.203(2)	92.8	N / 158.98(7) N / 78.36(9)	N / 119.01(8)	Se / 100.97(9)	C / 126.90(15)		
137	3.2204(4)	93.3	N / 172.56(16) N / 77.21(16)	Cl / 88.36(8)	Se / 102.79(18)	P / 134.57(19)	KEHYUR	[157]
138	3.254(3)	94.3	N / 151.20(8) N / 75.24(8)	Cl / 107.15(6)	Se / 104.76(9)	P / 135.91(10)	JAXBOZ	[158]
139	3.3406(18)	96.8	C / 158.37(6) C / 78.07(5)	O / 100.95(5)	N / 114.06(11)	C / 95.17(10)	ERUWAQ	[159]
140	3.257(7)	94.4	C / 157.6(3) O / 78.8(2)	O / 116.1(2)	O / 134.3(4)	C / 108.8(5)	JATHIV	[160]
141	3.386(3)	98.1	N(C) / 148.42(9)	F / 109.68(7)	C / 156.7(2)		QUHYEZ	[155]

			F / 72.60(6)	N(C) / 63.68(9)			
142	3.043(8)	88.2	N / 175.9(3)	Cl / 80.68(18)	Se / 94.8(3)	C / 137.8(7)	DUVFAB10 [161]
			N / 78.4(3)				
	3.138(8)	91.0	N / 159.8(3)	Cl / 99.83(18)	Se / 91.5(3)	C / 136.5(7)	
			N / 75.6(3)				

a $\%(\text{d/vdW}) = [\text{d}(\text{Se}\cdots\text{N})/3.45] \times 100$

b There are two independent pairs of molecules forming a dimeric aggregate

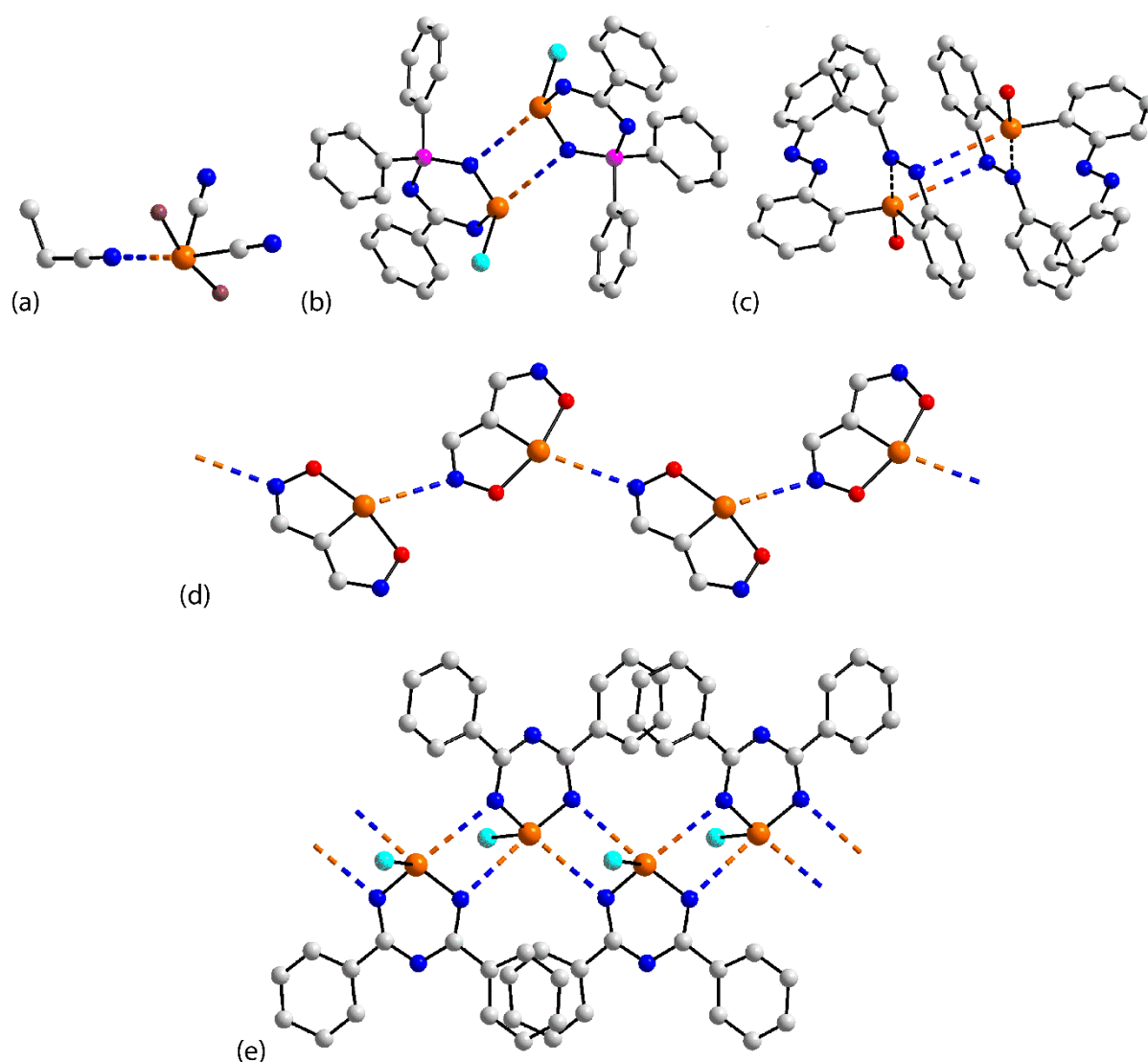


Fig. 28. Diagrams of aggregates featuring Se...N secondary-bonding interactions in the crystals of selenium(IV)-containing species: (a) **135**, (b) **138**, (c) **139**, (d) **140** and (e) **142**.

Zig-zag chains featuring Se...N interactions are formed in the crystals of **140** [160] and **141** [155]. In each of the former, shown in Fig. 28d, and latter, there is an approximately linear C–Se...N arrangement, Table 11. Finally, in **142** [161], a zig-zag tape arises as a result of the selenium atom forming two Se...N interactions. Here, confirming the universal adoption of chalcogen-bonding interactions among the selenium(IV) compounds there are approximately linear N–Se...N arrangements.

4 Evaluating the crystals of congeners of 1-142 for the presence of related secondary-bonding interactions

In this section, the molecular packing patterns in congeners of **1-142** were evaluated. Thus, the CSD [10] was searched with the aid of ConQuest [52] for structures where the selenium atom in each of **1-142** was substituted for an oxygen, sulphur or tellurium atom, that is, a Group 16 congener. The purpose of this survey was to evaluate the persistence or otherwise of contacts analogous to the secondary-bonding Se \cdots N contacts observed in **1-142** in the crystals of congeners of the same composition save for the variation in the Group 16 element. The sums of the van der Waals radii employed in the search are those assumed in the CSD [10], that is, 3.61, 3.45, 3.35 and 3.07 Å for Te + N, Se + N, S + N and O + N, respectively. The results of this survey are presented in Table 12. Here, the 34 selenium structures having congeners that have been structurally characterised are listed by their CSD REFCODES. Also, listed are the REFCODES for the structures of the congeners which are colour coded. Thus, REFCODES for the congeners which are highlighted with a green background correspond to isostructural crystals, that is, crystals with the same space group symmetry, similar unit-cell parameters and same value of Z'. The structures highlighted in bold green font correspond to congeners which do not fall in the definition of isostructurality just advanced but, do feature Te \cdots N or S \cdots N secondary-bonding interactions; as detailed below, in the case of S \cdots N interactions, some of the separations are beyond the accepted values of the van der Waals radii but the structures are include for the sake of the completeness of discussion. Finally, structures of sulphur- and oxygen-congeners highlighted in black font do not feature identifiable S \cdots N or O \cdots N secondary-bonding interactions, respectively. For example, none of the three polymorphs of the oxygen-congener of **5** feature S \cdots O secondary-bonding interactions, Table 12.

Table 12

Structural comparisons between congeners of **1-142**, identified through their CSD REFCODES. For each entry, isostructural relationships are highlighted with a green background and structures featuring related Te \cdots N and S \cdots N secondary-bonding interactions are highlighted in bold green font.

Comp'd	Congener			
	Te	Se	S	O
5	–	BOPGOD [67]	MOSXIC01 [162]	PCBZAM03 [163] PCBZAM11 [164] PCBZAM12 [164]
9	–	BEVPOJ [70]	BEVPEZ [70]	–
11	–	BEVQEA [70]	HULHIF [165]	–
13	–	HARCOU [71]	HARCIO [71]	HARCEK [71]
14	–	ANQSDZ [72]	ANQTDZ [166]	ANQDAZ [167]
25	–	GAJRIV [69]	GAJSUI [69]	–
26	–	VEHVUC [76]	VEHVOW [76]	–
27	–	BEVPID [70]	UZANAM [168]	–

29	–	DPSEAZ [78]	DPSDAZ [78]	ZZZTQC01 [169]
40	BEYGAQ [84]	BEYJEX [84]	–	–
41	WUMDIU [85]	WUMCIT [85]	–	–
46	–	DANJIM [89]	VIRGUY [170]	–
52	–	NUXRIK [95]	ZOKDUB [171]	–
56	OLUFOS [98]	OLUQOD [98]	CAMBAV01 [172]	–
62	–	BOPFUI [67]	XOGSAP [162]	RECQIA [163]
70	–	SADVUQ01 [102]	DPTHAZ [174]	NAXDIZ02 [175] NAXDIZ05 [176]
72	OLUQIX [93]	OLUGEJ [93]	–	–
73	OLUNEQ [93]	OLUFUY [93]	SERZEU10 [177]	LILMAV [178]
74	VIGCOD [179]	OLUGAF [93]	–	–
78	BECGAT [117]	BECFUM [117]	–	–
80	–	ATABAZ01 [112]	NAXDUL01 [180]	–
85	–	TEFBOW [104]	MEWXOD [181]	–
88	–	XOQBUA [125]	XOQBEK [125]	–

89	DEBHEY [182]	BESEAZ01 [126]	BETHAZ01 [125]	BEOXAZ01 [183]
91	–	AHINUC [128]		DAFRAD [184]
100	–	DERQOJ [90]	DESFEP [90]	–
105	IMUTEQ [185]	NABSAN [137]	–	–
	IMUTEQ01 [185]			
106	LOSLUD [186]	LOSMAK [138]	–	–
110	–	NABSER [137]	NABREQ [137]	–
115	–	NONZIZ [144]	KANWEB01 [144]	NONZAR [144]
121	–	PUBBAS [149]	POZYUB [149]	–
			POZYUB02 [149]	
			POZYUB04 [149]	
123	AREGEK01 [187]	HAMFUY [151]	HAMFOS [151]	–
140	–	JATHIV [160]	GIPVUW03 [160]	–
142	–	DUVFAB10 [161]	CILSAR [188]	–

The most striking feature of the data collated in Table 12 is the clear indication (lack of green highlighting) of the absence of O \cdots N secondary-bonding interactions in any of the oxygen-congeners that have been structurally characterised. Also noticeable is the predominance of highlighted REFCODES for the tellurium-congeners indicating isostructural relationships or structures with analogous Te \cdots N interactions. Thus, of the 12 tellurium-congeners, seven are isostructural giving rise to the same supramolecular aggregation patterns as detailed for the selenium-congeners. In the five other structures without strict isostructural relationships, OLUQIX [93] features a zig-zag chain as does selenium-congener **72**, and the same is true for the pair of structures LOSLUD [186] and **106**. Similarly, a non-isostructural relationship exists between AREGEK01 [187] and **123** yet both crystals feature secondary-bonding interactions operating in three-dimensions. Differences in secondary-bonding occur in the two remaining pairs of structures. In DEBHEY [182] extra Te \cdots N interactions occur leading to a zig-zag tape whereas in the selenium analogue **117**, a helical chain is formed as each selenium atom forms a single Se \cdots N interaction only. Mixed trends are noted in the final set of structures. Whereas IMUTEQ [185] is isostructural with selenium-congener, **105**, both adopting supramolecular tapes in their crystals, a polymorph is known for the tellurium-congener, that is, IMUTEQ01 [185] where the number of Te \cdots N secondary-bonding interactions is reduced so a centrosymmetric dimer is generated instead.

It is also instructive to compare the lengths and directionality of the Se \cdots N secondary-bonding interactions with the analogous Te \cdots N interactions in their isostructural congeners. The pertinent geometric data for the chalcogen-bonding in these isostructural crystals are listed in Table 13 from which several general trends may be discerned. While there is no systematic variation between the Se \cdots N and Te \cdots N separations, being experimentally equivalent in several pairs of structures, for example in **40** and **78**, with Se \cdots N being longer than Te \cdots N, for example in **41**, sometimes with Se \cdots N shorter than Te \cdots N, for example in **74** and there is an example,

namely **56**, where two independent secondary-bonding interactions are apparent with one Se \cdots N separation being shorter and the other equivalent to the comparable Te \cdots N distances. Perhaps more telling are the relative percentages of the Se \cdots N and Te \cdots N separations compared with their respective sums of the van der Waals radii [10], that is, 3.45 and 3.61 Å, expressed as percentages in Table 13. With one exception, that is, for one of the interactions in **56**, the percentage values indicate the Te \cdots N interactions are relatively stronger than their Se \cdots N counterparts. However, it should also be noted that the generally high values in the listed percentages are consistent with weak intermolecular interactions. Finally, as a general trend, the C–Se \cdots N angles are wider than the corresponding C–Te \cdots N angles in the congeners; N–Se/Te \cdots N angles pertain in **105**. The exceptional pairs of structures are found for co-crystal **41**, where the C–Te \cdots N angle is about 2° wider than C–Se \cdots N, and **56** where each pair of comparable angles is equal within experimental error.

Even though some general trends are evident, the foregoing highlights the influence of global molecular packing upon inherently weak intermolecular interactions. However, high-level calculations on isostructural pairs of structures show the interactions in the tellurium congeners are stronger relative to those in the selenium aggregates of **40** and **41**, reflecting the more significant electron-deficiency of the relevant σ -hole about the more electrophilic tellurium atoms [84, 85].

A much more complicated situation pertains for the sulphur-containing congeners. A total of 26 selenium compounds have sulphur-congeners with one, **121**, having three sulphur-containing polymorphs giving a total of 28 matching molecular structures. Strict isostructural relationships are found in 13 pairs, that is, in nearly half the examples. Seven crystals of sulphur-containing analogues not having an isostructural relationship, that is, about a quarter of the examples, exhibited no comparable S \cdots N secondary-bonding interactions. This leaves eight examples deserving of individual mention.

Firstly, to the isostructural pairs. While isostructural relationships are apparent between 13 pairs of structures this does not imply the formation of structure-directing S \cdots N secondary-bonding interactions in the sulphur-congeners. Referring to the data in Table 13, for the isostructural pairs, in all cases but one, namely **62**, already noted above as being unusual in terms of potential cooperative hydrogen-bonding interactions, the Se \cdots N separation is shorter than the corresponding S \cdots N separation. This is borne out in the comparison of the percentage values for (Se \cdots N/3.45) versus (S \cdots N/3.35) for the congeners. Particularly noteworthy is that in two of the sulphur-congeners, the S \cdots N separation is greater than the assumed sum of the van der Waals radii. This perhaps suggests the secondary-bonding interactions are not structure-directing and arise as a result of the global packing requirements. It is also of interest to compare the C–Se \cdots N and N–Se \cdots N angles with the corresponding angles in their sulphur-congeners. From the data compiled in Table 13, the angles in the latter have increased for seven and decreased for seven S \cdots N contacts in comparison with their heavier congeners, clearly implying no consistent correlation.

Finally, there are eight sulphur-congeners remaining for which special comment is appropriate. Two congeners adopt the same supramolecular aggregate as in the selenium crystals, namely a centrosymmetric dimer and three-dimensional architecture akin to **11** and **123**, respectively, but differ in their crystal symmetry. In the following six examples, the number of S \cdots N contacts is reduced compared with their selenium-congeners. Thus, centrosymmetric dimers are apparent in the sulphur-congener of **110** (tape) and in the three sulphur-congeners of **121** (a two-dimensional array). While the aggregate in **80** is a zig-zag chain, a two-molecule aggregate sustained by a single S \cdots N interaction is evident in the crystal of the sulphur-congener. A supramolecular tape is noted in **115** whereas a helical chain is apparent in the crystal of the sulphur analogue but the S \cdots N separation of 3.593(3) Å is greater than the sum of the van der Waals radii.

Table 13Selected geometric parameters (Å, °) characterizing Se/Te/S \cdots N secondary-bonding interactions in isostructural crystals

Aggregate	Se \cdots N	C–Se \cdots N	Te \cdots N	C–Te \cdots N	%(Se \cdots N/3.45)	%(Te \cdots N/3.61)
	(Å)	(°)	(Å)	(°)		
40	2.964(5)	175.17(17)	2.971(4)	169.91(15)	86	82
41	3.294(5)	156.93(16)	3.164(4)	159.03(15)	96	88
56	3.217(15)	166.4(3)	3.366(15)	165.0(5)	93	93
	3.423(15)	159.2(4)	3.419(15)	160.1(5)	99	95
73	3.327(13)	166.5(6)	3.231(16)	158.3(6)	96	90
74	3.355(2)	171.04(8)	3.428(4)	165.00(14)	97	95
78	3.146(3)	171.94(10)	3.124(5)	167.33(15)	91	87
	3.217(3)	170.79(10)	3.277(5)	162.77(15)	93	91
105 ^{a,b}	2.884(15)	164.4(6)	2.665(17)	157.7(6)	84	74
	3.174(15)	158.6(5)	2.947(17)	149.0(6)	92	82
Aggregate	Se \cdots N	C–Se \cdots N	S \cdots N	C–A \cdots S	%(Se \cdots N/3.45)	%(S \cdots N/3.35)

	(Å)	(°)	(Å)	(°)		
9 ^a	2.820(3)	N 168.11(10)	2.968(4)	175.33(17)	82	89
13 ^a	2.877(5)	N 168.1(2)	3.134(7)	167.5(3)	83	94
14 ^{a,c}	2.88	N 168.4	3.02	166.6	84	90
27 ^a	2.9487(18)	N 157.42(8)	3.164(2)	150.50(9)	86	94
52	3.403(3)	158.66(9)	3.4099(19)	155.61(8)	99	99
62	3.403(3)	133.63(12)	3.3778(19)	136.85(7)	99	98
70 ^c	3.250(5)	151.9(2)	3.38	148.6	94	101
73	3.327(13)	166.5(6)	3.469(6)	169.3(3)	96	104
85	3.1452(19)	161.35(8)	3.309(3)	162.28(12)	91	99
89 ^a	3.155(6)	N 169.16(11)	3.216(11)	167.98(6)	92	96
100 ^a	2.962(3)	N 159.87(12)	3.014(4)	162.93(18)	86	90
140	3.257(7)	157.6(3)	3.292(4)	161.98(13)	94	98
142 ^a	3.043(8)	N 175.9(3)	3.297(4)	154.95(16)	88	98
	3.138(8)	N 159.8(3)	3.309(4)	170.86(15)	91	99

^a Angle is N–Se···N.

b Only the shortest and longest A···N separations are listed; full details are found in Table S13 of the Supplementary Materials.

c Standard uncertainty values for the fractional atomic coordinates are not available.

5. Overview

A systematic survey of the CSD [10] has been conducted for the presence of Se \cdots N secondary-bonding interactions in crystals of molecules containing one selenium atom and nitrogen. A total of 142 crystals were found to feature at least one Se \cdots N contact operating in isolation of other apparent supramolecular synthons. The first crystal structure determined that displayed Se \cdots N interactions was **89** which forms a helical chain; this was published in 1951 [189] with a redetermination in 1989 [126]. The majority of aggregation patterns are zero-dimensional, comprising two-molecule aggregates but there are a small number of examples of three- and four-molecule aggregates. Complimenting the 71 zero-dimensional aggregates are 63 one-dimensional chains encompassing linear, zig-zag and helical chains featuring a single Se \cdots N contact per selenium atom and supramolecular tapes with two Se \cdots N contacts per selenium atom. There are seven examples of crystals featuring Se \cdots N interactions within two-dimensional arrays and one example with Se \cdots N interactions extending in three-dimensions. Selenium(II) compounds are the most represented in the survey, comprising 134 of the examples with the remaining eight crystals containing selenium(IV) centres, there being no examples of selenium(VI) compounds. The overwhelming majority of aggregation arrangements feature a single Se \cdots N interaction per selenium atom with the zero-dimensional aggregates normally sustained in this manner with few exceptions, for example, **53**, **54** and **56**. A similar situation pertains for the one-dimensional chains with notable exceptions being for **69**, **70**, **87** and **104**. Two and three Se \cdots N contacts per selenium are the normal for the two- and three-dimensional aggregates. In summary, 112 of the aggregates feature a single Se \cdots N contact per selenium atom, 26 with two Se \cdots N contacts and four with three.

It is now well established [190, 191], including for supramolecular interactions involving selenium [45, 49, 50], that distance/angle relationships involving these inherently weak interactions is not possible. This is because the interacting donor and acceptor atoms are more

often than not in different environments and hence, subject to varying electronic and steric influences, all of which impacts upon the Se \cdots N interaction. Over and above this, the bonding nature of the Se \cdots N interaction, generally, σ -hole versus π -hole, and the number of Se \cdots N contacts formed by the selenium atom, that is, one, two or three contacts, will also exert a significant influence upon the separation and relevant angles. Further, the conditions under which the X-ray experiments are run, in particular temperature, also impact upon these geometric parameters. As such, this lack of correlation between the magnitude of the Se \cdots N separation and the atom–Se \cdots N angle (more often than not, “atom” is C or N) has been highlighted in sections 3 and 4.

By contrast, angle considerations give insight into the nature of the bonding leading to the Se \cdots N interaction; such information was not readily discerned in the recent survey of Se \cdots O secondary-bonding interactions [50]. A σ -hole chalcogen bond occurs at the extension of atom–Se bond and hence atom–Se \cdots N angles tend to be linear. By contrast, a π -hole interaction will have the selenium positioned plumb to a sp^2 -hybridised nitrogen atom. Based on the geometric data collated in Tables 1-11, the overwhelming majority of Se \cdots N contacts described herein can be classified as chalcogen-bonding interactions, explained in terms of the σ -hole concept of bonding, as the atom–Se \cdots N angles tend to be linear, lying in the range 150-180°. Complimenting this is a small number of aggregates apparently sustained by Se \cdots N interactions best described as π -hole interactions with atom–Se \cdots N angles in the range 90-120°. Even a smaller number of aggregates feature Se \cdots N interactions that do not fall neatly into either category, often with atom–Se \cdots N angles midway between the 180 and 90° extremes. This was highlighted recently in particular for nitrile derivatives, well-represented herein, which were established to have a bimodal distribution of angles when forming X \cdots N \equiv CR halogen bonds [192]. The interplay between σ -hole and π -hole interactions has been discussed in the literature [193-196] and in this context, a recent publication discussed the co-existence of σ -hole and π -

hole Br $\cdots\pi$ (arene) interactions [197]. The latter study employed sophisticated crystallographic investigations and these, along with supporting high-level computational chemistry, are required to resolve the true nature of the bonding in these non-standard systems.

Next, focus is turned to an evaluation of the likelihood of forming Se \cdots N interactions in crystals where such interactions are theoretically possible. A crude guide is simply to ascertain the number of crystals in the CSD where such interactions can possibly occur, that is, in molecules having one selenium atom and at least one nitrogen atom. Such a search, employing the parameters leading to the 142 aggregates included herein, less the distance criterion, yielded 1681 crystals (no additional filtering for duplicates, interactions operating in concert with hydrogen-bonding, etc.) indicating a percentage adoption of approximately 9%. This value is intermediate to the 13% adoption rate for Se \cdots O secondary-bonding interactions [50] and 6% for delocalised [97] selenium(lone-pair) $\cdots\pi$ (arene) interactions [45, 198]; both these surveys allowed for the presence of multi-nuclear selenium compounds. As performed for the recent survey of Se \cdots O secondary-bonding interactions [50], specific classes of compounds were evaluated for their propensity to form secondary-bonding interactions. For example, Se \cdots O secondary-bonding interactions were noted to form 50% of the time when the crystal contained both selenium and carbonyl-oxygen [50]. An analogous analysis was made in the context of Se \cdots N interactions.

It has already been mentioned several times that molecules having a selenadiazole ring, first encountered in **8**, featured prominently in the present survey. Accordingly, a search of the CSD for residues containing a selenadiazole ring in single-selenium atom systems with no substituents at the selenium and nitrogen atoms was conducted. There were 67 examples and given that among the 142 aggregates herein, 50 (32, 13, 4 and 1 in zero-, one-, two- and three-dimensional aggregation patterns, respectively) participated in Se \cdots N interactions: this represents an adoption rate of nearly 75%; early studies point to the high tendency for the

formation of the four-membered $\{\text{SeN}\cdots\}_2$ for these systems [199]. Selenocyanate molecules were also prominent herein. The CSD archives 31 mono-nuclear $\text{RSe-C}\equiv\text{N}$ molecules and these formed $\text{Se}\cdots\text{N}$ interactions in about 50% of cases (13 and 2 examples in one- and two-dimensional aggregation patterns, respectively). To place these percentage values in context, the eight-membered carboxylic acid dimer synthon forms in 33% of (all-organic) crystals [200]. Next to be considered is the pervasive adoption of $\text{Se}\cdots\text{N}$ interactions in polymorphs and within crystals in examples where more than one molecule comprises the crystallographic asymmetric-unit.

There are four pairs of polymorphs among **1-142**. Three pairs, **17 & 20**, **59 & 60** and **92 & 93** adopt the same supramolecular motifs in their respective crystals, namely dimers, linear chains and helical chains, respectively; the dimer for **17** is centrosymmetric whereas for **20**, it is disposed about a 2-fold axis of symmetry. The exception is found for **80** (orthorhombic, $\text{Pna}2_1$ with $Z' = 1$) which forms a zig-zag chain in its crystals in contrast to a polymorph (monoclinic, $\text{P}2_1/\text{c}$, $Z' = 1$) which does not feature analogous interactions, the closest contact of 3.740(7) Å leading to a centrosymmetric dimer [201].

In terms of multiple molecules comprising the asymmetric-unit, there are 34 examples among **1-142**. If one allows molecules to connect via one interaction, implying one molecule is acting as a donor and the other as the acceptor, and disregards the resulting aggregation pattern there are four examples where molecules comprising the asymmetric-unit behave differently when considering the formation of $\text{Se}\cdots\text{N}$ interactions. In **1**, four independent molecules comprise the asymmetric-unit, two associate to form a two-molecule aggregate whereas the remaining two molecules do not form $\text{Se}\cdots\text{N}$ contacts. Four molecules also comprise the asymmetric-unit of **7**, two form a two-molecule aggregate via a single $\text{Se}\cdots\text{N}$ interaction, another forms a centrosymmetric dimer (**45**) whereas the fourth molecule does not form a $\text{Se}\cdots\text{N}$ contact. In **41**, one of the two independent molecules does not form a $\text{Se}\cdots\text{N}$

contact. The asymmetric-unit of **53** is rather complicated as described in section 3.3. Suffice to mention here the second molecule related to the dimer in **53**, does not form a Se \cdots N contact.

While the foregoing has focussed on propensity of Se \cdots N secondary-bonding interactions in crystals of mono-nuclear selenium compounds, a comparison was also made with their congeners. This analysis showed for oxygen-congeners, analogous O \cdots N interactions to those observed in the selenium compounds were not apparent. By contrast, Te \cdots N interactions were always present, sometimes leading to different aggregation patterns. These trends are in accord with expectation [28, 202, 203] with oxygen being least likely to form chalcogen-bonding interactions and tellurium most likely; it is noted that mass spectroscopic evidence for Te \cdots N interactions in the gas-phase has been reported [204]. The greatest number of congeners were noted for sulphur analogues and these presented capricious behaviour. Isostructural relationships were evident but, sometimes the S \cdots N contact was longer than the sum of the van der Waals radii, occasionally S \cdots N contacts persisted in crystals that were not strictly isostructural and in other examples, S \cdots N contacts were not present at all. As alluded to several times, systematic variations in A \cdots N separations were not apparent.

The description and discussion of Se \cdots N interactions in the crystals of mono-nuclear selenium compounds and their relationship with congeners points to an exciting future for investigations in this area, especially when the dimensionality of the supramolecular aggregates can be readily increased by increasing the number of selenium (or tellurium) atoms, having mixed species, etc. While opportunities exist for interesting crystal engineering exercises [30, 33, 205, 206], the importance of chalcogen-bonding in biological applications and materials chemistry provide future impetus for work in this area [32, 207-209].

6. Conclusions

The presence of Se \cdots N secondary-bonding interactions has been established in nearly 9% of crystals of mono-nuclear selenium compounds where such interactions can potentially form. Half of the aggregates stabilised by Se \cdots N interactions are one-dimensional chains and tapes or two- and three-dimensional aggregates. The great propensity of selenadiazole rings and selenocyanates to form Se \cdots N interactions in their crystals is particularly noteworthy. Clearly there is great scope for expanding this supramolecular chemistry into crystal engineering pursuits with potential materials applications.

Declaration of Competing Interest

The author declares that there are no known competing financial interests or personal relationships that could have appeared to influence the work reported in this paper.

Acknowledgements

The author gratefully acknowledges Sunway University Sdn Bhd (Grant no. GRTIN-IRG-01-2021) for support of structural studies.

Appendix A. Supplementary data

Supplementary data associated with this article (details of crystals featuring Se \cdots N secondary-bonding interactions: composition, diagram, distance and angle data, citation and commentary) can be found, in the online version, at doi:10.1016/j.ccr.20201.xx.xxx.

References

- [1] H.A. Bent, Chem. Rev. 68 (1968) 587–648, <https://doi.org/10.1021/cr60255a003>.
- [2] O. Hassel, Science 170 (1970) 497–502, <https://doi.org/10.1126/science.170.3957.497>.
- [3] N.W. Alcock, Adv. Inorg. Chem. Radiochem. 15 (1972) 1–58, [https://doi.org/10.1016/S0065-2792\(08\)60016-3](https://doi.org/10.1016/S0065-2792(08)60016-3).
- [4] N.W. Alcock, Bonding and Structure: Structural Principles in Inorganic and Organic Chemistry, Ellis Horwood, New York, 1990.
- [5] A.S. Mahadevi, G.N. Sastry, Chem. Rev. 116 (2016) 2775–2825, <https://doi.org/10.1021/acs.joc.8b03197>.
- [6] A. Gavezzotti, Acc. Chem. Res. 27 (1994) 309–314, <https://doi.org/10.1021/jp055982e>.
- [7] J.D. Dunitz, A. Gavezzotti, Acc. Chem. Res. 32 (1999) 677–684, <https://doi.org/10.1021/jp509195d>.
- [8] J.D. Dunitz, A. Gavezzotti, Chem. Soc. Rev. 38 (2009) 2622–2633, <https://doi.org/10.1039/B822963P>.
- [9] E.R.T. Tiekink, Chem. Commun. 50 (2014) 11079–11082, <https://doi.org/10.1039/C4CC04972A>.
- [10] R. Taylor, P.A. Wood, Chem. Rev. 119 (2019) 9427–9477, <https://doi.org/10.1021/acs.chemrev.9b00155>.
- [11] G. Cavallo, P. Metrangolo, R. Milani, T. Pilati, A. Priimagi, G. Resnati, G. Terraneo, Chem. Rev. 116 (2016) 2478–2601, <https://doi.org/10.1021/acs.chemrev.5b00484>.
- [12] I. Alkorta, J. Elguero, A. Frontera, Crystals 10 (2020) 180, <https://doi.org/10.3390/cryst10030180>.
- [13] S. Kolb, G. A. Oliver, D. B. Werz, Angew. Chem. Int. Ed. 2020, 59, 22306–22310, <https://doi.org/10.1002/anie.202007314>.

- [14] M. Savastano, *Dalton's Trans.* 50 (2021) 1142–1165, <https://doi.org/10.1039/D0DT04091F>
- [15] S.J. Grabowski, *ChemPhysChem* 15 (2014) 2985–2993, <https://doi.org/10.1002/cphc.201402344>.
- [16] S.J. Grabowski, *Struct. Chem.* 30 (2019) 1141–1152, <https://doi.org/10.1007/s11224-019-01358-1>.
- [17] S. Scheiner, *J. Chem. Phys.* 134 (2011) 094315, <https://doi.org/10.1063/1.3562209>.
- [18] W. Wang, B. Ji, Y. Zhang, *J. Phys. Chem. A* 113 (2009) 8132–8135, <https://doi.org/10.1021/jp904128b>.
- [19] J.S. Murray, P. Lane, T. Clark, P. Politzer, *J. Mol. Model.* 13 (2007) 1033–1038, <https://doi.org/10.1007/s00894-007-0225-4>.
- [20] P. Politzer, J.S. Murray, T. Clark, *Phys. Chem. Chem. Phys.* 12 (2010) 7748–7757, <https://doi.org/10.1039/C004189K>.
- [21] P. Politzer, J.S. Murray, *Phys. Chem. Chem. Phys.* 15 (2013) 11178–11189, <https://doi.org/10.1039/C3CP00054K>.
- [22] P. Politzer, J.S. Murray, *Crystals* 7 (2017) 212, <https://doi.org/10.3390/cryst7070212>.
- [23] J.S. Murray, P. Politzer, *Crystals* 10 (2020) 76, <https://doi.org/10.3390/cryst10020076>.
- [24] A. Bauzá, T.J. Mooibroek, A. Frontera, *ChemPhysChem* 16 (2015) 2496–2517, <https://doi.org/10.1002/cphc.201500314>.
- [25] E.R.T. Tiekink, *Dalton's Trans.* 41 (2012) 6390–6395, <https://doi.org/10.1039/c2dt12225a>.
- [26] H.-L. Seng, E.R.T. Tiekink, *Appl. Organomet. Chem.* 26 (2012) 655–662, <https://doi.org/10.1002/aoc.2928>.
- [27] N.V. Barbosa, C.W. Nogueira, P.A. Nogara, A.F. de Bem, M. Aschner, J.B.T. Rocha, *Metallomics* 9 (2017) 1703–1734, <https://doi.org/10.1039/c7mt00083a>.

- [28] M. Michalczyk, M. Malik, W. Zierkiewicz, S. Scheiner, *J. Phys. Chem. A* 215 (2021) 657–668, <https://doi.org/10.1021/acs.jpca.0c10814>.
- [29] M. Michalczyk, W. Zierkiewicz, R. Wysokiński, S. Scheiner, *Molecules* 24 (2019) 3329, <https://doi.org/10.3390/molecules24183329>.
- [30] E.R.T. Tiekink, *Coord. Chem. Rev.* 345 (2017) 219–228, <https://doi.org/10.1016/j.ccr.2017.01.009>.
- [31] R. Gleiter, G. Haberhauer, D.B. Werz, *Chem. Rev.* 118 (2018) 2010–2041, <https://doi.org/10.1021/acs.chemrev.7b00449>.
- [32] L. Vogel, P. Wonner, S.M. Huber, *Angew. Chem. Int. Ed.* 58 (2019) 1880–1891, <https://doi.org/10.1002/anie.201809432>.
- [33] P. Scilabra, G. Terraneo, G. Resnati, *Acc. Chem. Res.* 52 (2019) 1313–1324, <https://doi.org/10.1021/acs.accounts.9b00037>.
- [34] A.C. Legon, *Phys. Chem. Chem. Phys.* 19 (2017) 14884–14896, <https://doi.org/10.1039/c7cp02518a>.
- [35] A. F. Cozzolino, P. J. W., Elder, I. Vargas-Baca, *Coord. Chem. Rev.* 255 (2011) 1426–1438, <https://doi.org/10.1016/j.ccr.2010.12.015>.
- [36] V. Kumar, Y. Xu, C. Leroy, D.L. Bryce, *Phys. Chem. Chem. Phys.* 22 (2020) 3817–3824, <https://doi.org/10.1039/C9CP06267J>.
- [37] E.R.T. Tiekink, *CrystEngComm* 5 (2003) 101–113, <https://doi.org/10.1039/B301318A>.
- [38] M.A. Buntine, F.J. Kosovel, E.R.T. Tiekink, *CrystEngComm* 5 (2003) 331–336, <https://doi.org/10.1039/B308922C>.
- [39] Y. Liu, E.R.T. Tiekink, *CrystEngComm* 7 (2005) 20–27, <https://doi.org/10.1039/B416493H>.
- [40] E.R.T. Tiekink, *CrystEngComm* 8 (2006) 104–118, <https://doi.org/10.1039/B517339F>.

- [41] C.S. Lai, E.R.T. Tiekink, Z. Kristallogr. Cryst. Mater. 222 (2007) 532–538, <https://doi.org/10.1524/zkri.2007.222.10.532>.
- [42] E.R.T. Tiekink, Appl. Organomet. Chem. 22 (2008) 533–550, <https://doi.org/10.1002/aoc.1441>.
- [43] E.R.T. Tiekink, J. Zukerman-Schpector, Coord. Chem. Rev. 254 (2010) 46–76, <https://doi.org/10.1016/j.ccr.2009.09.007>.
- [44] I. Caracelli, J. Zukerman-Schpector, E.R.T. Tiekink, Coord. Chem. Rev. 256 (2012) 412–438, <https://doi.org/10.1016/j.ccr.2011.10.021>.
- [45] I. Caracelli, I. Haiduc, J. Zukerman-Schpector, E.R.T. Tiekink, Coord. Chem. Rev. 257 (2013) 2863–2879, <https://doi.org/10.1016/j.ccr.2013.05.022>.
- [46] I. Caracelli, I. Haiduc, J. Zukerman-Schpector, E. R. T. Tiekink, Coord. Chem. Rev. 281 (2014) 50–63, <https://doi.org/10.1016/j.ccr.2014.09.001>.
- [47] E.R.T. Tiekink, Crystals 8 (2018) 292, <https://doi.org/10.3390/cryst8070292>.
- [48] S.M. Lee, P.J. Heard, E.R.T. Tiekink, Coord. Chem. Rev. 375 (2018) 410–423, <https://doi.org/10.1016/j.ccr.2018.03.001>.
- [49] E.R.T. Tiekink, Crystals 10 (2020) 503, <https://doi.org/10.3390/cryst10060503>.
- [50] E.R.T. Tiekink, Coord. Chem. Rev. 427 (2021) 213586, <https://doi.org/10.1016/j.ccr.2020.213586>.
- [51] E.R.T. Tiekink, Crystals 11 (2021) 433, <https://doi.org/10.3390/cryst11040433>.
- [52] I.J. Bruno, J.C. Cole, P.R. Edgington, M. Kessler, C.F. Macrae, P. McCabe, J. Pearson, R. Taylor, Acta Crystallogr., Sect. B: Struct. Sci., Cryst. Eng. Mater. 58 (2002) 389–397, <https://doi.org/10.1107/S0108768102003324>.
- [53] A. Spek, Acta Crystallogr., Sect. E: Cryst. Commun. 76 (2020) 1–11, <https://doi.org/10.1107/S2056989019016244>.

- [54] K. Brandenburg, DIAMOND. Visual Crystal Structure Information System, version 3.1, Crystal Impact, Bonn, Germany, 2006.
- [55] D. Gallenkamp, E.R.T. Tiekink, F. Mohr, Phosphorus, Sulfur, Silicon, Relat. Elem. 183 (2008) 1050–1056, <https://doi.org/10.1080/10426500801901087>.
- [56] A. Chand, D.K. Sahoo, A. Rana, S. Jena, H.S. Biswal, Acc. Chem. Res. 53 (2020) 1580–1592, <https://doi.org/10.1021/acs.accounts.0c00289>.
- [57] P.C. Ho, J. Rafique, J. Lee, L.M. Lee, H.A. Jenkins, J.F. Britten, A.L. Braga, I. Vargas-Baca, Dalton Trans. 46 (2017) 6570–6579, <https://doi.org/10.1039/C7DT00612H>.
- [58] S. Goswami, A. Hazra, R. Chakrabarty, H.-K. Fun, Org. Lett. 11 (2009) 4350–4353, <https://doi.org/10.1021/ol901737s>.
- [59] S. Alvarez, Dalton Trans. 42 (2013) 8617–8636, <https://doi.org/10.1039/C3DT50599E>.
- [60] A. Mukherjee, G.R. Desiraju, IUCrJ 1 (2014) 49–60, <https://doi.org/10.1107/S2052252513025657>.
- [61] Y. Balmohammadi, H.R. Khavasi, S.S. Naghavi, CrystEngComm 22 (2020) 2756–2765, <https://doi.org/10.1039/C9CE01885A>.
- [62] P. Politzer, J.S. Murray, Struct. Chem. 32 (2021) 623–629, <https://doi.org/10.1007/s11224-020-01713-7>.
- [63] A.Yu. Makarov, V.V. Zhivonitko, A.G. Makarov, S.B. Zikirin, I.Yu. Bagryanskaya, V.A. Bagryansky, Yu.V. Gatilov, I.G. Irtegorova, M.M. Shakirov, A.V. Zibarev, Inorg. Chem. 50 (2011) 3017–3027, <https://doi.org/10.1021/ic102565x>.
- [64] G. Karabanovich, J. Roh, Z. Padělková, Z. Novák, K. Vávrová, A. Hrabálek, Tetrahedron 69 (2013) 8798–8808, <https://doi.org/10.1016/j.tet.2013.07.103>.
- [65] G. Hua, J. Du, A.M.Z. Slawin, J.D. Woollins, J. Org. Chem. 79 (2014) 3876–3886, <https://doi.org/10.1021/jo500316v>.

- [66] J.M. White, J.B. Lambert, M. Spiniello, S.A. Jones, R.W. Gable, *Chem. - Eur. J.* 8 (2002) 2799–2811, [https://doi.org/10.1002/1521-3765\(20020617\)8:12<2799::AID-CHEM2799>3.0.CO;2-Y](https://doi.org/10.1002/1521-3765(20020617)8:12<2799::AID-CHEM2799>3.0.CO;2-Y).
- [67] Y. Li, G.-X. Hua, A.M.Z. Slawin, J.D. Woollins, *Molecules* 14 (2009) 884–892, <https://doi.org/10.3390/molecules14020884>.
- [68] T. Pasinszki, D. Dzsotján, G.G. Lajgut, V. Harmat, A. Bor, I. Zupkó, A. Csámpai, J. *Organomet. Chem.* 863 (2018) 70–76, <https://doi.org/10.1016/j.jorganchem.2018.03.031>.
- [69] K. Eichstaedt, A. Wasilewska, B. Wicher, M. Gdaniec, T. Połośki, *Cryst. Growth Des.* 16 (2016) 1282–1293, <https://doi.org/10.1021/acs.cgd.5b01356>.
- [70] B.D. Lindner, B.A. Coombs, M. Schaffroth, J.U. Engelhart, O. Tverskoy, F. Rominger, M. Hamburger, U.H.F. Bunz, *Org. Lett.* 15 (2013) 666–669, <https://doi.org/10.1021/ol303490b>.
- [71] B.A. Coombs, B.D. Lindner, R.M. Edkins, F. Rominger, A. Beeby, U.H.F. Bunz, *New J. Chem.* 36 (2012) 550–553, <https://doi.org/10.1039/c2nj20847d>.
- [72] N.L. Klimasenko, L.A. Chetkina, G.A. Gol'der, *Zh. Strukt. Khim.* 14 (1973) 515–520.
- [73] S. Deng, D. Zeng, Y. Luo, J. Zhao, X. Li, Z. Zhao, T. Chen, *RSC Adv.* 7 (2017) 16721–16729, <https://doi.org/10.1039/C6RA28801D>.
- [74] D.O. Prima, E.V. Vorontsova, A.G. Makarov, A.Yu. Makarov, I.Yu. Bagryanskaya, T.F. Mikhailovskaya, Y.G. Slizhov, A.V. Zibarev, *Mendeleev Commun.* 27 (2017) 439–442, <https://doi.org/10.1016/j.mencom.2017.09.002>.
- [75] J. Xiao, X. Xiao, Y. Zhao, B. Wu, Z. Liu, X. Zhang, S. Wang, X. Zhao, L. Liu, L. Jiang, *Nanoscale* 5 (2013) 5420–5425, <https://doi.org/10.1039/C3NR00523B>.
- [76] S. Ghosh, S. Das, N.R. Kumar, A.R. Agrawal, S.S. Zade, *New J. Chem.* 41 (2017) 11568–11575, <https://doi.org/10.1039/C7NJ02394D>.

- [77] S. Mondal, M. Konda, B. Kauffmann, M.K. Manna, A.K. Das, *Cryst. Growth Des.* 15 (2015) 5548–5554, <https://doi.org/10.1021/acs.cgd.5b01179>.
- [78] M. Mellini, S. Merlino, *Acta Crystallogr., Sect. B: Struct. Crystallogr. Cryst. Chem.* 32 (1976) 1074–1078, <https://doi.org/10.1107/S056774087600469X>.
- [79] H. Ouahine, M. Ait Ali, L. El Firdoussi, A. Spannenberg, *IUCrData* 2 (2017) x170226, <https://doi.org/10.1107/S2414314617002267>.
- [80] K. Selvakumar, H.B. Singh, N. Goel, U.P. Singh, R.J. Butcher, *Chem. - Eur. J.* 18 (2012) 1444–1457, <https://doi.org/10.1002/chem.201003725>.
- [81] P.B. Pati, S.S. Zade, *Cryst. Growth Des.* 14 (2014) 1695–1700, <https://doi.org/10.1021/cg401830f>.
- [82] J. Lee, L.M. Lee, Z. Arnott, H. Jenkins, J.F. Britten, I. Vargas-Baca, *New J. Chem.* 42 (2018) 10555–10562, <https://doi.org/10.1039/C8NJ00553B>.
- [83] S. Plebst, M. Bubrin, D. Schweinfurth, S. Zális, W. Kaim, *Z. Naturforsch., B: Chem. Sci.* 72 (2017) 839–846, <https://doi.org/10.1515/znb-2017-0100>.
- [84] N. Biot, D. Bonifazi, *Chem. - Eur. J.* 24 (2017) 5439–5443, <https://doi.org/10.1002/chem.201705428>.
- [85] N. Biot, D. Bonifazi, *Chem. - Eur. J.* 26 (2020) 2904–2913, <https://doi.org/10.1002/chem.201904762>.
- [86] S. Saravanan, K. Namitharan, S. Muthusubramanian, *Indian J. Chem., Sect. B: Org. Chem. Incl. Med. Chem.* 47 (2008) 305–309.
- [87] A. Marx, S. Saravanan, S. Muthusubramanian, V. Manivannan, N.P. Rath, *Acta Crystallogr., Sect. E: Struct. Rep. Online* 64 (2008) o349, <https://doi.org/10.1107/S1600536807067487>.
- [88] P. Arsenyan, K. Oberte, S. Belyakov, *Chem. Heterocycl. Compd.* (2007) 289–293, <https://doi.org/10.1007/s10593-007-0036-7>.

- [89] P. Arsenyan, K. Oberte, K. Rubina, S. Belyakov, E. Lukevics, *Chem. Heterocycl. Compd.* (2004) 599–603.
- [90] L.S. Konstantinova, I.V. Baranovsky, E.A. Pritchina, M.S. Mikhailov, I.Yu. Bagryanskaya, N.A. Semenov, I.G. Irtegorova, G.E. Salnikov, K.A. Lyssenko, N.P. Gritsan, A.V. Zibarev, O.A. Rakitin, *Chem. - Eur. J.* 23 (2017) 17037–17047, <https://doi.org/10.1002/chem.201703182>.
- [91] S. J. Balkrishna, B. S. Bhakuni, S. Kumar, *Tetrahedron* 67 (2011) 9565–9575, <https://doi.org/10.1016/j.tet.2011.09.141>.
- [92] G.L. Sommen, A. Linden, H. Heimgartner, *Helv. Chim. Acta* 90 (2007) 472–487, <https://doi.org/10.1002/hlca.200790051>.
- [93] V.N. Nesterov, V.D. Dyachenko, Yu.A. Sharanin, Yu.T. Struchkov, *Russ. Chem. Bull.* (1994) 118–120, <https://doi.org/10.1007/BF00699148>.
- [94] D.S. Lamani, D. Bhowmick, G. Mugesh, *Org. Biomol. Chem.* 10 (2012) 7933–7943, <https://doi.org/10.1039/c2ob26156a>.
- [95] Y.-S. Zhu, Y. Xue, W. Liu, X. Zhu, X.-Q. Hao, M.-P. Song, *J. Org. Chem.* 85 (2020) 9106–9116, <https://doi.org/10.1021/acs.joc.0c01035>.
- [96] M. Seredyuk, I.O. Fritsky, R. Krämer, H. Kozłowski, M. Haukka, P. Gütllich, *Tetrahedron* 66 (2010) 8772–8777, <https://doi.org/10.1016/j.tet.2010.08.071>.
- [97] D. Schollmeyer, O. V. Shishkin, T. Rühl, M. O. Vysotsky, *CrystEngComm* 10 (2008) 715–723, <https://doi.org/10.1039/B716442D>.
- [98] A. Kremer, A. Fermi, N. Biot, J. Wouters, D. Bonifazi, *Chem. - Eur. J.* 22 (2016) 5665–5675, <https://doi.org/10.1002/chem.201504328>.
- [99] S. Dhole, J.-Y. Liao, S. Kumar, D.B. Salunke, C.-M. Sun, *Adv. Synth. Catal.* 360 (2018) 942–950, <https://doi.org/10.1002/adsc.201701256>.

- [100] M. Velusamy, K.R.J. Thomas, J.T. Lin, Y.S. Wen, *Tetrahedron Lett.* 46 (2005) 7647–7651, <https://doi.org/10.1016/j.tetlet.2005.08.166>.
- [101] T.M. Klapötke, B. Krumm, K. Polborn, *Eur. J. Inorg. Chem.* (1999) 1359–1366, [https://doi.org/10.1002/\(SICI\)1099-0682\(199908\)1999:8<1359::AID-EJIC1359>3.3.CO;2-3](https://doi.org/10.1002/(SICI)1099-0682(199908)1999:8<1359::AID-EJIC1359>3.3.CO;2-3).
- [102] M.J. Nasim, K. Witek, A. Kincses, A.Y. Abdin, E. Źeslawska, M.A. Marć, M. Gajdács, G. Spengler, W. Nitek, G. Latacz, E. Karczewska, K. Kieć-Kononowicz, J. Handzlik, C. Jacob, *New J. Chem.* 43 (2019) 6021–6031, <https://doi.org/10.1039/C9NJ00563C>.
- [103] K. Maartmann-Moe, K.A. Sanderud, J. Songstad, *Acta Chem. Scand.* 38 (1984) 187–200, <https://doi.org/10.3891/acta.chem.scand.38a-0187>.
- [104] G.L. Sommen, A. Linden, H. Heimgartner, *Tetrahedron* 62 (2006), 62, 3344–3354, <https://doi.org/10.1016/j.tet.2006.01.077>.
- [105] J.G. Leal, A.C. Sauer, J.C.P. Mayer, S.T. Stefanello, D.F. Gonçalves, F.A.A. Soares, B.A. Iglesias, D.F. Back, O.E.D. Rodrigues, L. Dornelles, *New J. Chem.* 41 (2017) 5875–5883, <https://doi.org/10.1039/C7NJ00920H>.
- [106] F. Cui, J. Chen, Z. Mo, S. Su, Y. Chen, X. Ma, H. Tang, H. Wang, Y. Pan, Y. Xu, *Org. Lett.* 20 (2018) 925–929, <https://doi.org/10.1021/acs.orglett.7b03734>.
- [107] L.R.S. Camargo, J. Zukerman-Schpector, A.M. Deobald, A.L. Braga, E.R.T. Tiekink, *Acta Crystallogr., Sect. E: Cryst. Commun.* 71 (2015) o202–o203, <https://doi.org/10.1107/S2056989015003230>.
- [108] P. Dubey, S. Gupta, A.K. Singh, *Dalton Trans.* 47 (2018) 3764–3774, <https://doi.org/10.1039/C7DT04326K>.
- [109] G. Mazumder, M. De, A. Mukhopadhyay, A.K. Das, S.K. Mazumdar, V. Bertolasi, R.F. Schinazi, *J. Chem. Crystallogr.* 29 (1999) 837–839, <https://doi.org/10.1023/A:1009560106913>.

- [110] N.A. Barnes, S.M. Godfrey, R.T.A. Halton, I. Mushtaq, S. Parsons, R.G. Pritchard, M. Sadler, *Polyhedron* 26 (2007) 1053–1060, <https://doi.org/10.1016/j.poly.2006.09.083>.
- [111] G. Hua, Y. Li, A.L. Fuller, A.M.Z. Slawin, J.D. Woollins, *Eur. J. Org. Chem.* (2009) 1612–1618, <https://doi.org/10.1002/ejoc.200900013>.
- [112] D.B. Cordes, G. Hua, A.M.Z. Slawin, J.D. Woollins, *Acta Crystallogr., Sect. C: Cryst. Struct. Commun.* 67 (2011) o509–o514, <https://doi.org/10.1107/S0108270111049900>.
- [113] Y. Liu, X.-L. Chen, K. Sun, X.-Y. Li, F.-L. Zeng, X.-C. Liu, L.-B. Qu, Y.-F. Zhao, B. Yu, *Org. Lett.* 21 (2019) 4019–4024, <https://doi.org/10.1021/acs.orglett.9b01175>.
- [114] S.J. Dunne, L.A. Summers, E.I. von Nagy-Felsobuki, M.F. Mackay, *Acta Crystallogr., Sect. C: Cryst. Struct. Commun.* 50 (1994) 971–974, <https://doi.org/10.1107/S0108270193013927>.
- [115] A.G. Makarov, A.Yu. Makarov, I.Yu. Bagryanskaya, M.M. Shakirov, A.V. Zibarev, *J. Fluorine Chem.* 144 (2012) 118–123, <https://doi.org/10.1016/j.jfluchem.2012.08.002>.
- [116] P. Arsenyan, E. Paegle, S. Belyakov, I. Shestakova, E. Jaschenko, I. Domracheva, J. Popelis, *Eur. J. Med. Chem.* 46 (2011) 3434–3443, <https://doi.org/10.1016/j.ejmech.2011.05.008>.
- [117] S. Aboulkacem, D. Naumann, W. Tyrra, I. Pantenburg, *Organometallics* 31 (2012) 1559–1565, <https://doi.org/10.1021/om201195j>.
- [118] S. Chitra, N. Paul, S. Muthusubramanian, P. Manisankar, P. Yogeewari, D. Sriram, *Eur. J. Med. Chem.* 46 (2011) 5465–5472, <https://doi.org/10.1016/j.ejmech.2011.09.007>.
- [119] T. Fellowes, J.M. White, *CrystEngComm* 21 (2019) 1539–1542, <https://doi.org/10.1039/C8CE01853G>.
- [120] M. Matsumura, Y. Sakata, A. Iwase, M. Kawahata, Y. Kitamura, Y. Murata, N. Kakusawa, K. Yamaguchi, S. Yasuike, *Tetrahedron Lett.* 57 (2016) 5484–5488, <https://doi.org/10.1016/j.tetlet.2016.10.095>.

- [121] A.S. Potapov, N.P. Chernova, V.D. Ogorodnikov, T.V. Petrenko, A.I. Khlebnikov, *Sci. World J.* 2014 (2014) 578762, <https://doi.org/10.1155/2014/578762>.
- [122] J. Fleischhauer, R. Beckert, D. Hornig, W. Gunther, H. Görls, V. Klimesova, *Z. Naturforsch., B: Chem. Sci.* 63 (2008) 415–424.
- [123] G.L. Sommen, A. Linden, H. Heimgartner, *Helv. Chim. Acta* 91 (2008) 209–219, <https://doi.org/10.1002/hlca.200890025>.
- [124] Z. Wei, X. Li, F. Wudl, Y. Zheng, *Tetrahedron* 73 (2017) 7100–7104, <https://doi.org/10.1016/j.tet.2017.10.072>.
- [125] T. Suzuki, T. Tsuji, T. Okubo, A. Okada, Y. Obana, T. Fukushima, T. Miyashi, Y. Yamashita, *J. Org. Chem.* 66 (2001) 8954–8960, <https://doi.org/10.1021/jo010808h>.
- [126] A.C. Gomes, G. Biswas, A. Banerjee, W.L. Duax, *Acta Crystallogr., Sect. C: Cryst. Struct. Commun.* 45 (1989) 73–75, <https://doi.org/10.1107/S0108270188008376>.
- [127] H.-C. Ting, Y.-H. Chen, L.-Y. Lin, S.-H. Chou, Y.-H. Liu, H.-W. Lin, K.-T. Wong, *ChemSusChem* 7 (2014) 457–465, <https://doi.org/10.1002/cssc.201301090>.
- [128] L.S. Konstantinova, I.E. Bobkova, Y.V. Nelyubina, E.A. Chulanova, I.G. Irtegov, N.V. Vasilieva, P.S. Camacho, S.E. Ashbrook, G. Hua, A.M.Z. Slawin, J. D. Woollins, A.V. Zibarev, O.A. Rakitin, *Eur. J. Org. Chem.* (2015) 5585–5593, <https://doi.org/10.1002/ejoc.201500742>.
- [129] H. Wang, J. Liu, W. Wang, *Phys. Chem. Chem. Phys.* 20 (2018) 5227–5253, <https://doi.org/10.1039/C7CP08215K>.
- [130] J.-A. Xiao, Y.-C. Li, X.-L. Cheng, W.-Q. Chen, J.-G. Cui, Y.-M. Huang, J. Huang, Q. Xiao, W. Su, H. Yang, *Org. Chem. Front.* 6 (2019) 1967–1971, <https://doi.org/10.1039/C9QO00358D>.
- [131] P.G. Jones, C. Wismach, G. Mugesh, W.-W. du Mont, *Acta Crystallogr., Sect. E: Struct. Rep. Online* 58 (2002) o1298–o1300, <https://doi.org/10.1107/S1600536802019323>.

- [132] T. Asamizu, W. Henderson, B.K. Nicholson, *J. Organomet. Chem.* 761 (2014) 103–110, <https://doi.org/10.1016/j.jorganchem.2014.03.005>.
- [133] K. Sidoryk, L. Rárová, J. Oklešťková, Z. Pakulski, M. Strnad, P. Cmoch, R. Luboradzki, *Org. Biomol. Chem.* 14 (2016) 10238–10248, <https://doi.org/10.1039/C6OB01938B>.
- [134] A.V. Kachanov, A.V. Zamaraev, A.V. Gerasimenkoc, K.V. Maslov, O.Yu. Slabko, V.A. Kaminskii, *Synlett* 29 (2018) 2035–2038, <https://doi.org/10.1055/s-0037-1609939>.
- [135] M. Yamada, M. Matsumura, E. Sakaki, S. Yen, M. Kawahata, T. Hyodo, K. Yamaguchi, Y. Murata, S. Yasuike, *Tetrahedron* 75 (2019) 1406–1414, <https://doi.org/10.1016/j.tet.2019.01.056>.
- [136] P. Arsenyan, A. Petrenko, S. Belyakov, *Tetrahedron* 71 (2015) 2226–2233, <https://doi.org/10.1016/j.tet.2015.02.078>.
- [137] T.F. Mikhailovskaya, A.G. Makarov, N.Yu. Selikhova, A.Yu. Makarov, E.A. Pritchina, I.Yu. Bagryanskaya, E.V. Vorontsova, I.D. Ivanov, V.D. Tikhova, N.P. Gritsan, Y.G. Slizhov, A.V. Zibarev, *J. Fluorine Chem.* 183 (2016) 44–58, <https://doi.org/10.1016/j.jfluchem.2016.01.009>.
- [138] A.L. Rheingold, Private Communication to the Cambridge Structural Database (2019) Refcode LOSMAK.
- [139] A.G. Makarov, N.Yu. Selikhova, A.Yu. Makarov, V.S. Malkov, I.Yu. Bagryanskaya, Y.V. Gatilov, A.S. Knyazev, Y.G. Slizhov, A.V. Zibarev, *J. Fluorine Chem.* 165 (2014) 123–131, <https://doi.org/10.1016/j.jfluchem.2014.06.019>.
- [140] W. Tian, S. Grivas, K. Olsson, *J. Chem. Soc., Perkin Trans. 1* (1993) 257–261, <https://doi.org/10.1039/p19930000257>.
- [141] H.A. Patel, V.J. Bhanvadia, H.M. Mande, S.S. Zade, A.L. Patel, *Org. Biomol. Chem.* 17 (2019) 9467–9478, <https://doi.org/10.1039/C9OB01762C>.

- [142] N.A. Barnes, S.M. Godfrey, R.T.A. Halton, I. Mushtaq, S. Parsons, R.G. Pritchard, M. Sadler, *Polyhedron* 26 (2007) 1053–1060, <https://doi.org/10.1016/j.poly.2006.09.083>.
- [143] M. Bürger, S.H. Röttger, M.N. Loch, P.G. Jones, D.B. Werz, *Org. Lett.* 22 (2020) 5025–5029, <https://doi.org/10.1021/acs.orglett.0c01582>.
- [144] T. Suzuki, Y. Yamashita, T. Fukushima, T. Miyashi, *Mol. Cryst. Liq. Cryst. Sci. Technol., Sect. A* 296 (1997) 165–180, <https://doi.org/10.1080/10587259708032319>.
- [145] T.M. Klapötke, B. Krumm, M. Scherr, *Inorg. Chem.* 47 (2008) 7025–7028, <https://doi.org/10.1021/ic801011g>.
- [146] D. Bhatt, P. Raj Singh, P. Kalaramna, K. Kumar, A. Goswami. *Adv. Synth. Catal.* 361 (2019) 5483–5489, <https://doi.org/10.1002/adsc.201900791>.
- [147] G. Mukherjee, P. Singh, C. Ganguri, S. Sharma, H.B. Singh, N. Goel, U.P. Singh, R.J. Butcher, *Inorg. Chem.* 51 (2012) 8128–8140, <https://doi.org/10.1021/ic3005272>.
- [148] C.P. Morley, S. Ford, M. Di Vaira, *Polyhedron* 23 (2004) 2967–2973, <https://doi.org/10.1016/j.poly.2004.08.011>.
- [149] R. Centore, F. Borbone, A. Carella, M. Causà S. Fusco, F.S. Gentile, E. Parisi, *Cryst. Growth Des.* 20 (2019) 1229–1236, <https://doi.org/10.1021/acs.cgd.9b01491>.
- [150] N.A. Semenov, E.A. Radiush, E.A. Chulanova, A.M.Z. Slawin, J.D. Woollins, E.M. Kadilenko, I.Yu. Bagryanskaya, I.G. Irtegorova, A.S. Bogomyakov, L.A. Shundrin, N.P. Gritsan, A.V. Zibarev, *New J. Chem.* 43 (2019) 16331–16337, <https://doi.org/10.1039/C9NJ04069B>.
- [151] E.A. Sutturina, N.A. Semenov, A.V. Lonchakov, I.Yu. Bagryanskaya, Y.V. Gatilov, I.G. Irtegorova, N.V. Vasilieva, E. Lork, R. Mews, N.P. Gritsan, A.V. Zibarev, *J. Phys. Chem. A* 115 (2011) 4851–4860, <https://doi.org/10.1021/jp2019523>.
- [152] T. Fellowes, M.P. Van Koeverden, J.M. White, *CrystEngComm* 22 (2020) 4023–4029, <https://doi.org/10.1039/D0CE00662A>.

- [153] V.F. Kaminskii, R.P. Shibaeva, M.Z. Aldoshina, R.N. Lyubovskaya, M.L. Khidekel, J. Struct. Chem. 20 (1979) 130–133, <https://doi.org/10.1007/BF00746308>.
- [154] V. Kumar, Y. Xu, D.L. Bryce, Chem. - Eur. J. 26 (2020) 3275–3286, <https://doi.org/10.1002/chem.201904795>.
- [155] S. Fritz, C. Ehm, D. Lentz, Inorg. Chem. 54 (2015) 5220–5231, <https://doi.org/10.1021/acs.inorgchem.5b00107>.
- [156] T. Maaninen, T. Chivers, R. Laitinen, G. Schatte, M. Nissinen, Inorg. Chem. 39 (2000) 5341–5347, <https://doi.org/10.1021/ic000598b>.
- [157] A.W. Cordes, K. Bestari, R.T. Oakley, Acta Crystallogr., Sect. C: Cryst. Struct. Commun. 46 (1990) 504–506, <https://doi.org/10.1107/S0108270189011753>.
- [158] H.W. Roesky, U. Scholz, M. Noltemeyer, Z. Anorg. Allg. Chem. 576 (1989) 255–266, <https://doi.org/10.1002/zaac.19895760129>.
- [159] K. Srivastava, T. Chakraborty, H.B. Singh, R.J. Butcher, Dalton Trans. 40 (2011) 4489–4496, <https://doi.org/10.1039/c0dt01319f>.
- [160] F.A. Amundsen, L.K. Hansen, A. Hordvik, Acta Chem. Scand. 36 (1982) 673–681, <https://doi.org/10.3891/acta.chem.scand.36a-0673>.
- [161] R.T. Oakley, R.W. Reed, A.W. Cordes, S.L. Craig, J.B. Graham, J. Am. Chem. Soc. 109 (1987) 7745–7749, <https://doi.org/10.1021/ja00259a024>.
- [162] K.S. Eccles, R.E. Morrison, A.R. Maguire, S.E. Lawrence, Cryst. Growth Des. 14 (2014) 2753–2762, <https://doi.org/10.1021/cg401891f>.
- [163] T. Hayashi, K. Nakata, Y. Takaki, K. Sakurai, Bull. Chem. Soc. Jpn. 53 (1980) 801–802, <https://doi.org/10.1246/bcsj.53.801>.
- [164] A. Schönleber, P. Pattison, G. Chapuis, Z. Kristallogr. Cryst. Mater. 218 (2003), 218, 507–513, <https://doi.org/10.1524/zkri.218.7.507.20713>.

- [165] M.S. Khan, B. Ahrens, M.F. Mahon, L. Male, P.R. Raithby, *Acta Crystallogr., Sect. E: Struct. Rep. Online* 58 (2002) o1202–o1203, <https://doi.org/10.1107/S1600536802017993>.
- [166] N.L. Klimasenko, L.A. Chetkina, S.L. Ginzburg, M.G. Neigauz, E.M. Smelyanskaya, *Zh. Strukt. Khim.* 14 (1973) 108–115.
- [167] L.A. Chetkina, S.L. Ginzburg, M.G. Neigauz, G.A. Gol'der, *Zh. Strukt. Khim.* 13 (1972) 91–98.
- [168] B.D. Lindner, F. Paulus, A.L. Appleton, M. Schaffroth, J.U. Engelhart, K.M. Schelkle, O. Tverskoy, F. Rominger, M. Hamburger, U.H.F. Bunz, *J. Mater. Chem. C* 2 (2014) 9609–9612, <https://doi.org/10.1039/C4TC01992J>.
- [169] M. Mellini, S. Merlino, *Acta Crystallogr., Sect. B: Struct. Crystallogr. Cryst. Chem.* 32 (1976) 1079–1082, <https://doi.org/10.1107/S0567740876004706>.
- [170] A.J. Mayr, B. Carrasco-Flores, F. Cervantes-Lee, K.H. Pannell, L. Párkányi, K. Raghuveer, *J. Organomet. Chem.* 405 (1991) 309–322, [https://doi.org/10.1016/0022-328X\(91\)86290-7](https://doi.org/10.1016/0022-328X(91)86290-7).
- [171] L.-L. Tian, S. Lu, Z.-H. Zhang, E.-L. Huang, H.-T. Yan, X. Zhu, X.-Q. Hao, M.-P. Song, *J. Org. Chem.* 84 (2019) 5213–5221, <https://doi.org/10.1021/acs.joc.9b00186>.
- [172] Y.-T. Huang, W.-C. Wang, C.-P. Hsu, W.-Y. Lu, W.-J. Chuang, M. Y. Chiang, Y.-C. Lai, H.-Y. Chen, *Polym. Chem.* 7 (2016) 4367–4377, <https://doi.org/10.1039/C6PY00569A>.
- [173] K. Moribe, M. Tsuchiya, Y. Tozuka, K. Yamaguchi, T. Oguchi, K. Yamamoto, *J. Inclusion Phenom. Macrocyclic Chem.* 54 (2006) 9–16, <https://doi.org/10.1007/s10847-005-3183-4>.
- [174] Z.V. Zvonkova, A.N. Khvatkina, *Kristallografiya* 10 (1965) 734–737.
- [175] O. Franco, G. Reck, I. Orgzall, B.W. Schulz, B. Schulz, *J. Mol. Struct.* 649 (2003) 219–230, [https://doi.org/10.1016/S0022-2860\(02\)00569-0](https://doi.org/10.1016/S0022-2860(02)00569-0).

- [176] T. Kotipalli, V. Kavala, A. Konala, D. Janreddy, C.-W. Kuo, C.-F. Yao, *Adv. Synth. Catal.* 358 (2016) 2652–2660, <https://doi.org/10.1002/adsc.201600274>.
- [177] S.-Z. Hu, D. Shi, T. Huang, J. Wan, Z. Huang, J. Yang, C. Xu, *Inorg. Chim. Acta* 173 (1990) 1–4, [https://doi.org/10.1016/S0020-1693\(00\)91046-6](https://doi.org/10.1016/S0020-1693(00)91046-6).
- [178] N.V. Likhanova, R. Martínez-Palou, M.A. Veloz, D.J. Matías, V.E. Reyes-Cruz, H. Höpfl, O. Olivares, J. Heterocycl. Chem. 44 (2007) 145–153, <https://doi.org/10.1002/jhet.5570440123>.
- [179] A.E. Mistryukov, I.D. Sadekov, V.S. Sergienko, G.M. Abakarov, M.A. Porai-Koshits, A.A. Schneider, A.D. Garnovskii, *Khim. Geterosikl. Soedin.* (1989) 1690–1692.
- [180] V.P. Kuznetsov, L.D. Patsenker, A.I. Lokshin, A.V. Tolmachev, *Kristallografiya* 43 (1998) 468–477.
- [181] O.K. Sakka, D.H. Fleita, W.T.A. Harrison, *Acta Crystallogr., Sect. E: Struct. Rep. Online* 69 (2013) o350, <https://doi.org/10.1107/S160053681300216X>.
- [182] A.F. Cozzolino, J.F. Britten, I. Vargas-Baca, *Cryst. Growth Des.* 6 (2006) 181–186, <https://doi.org/10.1021/cg050260y>.
- [183] M.R. Ams, N. Trapp, A. Schwab, J.V. Milić, F. Diederich, *Chem. - Eur. J.* 25 (2019) 323–333, <https://doi.org/10.1002/chem.201804261>.
- [184] A.S. Batsanov, Yu.T. Struchkov, *J. Struct. Chem.* 26 (1985) 52–56, <https://doi.org/10.1007/BF00747762>.
- [185] A.F. Cozzolino, P.S. Whitfield, I. Vargas-Baca, *J. Am. Chem. Soc.* 132 (2010) 17265–17270, <https://doi.org/10.1021/ja107252f>.
- [186] A.L. Rheingold, Private Communication to the Cambridge Structural Database (2019) Refcode LOSLUD.

- [187] N.A. Semenov, N.A. Pushkarevsky, J. Beckmann, P. Finke, E. Lork, R. Mews, I.Yu. Bagryanskaya, Y.V. Gatilov, S.N. Konchenko, V.G. Vasiliev, A.V. Zibarev, *Eur. J. Inorg. Chem.* (2012) 3693–3703, <https://doi.org/10.1002/ejic.201200376>.
- [188] A.W. Cordes, P.J. Haynes, P.D. Josephy, H. Koenig, R.T. Oakley, W.T. Pennington J. *Chem. Soc. Chem. Commun.* (1984) 1021–1022, <https://doi.org/10.1039/C39840001021>.
- [189] V. Luzzati, *Acta Crystallogr.* 4 (1951) 193–200, <https://doi.org/10.1107/S0365110X51000702>.
- [190] J.D. Dunitz, R. Taylor, *Chem. Eur. J.* 3 (1997) 89–98, <https://doi.org/10.1002/chem.19970030115>.
- [191] E.R.T. Tiekink, J. Zukerman-Schpector, *CrystEngComm* 11 (2009) 2701–2711, <https://doi.org/10.1039/B910209D>.
- [192] C.J. Setter, J.J. Whittaker, A.J. Brock, K.S. Athukorala Arachchige, J.C. McMurtrie, J.K. Clegg, M.C. Pfrunder, *CrystEngComm* 22 (2020) 1687–1690, <https://doi.org/10.1039/D0CE00176G>.
- [193] H. Wang, W. Wang, W.J. Jin, *Chem. Rev.* 116 (2016) 5072–5104, <https://doi.org/10.1021/acs.chemrev.5b00527>.
- [194] S.J. Grabowski *Phys. Chem. Chem. Phys.* 19 (2017) 29742–29759, <https://doi.org/10.1039/C7CP06393H>.
- [195] P. Politzer, J.S. Murray, *J. Comput. Chem.* 39 (2018) 464–471, <https://doi.org/10.1002/jcc.24891>.
- [196] W. Zierkiewicz, M. Michalczyk, R. Wysokiński, S. Scheiner, *J. Molec. Model.* 25 (2019) 152, <https://doi.org/10.1007/s00894-019-4031-6>.
- [197] R. Shukla, N. Claiser, M. Souhassou, C. Lecomte, S.J. Balkrishna, S. Kumar, D. Chopra, *IUCrJ* 5 (2018) 5, 647–653, <https://doi.org/10.1107/S2052252518011041>.

- [198] I.S. Đorđević, M. Popadić, M. Sarvan, M. Petković-Benazzouz, G.V. Janjić, *Acta Crystallogr B. Sect Struct. Sci., Cryst. Eng. Mater.* 76 (2020) 122–136, <https://doi.org/10.1107/S2052520619016287>.
- [199] A.F. Cozzolino, I. Vargas-Baca, S. Mansour, A.H. Mahmoudkhani, *J. Am. Chem. Soc.* 127 (2005) 3184–3190, <https://doi.org/10.1021/ja044005y>.
- [200] F.H. Allen, W D.S. Motherwell, P.R. Raithby, G.P. Shields, R. Taylor, *New J. Chem.* 23 (1999) 25–34, <https://doi.org/10.1039/A807212D>.
- [201] G. Hua, D.B. Cordes, Y. Li, A.M.Z. Slawin, J.D. Woollins, *Tetrahedron Lett.* 52 (2011) 3311–3314, <https://doi.org/10.1016/j.tetlet.2011.04.058>.
- [202] P.R. Varadwaj, A. Varadwaj, P.J. MacDougall, *Phys. Chem. Chem. Phys.* 21 (2019) 19969–19986, <https://doi.org/10.1039/c9cp03783g>.
- [203] T. Chivers, R.S. Laitinen, *Chem. Soc. Rev.* 44 (2015) 1725–1739, <https://doi.org/10.1039/C4CS00434E>.
- [204] A.F. Cozzolino, G. Dimopoulos-Italiano, L. Myongwon Lee, I. Vargas-Baca, *Eur. J. Inorg. Chem.* (2013) 2751–2756, <https://doi.org/10.1002/ejic.201201439>.
- [205] H.-T. Huynh, O. Jeannin, E. Aubert, E. Espinosa, M. Fourmigué, *New J. Chem.* 45 (2021) 76–84, <https://doi.org/10.1039/d0nj05293k>.
- [206] A. Dhaka, O. Jeannin, I.-R. Jeon, E. Aubert, E. Espinosa, M. Fourmigué, *Angew. Chem. Int. Ed.* 59 (2020) 23583–23587, <https://doi.org/10.1002/anie.202011981>.
- [207] P.C. Ho, J.Z. Wang, F. Meloni, I. Vargas-Baca, *Coord. Chem. Rev.* 422 (2020) 213464, <https://doi.org/10.1016/j.ccr.2020.213464>.
- [208] B. Zhou, F.P. Gabbaï, *Chem. Sci.* 11 (2020) 7495–7500, <https://doi.org/10.1039/D0SC02872J>.
- [209] N. Biot, D. Bonifazi, *Coord. Chem. Rev.* 413 (2020) 213243, <https://doi.org/10.1016/j.ccr.2020.213243>.